INFLUENCE OF A CONSTANT MAGNETIC FIELD ON THE LOBSTER NERVE: CONDUCTION VELOCITY AND VOLTAGE CLAMP STUDIES

by

Jean-Louis Schwartz

Submitted to the School of Graduate Studies
in partial fulfilment of the requirements
for the degree of Doctor of Philosophy

Department of Electrical Engineering
Faculty of Science and Engineering
University of Ottawa
Ottawa, Canada
April 1977

à Christiane

à la mémoire d'Edgar Schwartz
à celle de Georges Renouard
et à celle de George Glinski

ABSTRACT

This thesis presents a study on the biomagnetic response of the lobster nerve. Experiments have been made on the circum-esophageal connective of the lobster in order to investigate the influence of a constant intense magnetic field upon (i) the nerve impulse conduction velocity of the entire trunk by recording the compound action potentials, and (ii) the membrane potentials and the transmembrane currents under voltage-clamp conditions of the giant axon of this nerve, using the double sucrose gap technique.

It was found that within the limitations of these exploratory experiments the conduction velocity, the membrane potentials and the transmembrane currents of the lobster nerve are not affected in any detectable manner by a constant 1.2 T magnetic field parallel or perpendicular to the nerve.

RESUME(*)

Cette thèse présente une étude de la réponse biomagnétique du nerf du homard. Le nerf péri-oesophageal du homard a été soumis à des expériences visant à déterminer l'influence d'un champ magnétique intense et continu sur : a) la vitesse de conduction nerveuse du nerf intégral par la mesure du potentiel d'action multi-fibre, et b) les potentiels de membrane et les courants transmembranaires, en condition de potentiel imposé, de l'axone géant de ce nerf, au moyen de la technique de la double séparation de saccharose.

Les résultats montrent que, dans les limites de cette étude exploratoire, la vitesse de conduction, les potentiels membranaires et les courants transmembranaires du nerf du homard ne sont pas modifiés de façon détectable par un champ magnétique continu de 1.2 T parallèle ou perpendiculaire au nerf.

(*) Chaque chapitre est précédé d'un résumé en français.

CONTENTS

ILLUSTRATIONS

FIGURE

PREFACE

"Depuis quelques années, la magie cherche à revêtir une robe scientifique. Elle ne se satisfait plus de pythies balkaniques ou de gourous du Népal. Elle rend en quelque sorte hommage à la science en lui demandant le secours de sa machinerie. De sa machinerie. Non de ses méthodes. C'est ainsi que sont préparés d'horribles mélanges où se trouvent associés la sagesse hindoue, la caverne de Platon, William Blake, l'électroencéphalographie, les réflexes conditionnés, les enzymes les plus raffinées, les rythmes circadiens, les champs magnétiques.

La technique employée par les fabricants de ces horribles mélanges mérite d'être analysée.

1° La magie est initiale. Il est recommandé d'avoir à sa disposition un Tibétain entraîné et centenaire, un aliéné de bonne volonté ; mieux encore, de petites escouades de Tibétains ou d'aliénés.

2° Une connaissance imparfaite des données scientifiques modernes est indispensable. Il convient d'être informé des progrès récents de la science; mais il est nécessaire que cette information soit approximative, mal assimilée, inexacte, ce qui permettra les développements les plus incertains, les extrapolations les plus téméraires. Les disciplines scientifiques les plus utilisées sont l'électrophysiologie (l'électricité du cerveau est un élément fondamental des magies modernes), la toxicologie et la chimie du cerveau (formes contemporaines de la soupe et du chaudron des sorcières), certaines formes d'expérimentations animales: les rats, les chimpanzés sont les bienvenus.

3° Un vocabulaire renouvelé est recommandé. On doit, dans les descriptions, trouver les mots psychédéliques, L.S.D., ondes alpha, phénomènes psi, suggestologie.

4° La magie qui était initiale est également terminale. Les affirmations sont péremptoires, les vérifications sont inutiles.

Ainsi s'étend une magie neuve enveloppée des oripeaux d'une pseudo-science. [...] Elle est doublement dangereuse, elle donne de fausses descriptions, établit des corrélations inexactes. Elle décourage les vrais chercheurs, peu enclins à s'engager sur des chemins mal assurés."

d'après JEAN BERNARD
de l'Académie française

(L'homme changé par l'homme,
Buchet-Chastel, Paris, 1976)

REMERCIEMENTS

Je remercie M. C.Lemyre, directeur du département de Génie Electrique de l'université d'Ottawa, de m'avoir permis d'entreprendre ce projet et d'avoir relu avec beaucoup de soin le manuscrit de cette thèse. Je remercie M. J.A. Tanner, directeur du laboratoire des Systèmes de Commande et d'Ergonomie du Conseil National de Recherche Canada, pour le soutien technique et financier qu'il m'a apporté pendant ces deux dernières années. Je remercie aussi M. C.Romero-Sierra, professeur au département d'Anatomie de l'université Queen's, de m'avoir introduit au domaine du biomagnétisme et de l'électrophysiologie à l'occasion d'intéressantes discussions.

Que M. G.W.Mainwood, professeur au département de Physiologie de l'université d'Ottawa, soit assuré de ma plus profonde gratitude pour m'avoir si adroitement conseillé sur le plan scientifique pendant la période la plus critique de mon travail, et jusqu'au dernier jour.

Je remercie M. D.Poussart, professeur à l'université Laval, et M. P.Blondeau, professeur à l'Ecole Polytechnique de Montréal, pour m'avoir accueilli à Laval en mai 1973 et m'avoir initié à la méthode du potentiel imposé.

Je tiens à remercier tout particulièrement Frank Prat qui a passé deux étés dans mon laboratoire et avec qui j'ai eu les discussions les plus passionnantes sur mon travail. Il a su me redonner espoir dans les moments les plus délicats et m'a fourni d'innombrables et fort judicieux commentaires. Merci aussi à Jean-Pierre Dion, si souvent mon compagnon et mon interlocuteur.

Je remercie chaleureusement René LeHénaff et Alfred Sierhuis pour leur aide sympathique et toujours précieuse.

Mme L.Leblanc a dactylographié avec célérité et précision cette thèse. Susan Eng et Eric Lavarack ont passé de nombreuses heures à en rendre le manuscript anglais plus concis et ... plus anglais. Qu'ils soient tous trois assurés de ma reconnaissance.

Christiane, tu as lu et relu cette thèse, tu en as dactylographié les multiples versions, et surtout tu as supporté avec bonne humeur cette période difficile de notre existence. Je t'en suis gré de tout coeur.

CHAPTER I

INTRODUCTION

CHAPITRE I

INTRODUCTION

Résumé: dans ce chapitre introductif, on a tenté de cerner de façon générale le problème du biomagnétisme. A cet effet, les articles récents donnant une analyse critique dans ce domaine sont présentés, et une mention spéciale est faite du travail d'Amer qui a mis en évidence le fait que l'action du champ magnétique sur un système vivant se manifeste parfois en relation avec celle d'autres sources d'énergie physique: température et rayons X. On insiste sur le besoin d'une meilleure preuve expérimentale de l'existence des réponses biomagnétiques, de la nécessité d'une méthodologie plus rigoureuse, et de l'importance éventuelle du biomagnétisme comme outil de recherche en biophysique membranaire.

On énonce ensuite les objectifs de cette thèse:

a) étude de la vitesse de conduction nerveuse du nerf du homard soumis à un champ magnétique constant et intense;

b) étude exploratoire des phénomènes membranaires associés à la réponse biomagnétique de l'axone géant du homard, au moyen de la méthode de la double séparation de saccharose.

Finalement, les aspects originaux de ce travail sont énumérés:

a) cette thèse contient une revue détaillée de la littérature récente dans le domaine des méthodes du potentiel imposé, dans celui de la biophysique membranaire et dans celui du biomagnétisme;

b) il s'agit de la première étude biomagnétique du nerf du homard;

c) il s'agit de la première étude biomagnétique de la membrane nerveuse au moyen de la méthode du potentiel imposé:

d) pour la première fois, on a essayé d'évaluer la possibilité d'utiliser l'exposition au champ magnétique comme outil de recherche en biophysique membranaire;

e) le dispositif expérimental est décrit et analysé complètement;

f) cette thèse contient la description d'améliorations originales du dispositif de potentiel imposé, en particulier dans le sens d'une automatisation plus poussée.

CHAPTER I

INTRODUCTION

Mankind has always been fascinated by the invisible and sometimes disturbing effects of obscure physical phenomena and even in recent centuries when rationalism and scientific approaches have become the generally accepted way of attacking and sometimes solving unexplained questions of the Universe, man is still attracted by some strange aspects of its relationship to Nature. Among these are the effects of magnetic fields on living systems.

Biomagnetic phenomena have been,and are still used by charlatans to impress people and exploit their credulity. They have also been submitted in the last two decades to scientific investigation. However, there is still a tendency among some scientists to associate research in biomagnetism with Magic, or even with the most heretical parascience. This is not surprising given the often controversial aspect of the explanations of magnetic field and biological system interactions and the lack of rigor in many investigations.

The present study was undertaken with three major guidelines in mind. First, it was thought that more experimental evidence is needed to establish the existence of biomagnetic effects. Second, it is essential that a careful methodological approach should be developed to assess properly any possible biomagnetic effects. And finally, the whole attitude towards the interaction between magnetic fields and living systems might have to be reconsidered: instead of stressing the importance of the magnetic fields as such, one might be able to realize their importance as a tool in biophysics, particularly in membrane research.

The next sections of this chapter are devoted to define more precisely the ideas that have been presented above. They are followed by the statement of the thesis objectives.

I.1 Biomagnetism

The biological effects of magnetic fields have been a subject of interest for more than a century, and extensive studies have been carried out at experimental and theoretical levels in the last twenty-five years.

Magnetic fields that exist in the biosphere range from a few tenth of a Gauss(*) to many Teslas. The increasing use of superconductive magnets in laboratories and their forthcoming application in industry and urban transportation will extend the range to tens of Teslas. These fields can be constant (d.c.) or variable (a.c., time-varying). Furthermore, they can be homogeneous (low-gradient) or highly inhomogeneous (high-gradient). It is expected that the effects they will have upon biological systems will depend on the field characteristics, as related to the magnetic characteristics of the biosystems.

Numerous review papers and bibliographies of research on biological effects of magnetic fields have been published since 1960 (Davis(**) et al., 1962; Alexander, 1962; Beischer, 1963; Gross, 1964a; Becker, 1963; Barnothy, 1963; Lenzi, 1966; Gauquelin, 1966; Kholodov, 1967a; Kolin, 1968; Busby, 1968; Mutshall, 1969; Piruzian et al., 1973; Aceto et al., 1970; Presman, 1970; Kholodov, 1973; Frei, 1972).

(*) The SI unit for magnetic fields is the Tesla (T).
1 Gauss = 10^{-4} Tesla.

(**) References are given in alphabetical order at the end of the thesis.

Their number reflects the increasing interest in biomagnetism. Among the recent papers, the best coverage of the work by western scientists is found in Busby (1968), Aceto et al. (1970), and Frei (1972), while Mutschall (1969) and Piruzian et al. (1973) provide a good review of the investigations that have been carried out in the Soviet Union. The following review will be restricted to the action of constant magnetic fields on biological systems.

Exposure of man to very low magnetic fields (100 gammas or less, 1 gamma = 10^{-9} Tesla) yielded negative results, except for a decrease of the scotopic critical flicker-fusion frequency and a decrement in the visual field (Beischer, 1963).

Biomagnetic research has led to interesting discoveries when low to high intensity fields were used (10^{-2} to 10 Teslas). It has been found that magnetic fields have an effect on plant growth and orientation (Dunlop et al., 1969; Audus et al., 1964); on tumor and cell growth (Mulay et al., 1964; Butler et al., 1964), although negative results have also been reported in this case (Hall et al., 1964; Eiselein et al., 1961); on cellular respiration (Reno et al., 1963); on food requirements, sexual development, aging, morphological and cytochemical features of tissues for whole animals (Barnothy, 1964a,b; Barnothy et al., 1969 ; Gross, 1963); on morphogenesis of flies (Levengood, 1967); on the rates of enzymatically catalysed chemical reactions (Maling et al., 1965; Rabinovitch et al., 1967a, b); on orientation of Paramecia (Ozhigova et al., 1966) and algae (Palmer, 1963); on blood (Murayama, 1965; Bresson et al., 1969; Bellossi et al., 1971; Bellossi et al., 1972; Bellossi et al., 1974); on the nervous system (this will be reviewed in detail in the following chapter).

Unfortunately, many of the conclusions in the early reports

were based on limited data and on experimentation of the crudest nature. Consequently, it is not surprising that there are contradictory results in experiments that appear to have been made under the same conditions. Many of the experimental results are controversial and the theories formulated to explain them are still very hypothetical. Although a number of positive results have been obtained, no definite biophysical interpretation can be found in the literature that would explain satisfactorily the mechanisms of the interaction between magnetic fields and living systems.

It is now recognized that highly refined experimental procedures are needed in order to achieve a good degree of replication. Theoretical explanations will involve the discussion of very complex interaction mechanisms, from behavioural and cybernetic concepts to molecular or even submolecular biophysics and biochemistry.

To illustrate this, and to show the inherent complexity that is associated with biomagnetic investigations, a typical experiment has been selected. Amer (1966) in his study of the coupling effect of homogeneous magnetic fields with temperature, oxygen tension and ionizing radiation on Tribolium Confusum (flour beetle) observed the failure of pupae to moult, and wing abnormalities in the adult beetle. He found that the influence of the magnetic field on development depends strongly on the environmental conditions, i.e. temperature, oxygen tension and ionizing radiation:

(1) At normal temperature ($30^{\circ}C$), magnetic fields do not change the normal eclosion and development of Tribolium.

(2) At higher temperatures, the effect of a constant magnetic field at normal oxygen tension is to

protect the pupae from the disorganizing effects of temperature.

(3) Oxygen is more toxic in presence of a magnetic field at given temperature.

(4) Magnetic fields reduced wing malformations induced by ionizing radiation at 38°C, but this protective effect was absent at normal temperature (30°C).

Amer's work is interesting in many respects. On the one hand, it shows that the magnetic field has a definite effect on the growing process of Tribolium. On the other hand, it shows also that this effect could well have remained undetected if the effect of temperature had not been studied simultaneously. Another interesting result is the protective action of the magnetic field, which is most effective when synergism between X-rays and temperature occurs. All these factors might explain the different and sometimes contradictory results that have been reported in the literature despite apparent similarities in the experimental approach.

I.2 Methodological problems in biomagnetism

It has been mentioned before that the results reported in biomagnetism are often unreplicable and diametrically opposed. The main problem lies in the existence of numerous parameters on both the biological side and the physical side of the experiment. One is the kind of biological specimen that should be selected. Size plays a predominant role in this choice, since magnets will provide fields of reasonable strength and at acceptable energy cost only in a relatively small volume. Consequently, many experiments have been made on mice (Barnothy, 1960). Another parameter is the biological level at which the investigation should be undertaken. Experiments on whole animals are difficult to

control and interpret in physical terms. In vitro experiments are more controversial for assessing biomagnetic effects although they have proven very useful in the development of our knowledge of life's mechanisms. Here again one can consider different levels: groups of organs or cells, isolated cells or even subcellular entities. With simple specimens, the amount of variables to be controlled is smaller, and interpretations are, theoretically at least, easier. But, in addition to the experimental difficulties encountered in handling isolated structures, the biomagnetic response could be much smaller or even impossible to detect with available instruments. Furthermore, by breaking the chain of elements which constitute the overall living system, it is possible that no biomagnetic action will be recorded, although the magnetic field might in fact have an effect on the overall system (Becker, 1969; Kholodov, 1973).

I. 3 Membrane research

Relating structure and function is one of the main goals of investigators in membrane biology. Excitable membranes have been studied extensively in the last fifty years but most of our knowledge about excitation is less than twenty-five years old. On the one hand, neurophysiologists and biophysicists have obtained results using electrical measurements on the axonal membrane (Hodgkin et al., 1952 a, b; Cole, 1956). However, the relation of the membrane function, or excitability, to its biochemical structure is not yet fully understood (Johnston et al., 1972). In addition to the ionic and pharmacological approaches (Hille, 1968) which have provided much useful information, electromagnetic radiations have been used both to evaluate the optical properties of normal membranes (Cohen, 1973) and to provide the initial energy to modify the membrane conductance properties (Lieberman, 1970; Pooler, 1972). On the other hand, new parameters from excitable structures have also been recorded:

microwave emissions (Fraser et al., 1968) and magnetic fields (Cohen, 1968). It seems that the use of more diversified techniques that alter excitable membranes might bring new information relevant to the molecular basis for cellular excitation.

I.4 Statement of thesis objectives

The literature survey (see Chapter II for a review) on the biological effects of magnetic fields shows that there is some evidence of the existence of such effects, but in the case of the nervous system, there is really no firm experimental basis for the underlying mechanisms of these biomagnetic responses. Therefore, a logical approach to the problem would be to study the influence of magnetic fields on the basic electrophysiological response of excitable tissues.

This can be done in two ways: the normal propagated action potential can be studied in relation to applied magnetic fields, and the underlying membrane conductance changes can be investigated in the same conditions. However, a choice has to be made among the various electrophysiological variables that can be measured in relation to the propagated action potential, i.e. velocity, amplitude, excitation threshold and so on, and to the transmembrane phenomena, i.e. capacitance, total current, ionic currents, etc.. This choice will determine the degree of sophistication of the measurement technique that will be used.

In addition, the choice of the biological specimen is not completely arbitrary. The excitable structure that will be selected should have a well-known behaviour under normal physiological conditions. In addition, it should be compatible with the geometrical constraints imposed by the magnetic exposure apparatus. This is probably one of the most difficult requirement to meet,

because modern electrophysiological methods require a large amount of peripheral equipment. Therefore, a compromise has to be found between sophistication of the electrophysiological method and the feasibility of the biomagnetic experiment. It should be possible by proper choice of the specimen to be able to use a measurement technique that is refined enough and compatible with the magnetic field generation facilities.

Finally, the choice of the physical parameters associated with the magnetic field is also important. Should constant or time varying magnetic fields be used? Over what intensity range? Should the field be homogeneous or not? What exposure time is going to be used? How will the specimen be located (or oriented) with respect to the field? The power of the magnet, the size of the specimen, the space available in close vicinity of the pole caps are all important factors in the determination of the experimental conditions. There is still a great deal of choice in exposure time, in specimen orientation with respect to field direction and in field intensity range.

The search for a fundamental biophysical phenomenon underlying many electrophysiological, neurophysiological and behavioural activities of living systems, was therefore undertaken. When planning the experiments that are reported in this thesis, the following guidelines were adopted:

(1) the experimental method should limit the number of variables to a minimum, ideally one, so that any effects of a magnetic field can be determined without ambiguity;

(2) the experimental method should be versatile enough to permit the use of more refined procedures if biomagnetic effects are undetected at first;

(3) the experimental apparatus and method should allow different possible orientations of the specimen in the

magnetic field;

(4) the field characteristics should be well defined in time, amplitude and geometry.

(5) if possible, the experimental specimen should be taken at cellular level, in order to minimize the amount of variables that could be affected by the magnetic field ;

(6) if possible, the experimental specimen should be one that has been extensively studied under normal conditions.

In view of these guidelines, and because of the availability of a powerful d.c. electromagnet(*) offering a reasonable amount of space for inserting a nerve chamber between the pole caps, it was found that conduction velocity and voltage-clamp experiments could be made on a nerve specimen that could be either parallel or perpendicular to the constant magnetic field. Due to the rather restricted experimental space between the coils of the magnet, experiments involving micro-electrodes and their bulky micro-manipulators could not be envisaged, thus the double sucrose gap method appeared to be the most appropriate technique to be used. It was found that it is suitable to the lobster circumesophageal connective which is available any time of the year to inland laboratories. This nerve can be used as a whole for conduction velocity measurements, although the compound action potential response has not been extensively studied. This nerve provides also a giant axon that has a well-known behaviour under current and voltage-clamp conditions (Julian et al., 1962 a,b).

The objective of the present investigation is to define the effects of magnetic fields on the basic characteristics of excitable membranes,

---

(*) The author wishes to acknowledge Dr. J.C. Wooley, Department of Physics, University of Ottawa, for making the electromagnet available.

which underlie the generation and propagation of nerve impulses.

This central objective was pursued in two independent experimental studies:

(1) the study of the effects of a constant magnetic field on the propagation velocity of nerve impulses along lobster nerve;

(2) the study of the effects of a constant magnetic field on the transmembrane conductance changes associated with the nerve excitation process under voltage-clamp conditions.

The work described in this thesis presents several original aspects :

a) it contains an up-to-date extensive review of the literature pertinent to voltage-clamp techniques, to membrane biophysics and to biomagnetism. This should be of help to both the engineer and the life scientist wishing to enter this multidisciplinary field;

b) for the first time, the lobster nerve is being used in biomagnetic studies;

c) it is the first biomagnetic investigation at neural membrane level using the voltage-clamp technique;

d) it is the first attempt to assess the value of magnetic exposure as a tool in membrane biophysics;

e) it describes and analyzes in full detail the voltage clamp apparatus that has been specially designed for these biomagnetic experiments;

f) it presents improvements of the standard voltage-clamp equipment in the direction of an extensive use of modern integrated electronics. It presents also

new hybrid circuits that have been specially designed to automatize the command signal generation and the voltage-clamp data processing without the need of a computer.

CHAPTER II

LITERATURE SURVEY

CHAPITRE II

REVUE DE LITTERATURE

Résumé : ce chapitre comprend quatre parties. La première partie introduit le lecteur au système de fibres nerveuses géantes qui existe chez le homard. La deuxième partie traite des méthodes de potentiel imposé qui sont utilisées en électrophysiologie pour l'étude des phénomènes transmembranaires. La troisième partie contient certains résultats fondamentaux relatifs aux membranes biologiques excitables. La dernière partie est une analyse des effets des champs magnétiques continus sur le système nerveux, ainsi que des théories et hypothèses qui s'y rapportent.

CHAPITRE II

LITERATURE SURVEY

Biomagnetic investigations are multidisciplinary by nature. When the present study was undertaken, it was found that a large amount of information, in each of the related fields, was necessary in order to be able to design and plan the investigation in a meaningful way. This chapter is a review of four main topics: the lobster giant axon system, the voltage-clamp technique, the biophysics of excitable membranes, and the biomagnetic response of the nervous system and nervous tissue, with related hypotheses and theories. From the statement of objectives that has been given at the end of Chapter I, it can be seen that these four subjects, although they seem to be only loosely related, are in fact strongly interdependent in the context of the planned biomagnetic investigation.

II. 1 The lobster giant fibre system

This section deals generally with the nervous system of the lobster. Several textbooks give a detailed description of this system (Bullock et al., 1965; Meglitsch, 1975; Waterman, 1961).

The lobster is a sea water invertebrate(*) belonging to the same superfamily as the crayfish which lives in fresh water. The general anatomical plan of the nervous system is a dorsal, anterior brain with circumesophageal connectives and a ventral cord of segmental ganglia, commissures and nerves, plus a peripheral nervous system of mixed sensory and motor elements, and a distinct stomatogastric system for the anterior alimentary canal. The

(*) Phylum Arthropoda, class Crustaceas, subclass Malacostra, series Eumalacostra, superorder Eucaridia, order Decapoda, suborder Reptantia, section Macrura, superfamily Nephrosidea, family Homarus.

ventral cord has a segmental pattern, with a pair of ganglia in each embryonic segment, joined longitudinally by connectives, and transversally by commissures. Fusion of ganglia is complete in each segment of the adult lobster. The first ganglion of the ventral cord is the subesophageal ganglion. Its function is twofold: it is the coordinating ganglion for chewing movements, and a source of tonic excitation for the partially autonomous activity of other ganglia. Each of the segmental ganglia is connected by a nerve to the appendage, by a dorsal nerve to the dorsal muscles, and by a nerve to the heart. The longitudinal connectives contain many primary sensory and motor axons and many interneurons. Cell bodies are restricted to the ganglia and are not found in the connectives. The ventral cord itself contains long interneurons, which run through several ganglia.

The ventral cord contains two to three pairs of giant fibres. The lateral pairs are composed of a series of end-to-end nerve sections. The medial pair is made of two large axons running from the brain, where the cell body can be found, to the end of the cord. These giant fibres are associated with the rapid tail flick coordination. Synapses occur in many different forms: "en passant", chemical or electrical synapses. The giant fibre system has been described in detail by Johnson (1924) and Wiersma (1947).

Analyses of the ultrastructure of the nervous tissue of the lobster (and other members of the same family) have shown that it is very similar to the vertebrate neural ultrastructure. Schwann cells, Schmidt-Lanterman incisures and even nodes of Ranvier can be observed (Mc Alear et al., 1958). The internodal distance, however, does not remain constant along a fibre, as it does in vertebrate myelinated nerves. Giant axons are surrounded by lamellated sheaths which consist of alternating layers of thin cell cytoplasm

and connective tissue (Hama, 1961).

The composition of the axonal membrane of the lobster has been studied by Balerna et al. (1975). They found that this membrane is characterized by a high content of lipids and a low content of proteins in comparison with other types of axonal membranes.

In spite of these differences, the giant axon of the lobster displays an electrophysiological behaviour that is very similar to that of other excitable membranes. It has been extensively studied by several investigators (Dalton, 1958; Wright et al., 1958; Dalton et al., 1960; Julian et al., 1962a,b; Brinley, 1965) who have shown that it is in many ways similar to other well-known neurophysiological specimens. For this reason, and due to the fact that lobsters are available to inland laboratories at any time of the year, the giant axon preparation is widely used in experimental work on excitable membranes.

II. 2 Voltage-clamp techniques

In contrast to the natural excitation process where both membrane current and membrane potential change as a function of time, excitation under voltage-clamp conditions is characterized by a known value of the membrane potential which remains constant and uniform over a given area of membrane. In addition to the fact that the voltage-clamp technique holds one membrane parameter to a constant and known value, it also allows measurements of pure transmembrane currents. A voltage-clamp apparatus is therefore essentially an electronic feedback circuit which passes a variable current through a biological membrane in such a way that the membrane potential matches a predetermined command voltage, in spite of the natural tendency of the membrane conductance to vary with voltage and time.

II.2.1 Historical notes

Using the potential control techniques of Marmont (1949) and Cole (1949), Hodgkin et al. (1952a) designed an experimental method for measuring the flow of current through a definite membrane area of the giant axon of the squid. The membrane potential was kept uniform over this area and changed in a stepwise manner by feedback control. The modern interpretation of the nervous function originated from the basic results obtained with the voltage-clamp technique (Hodgkin et al., 1952b). Furthermore, this technique has proven its value as a very powerful and reliable quantitative tool for membrane biophysics studies.

This method of measuring transmembrane ionic currents was soon improved and adapted to other specimens. Cole et al. (1960), using micropipettes and calomel half-cells, brought the potential electrodes as close to the membrane surface as physically possible, in order to improve accuracy. The isolated nerve fibre of the frog and of the toad were studied using the voltage-clamp technique by Del Castillo et al. (1957), Tasaki et al. (1958) and Dodge et al. (1958). Similar methods were used by other investigators on various excitable and inexcitable tissues (see Moore et al., 1963, and Cole, 1968, for descriptions of early investigations).

Examples of improvements of the original voltage-clamp technique are mentioned in the previous paragraph. Some were intended to adapt the technique to completely different specimens, such as spherical cells, muscle or cardiac fibres, and others to improve the accuracy and the ease of data processing through the use of more elaborate solid-state electronic and computing circuitry. There were important developments in the method used to separate the different ionic components of the transmembrane current, namely changing the type of command potentials from a simple step

function to more complicated functions like pulse trains, ramps, triangular or sinusoidal signals (Palti et al., 1969; Fishman, (1969), or using pharmacological agents having a specific action on the different ionic components of the current (Hille, 1966).

II.2.2 Nerve response and voltage-clamp data interpretation (Katz, 1966).

II.2.2.1 Normal nerve behaviour. There are three important concepts related to neural excitable structures: the concept of resting state, the concept of excited state and the concept of propagation.

The resting state is characterized by a resting potential due to differences in ionic concentrations maintained on the two sides of the neural membrane by metabolic processes. The value of this resting potential can be obtained from Goldman's equation. It ranges between 80 mV and 100 mV depending on the specimen, and it is negative inside the cell.

The excited state is attained when a stimulus of sufficient amplitude and length is applied to the membrane. An abrupt change in membrane potential occurs which is independent of the stimulation signal (all-or-none law). The voltage then returns to its resting value, and at the end of the refractory period, the nerve membrane is ready to fire again. The phenomenon of excitation can be explained by the ionic theory established by Hodgkin et al. (1952b) as a result of their voltage-clamp studies of the squid giant axon. According to this theory, the excitation process corresponds to a voltage and time dependent change in the membrane permeability to different ions.

The impulse propagation along the nerve cell axon is the third important characteristic of nervous function. The propagation

process can be explained by comparing the axon to a coaxial transmission line where the conducting axoplasm is separated from the conducting extracellular fluid by the membrane which behaves like a leaky capacitor. Due to the potential difference that exists between an active and an inactive patch of membrane, local electrical conducting paths are established in which the current is generally sufficient to stimulate the inactive patch, thus propagating the impulse. The propagation velocity can be predicted using the transmission line theory ("cable theory", Taylor, 1963). It can be found theoretically, and it has been recorded experimentally, that the impulse propagates at constant velocity and with constant amplitude.

II.2.2.2 Nerve behaviour under voltage-clamp conditions.

If the voltage in a given length of membrane is kept constant, there are no longitudinal currents in the axoplasm and in the extracellular medium. Propagation is therefore abolished and pure transmembrane currents are recorded. If the clamping voltage is hyperpolarizing, in other words if the inside of the neural membrane is made more negative, an entering current of potassium ions driven by electrostatic forces is observed. If the clamping voltage is depolarizing (the inside of the neural membrane is made less negative), current patterns that are recorded differ depending on the depolarization levels. For small depolarizations, there is an outgoing current of potassium ions driven by diffusion forces. For a higher depolarization, a large inward current of sodium ions enters the axon, rapidly reaches a maximum, reverses its polarity and is then followed by an outgoing current of potassium ions. If the depolarization of the membrane is made more positive than the sodium reversal potential, the inward current does not appear and only the slow outgoing current of potassium ions is recorded. To summarize, the inward current composed

of sodium ions corresponds to the transient depolarization process of the action potential and the delayed outward potassium current corresponds to the repolarization of the membrane. In addition to these two components of the membrane current, there is a leakage current proportional to the applied voltage step, as well as a capacitive current noticeable at the beginning and at the end of the clamping step.

A quantitative description of the excitation process has been put forward by Hodgkin et al. (1952b), together with the following membrane model (Fig. II-1). E_{Na}, E_K and E_ℓ are the sodium, potassium and leakage potentials, g_{Na} and g_K are the voltage-and-time dependent sodium and potassium conductances, g_ℓ is the constant leakage conductance, and C'_m is the membrane capacitance.

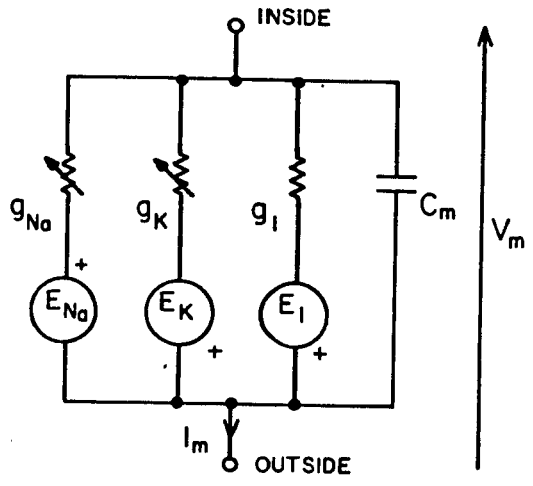

Fig. II-1. Hodgkin-Huxley Membrane Model

II.2.2.3 Voltage-clamp data interpretation.

In addition to the recorded time course of transmembrane currents under voltage-clamp conditions, it is standard practice to plot on I vs V graphs the peak transient current and the steady-state delayed current with respect to the applied voltage steps, as much physiological and biophysical information can be extracted from this kind of graph . Some of the techniques that are used will be mentioned here. A complete description is given by Blaustein et al. (1966a).

a) Membrane capacitance : the value of C_m can easily be found from expanded time scale oscilloscope traces of the current density under voltage-clamp. The area under the curve gives the electric charge stored by the capacitor. Dividing this value by the value of the clamping voltage corresponding to the recorded current gives the value of the membrane capacitance.

b) Sodium reversal potential: the potential is defined as the potential for which no sodium flow crosses the membrane. It can be obtained directly from the current-voltage characteristics, where the early transient inward current line crosses the horizontal axis before reversing its polarity. This is only true though, if one assumes that the early current is carried by sodium ions only.

c) Potassium reversal potential: the same technique as described in the previous paragraph could be used if it could be assumed that the steady-state current is carried by potassium ions exclusively. Here, the assumption has less validity because it has been established that there exists a leakage current (Cl^-, etc.).

d) Membrane conductances: probably the most interesting information that can be obtained from the current-voltage characteristics is the value of the membrane conductance. It can be determined by taking the slope of the characteristics at any given point. The steady-state characteristic only displays a positive slope, which means that the membrane has a positive conductance in the steady-state. The peak transient current curve displays a negative slope, which indicates negative conductance. This is not quite true though,because the different points on this curve are not taken at the same time. This phenomenon is of course responsible for the "unstable" or all-or-none behaviour of the nervous membrane.

The values of the Hodgkin-Huxley model parameters, obtained as described in the previous paragraphs, can be used to build models in order to predict the response of the nerve membrane in other experimental conditions. On the other hand, the variations in the I vs V curves under the influence of various environmental changes are of great interest to investigators in membrane biophysics.

II.2.3 The double sucrose gap voltage-clamp technique

This method has been developed by Julian et al. (1962a,b) in order to study single non-myelinated fibres of small size compared to the squid axon. The method consists of raising the external shunt resistance in order to reduce the external current that flows between two patches of membrane, one of which being depolarized with isotonic potassium chloride. This allows the use of external electrodes and more important, it allows the study of small biological specimens which could not be impaled as in the Hodgkin-Huxley-Katz technique . Two methods have been successfully used to increase the

external resistance: the air gap method introduced by Tasaki et al. (1955) and the sucrose gap method introduced by Stämpfli (1954), in which a deionized solution of sucrose is used as an outside insulator.

The schematic description of the double sucrose gap method is given in Fig. II-2. The two sucrose streams limit the membrane area, perfused by the test solution which may be artificial sea water, or any other solution containing pharmacological agents of interest. The membrane area can be adjusted by proper flow regulation of the different solutions. Typical values for the gap width are 80 to 100 microns. The isolated fibre extends beyond both sides of the sucrose gap (about 1mm each), in such a way that current can be injected for stimulation or for voltage-clamping on one side, while voltage is measured on the other side.

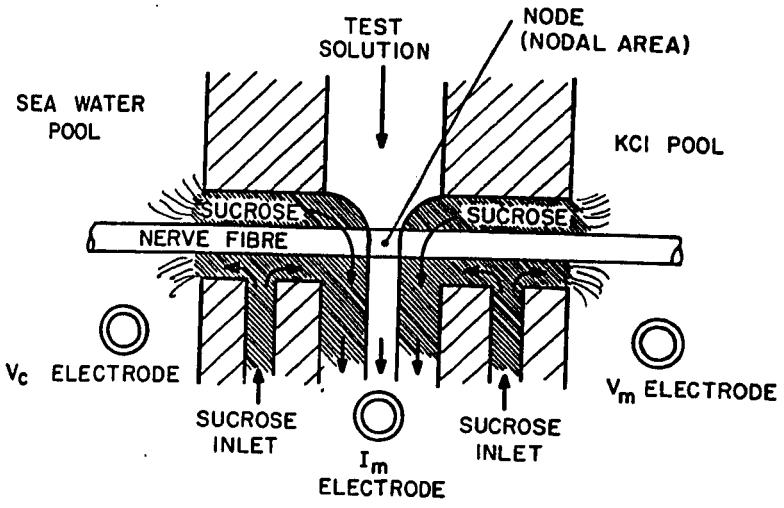

Fig. II-2. Double sucrose gap arrangement (top view)

The current is measured in central area (or "node") where the test solution is flowing. The lateral pool where the current is injected is filled with either potassium chloride or artificial sea water, and the lateral pool where the voltage is recorded is filled with potassium chloride. Electrodes are of the conventional type: glass tubes filled with saturated KCl-agar gel, with properly coated silver wires to allow electrical connections to the electronic instruments. If the isotonic sucrose solution has been carefully deionized to a conductivity of about 10^{-5} S/m, the electrical resistance across the sucrose gap without nerve preparation has a typical value of the order of 100 MΩ.

The sucrose gap technique offers several advantages: nerve axons of smaller diameter than the squid fibre can be studied, because the impalement by an axial electrode is not necessary; large size external electrodes can be used which results in a better frequency response of the measurement circuit and a lesser load to the control amplifier; more than one membrane patch can be measured by simply sliding the preparation along its longitudinal axis. Several difficulties are however encountered, and they will be reviewed in the next paragraphs.

II.2.4 Problems related to voltage-clamp techniques

Voltage-clamp results can be properly interpreted only if the membrane potential is spatially and temporally controlled. Spatially, the entire membrane patch where measurements are made must be forced to respond as a single and uniform unit. Temporarily, the membrane potential must accurately follow the command pulse. A lack of spatial control results generally in the appearance of

oscillations or "notches" in the membrane currents (Taylor et al., 1960). Results of simulation have shown that it is impossible to tell from the time variation of voltage and current alone whether the experiment is adequately close to an ideal clamp or not, and whether recordings are in fact characteristic of the membrane without experimental artifacts (Kootsey, 1975). In the case of the sucrose gap method, the tendency to oscillate can be prevented by reducing the area over which the current is measured to a value of less than one axon diameter (Blaustein et al., 1966b; Moore et al., 1975). Furthermore, proper temporal control is required for rapid response of the membrane at the leading edge of the command pulse, prior to excitation, and for fidelity during the pulse, when ionic conductance changes take place in the excitation process (Katz et al., 1974).

The use of sucrose around the axon is also responsible for additional problems: hyperpolarization of the membrane, limited survival time of the preparation and increased transmembrane leakage currents. The membrane hyperpolarization can be greater than 50mV. It has been attributed to the existence of junction potentials that results from the different mobilities of cations and anions at the junction of two solutions. This hyperpolarization can be reduced by increasing the width of the gap between the sucrose streams, which is in contradiction with the spatial control requirements (Blaustein et al., 1966b). Survival time reduction might be imputed to a lack of ions (K^+, Na^+ and Ca^{++}) in the extracellular medium (Mc Guigan, 1974). Leakage currents have been found to be hundred times larger in double sucrose gap arrangements than when measured with microelectrodes. These currents are voltage-dependent but do not vary if the membrane

area is changed. This phenomenon has been attributed to a parallel leakage path in sucrose along the axon (Pooler et al., 1972).

The exact determination of the membrane potential in the case of the double sucrose gap method is made difficult by the fact that the extracellular medium is divided in regions of different resistivity. Jirounek et al. (1971) have performed a theoretical analysis of the potential distribution in sucrose gap arrangements, and they have established that the true membrane potential of the patch in test solution can be obtained from its measured value if the longitudinal resistances, the membrane resistance , the extracellular potential in sucrose, and the junction potential at the test solution and sucrose interface are determined by separate measurements.

Another phenomenon that can lead to erroneous interpretations of voltage-clamp data is the existence of an electrical resistance between the membrane and the electrode located in the central pool. When this resistance takes a value of several Ω-cm^2, it can produce noticeable changes in amplitude and kinetics for both transient and delayed current recordings (Binstock et al., 1975). Reduction of this series resistance can be accomplished by reducing the distance between the voltage reference electrode and the preparation. This is relatively easy to do with microelectrodes but not in the case of large external electrodes such as those used in sucrose gap arrangements. Electronic circuits have been designed to compensate for the error introduced by the series resistance (Poindessault et al., 1976).

In spite of these difficulties, the voltage-clamp method has proven to be a very powerful technique, and it has been used successfully on many different specimens. It is one of the best tools

in electrophysiological research. However, the experimental results should be carefully analyzed before attempting to establish any theory, as systematic errors can be introduced both by the geometry of the preparation and the characteristics of the apparatus.

II.3 Membrane biophysics

II.3.1 Introduction

It is not intended to cover comprehensively in this section the accumulated knowledge and the unresolved questions related to membrane biophysics, but rather to provide some information on major trends and results in this field, with special reference to the nerve membrane and its excitability properties.

As a result of the work by Hodgkin, Huxley and Katz (Hodgkin et al., 1952a; Hodgkin et al., 1952b) the action potential of the squid axon can be completely explained in terms of ionic permeability changes in a patch of nerve membrane and by the transmission line properties of the axon. This phenomenological description corresponds to the so-called Hodgkin-Huxley model (H-H model) of the axon membrane. With only minor changes this model has also been successfully used to describe the excitation and conduction behaviour of many other membranes (see Noble, 1966, for a review).
However, a major question still remains unsolved: how do ions pass through the membrane. This problem has been actively studied in the last decade, through very different approaches: experimental studies of living and artificial membranes in various chemical or physical environmental conditions, theoretical investigations of model membranes, and biochemical and biophysical studies of membrane ultrastructure (for reviews, see Gitler, 1972; Ehrenstein and Lecar, 1972; Vaidhyanathan, 1974; de Levie and Abbey, 1976).
A clearer, although incomplete, picture of the nerve membrane

structure and of the process of ion permeation through it has appeared in the recent years, and some of its most important features will be reviewed in the following paragraphs.

II.3.2 Membrane structure

It is now established that membrane formation results from the intrinsic characteristic properties of constituent molecules and their behaviour in the presence of water. The major membrane components are lipids, proteins and carbohydrates. X-ray diffraction, spin label paramagnetic resonance and calorimetric studies have brought evidence of a bilayer arrangement of the membrane lipids. The protein packing is not as well elucidated, although it is thought that protein molecules are intercalated either into or through the lipid bilayer, with an asymmetric distribution, the major portion being located near the inner surface. There is also strong evidence that the lipid-protein interactions are small, thus allowing access for phospholipids to the aqueous medium. Membrane carbohydrates (glycolipids and glycoproteins) have been found to be readily accessible to the exterior of cells. They might be responsible for regions where formation of complexes with sugar and alkali metal cations is possible.

These components are in a metastable state giving the membrane a certain degree of lability. This ability of components to move with respect to each other is probably determined by the interaction between polar groups of the molecules, by the interaction of the molecules with their aqueous surrounding media, and by the cohesive forces between apolar regions of molecules. Lipids are arranged in a liquid-crystalline packing where tilting and inversions are possible. It has also been established, by means of low angle X-ray scattering measurements and by use of fluorescent probes

which bind to protein molecules, that proteins are also in movement in the membrane.

It is therefore possible to relate, at least tentatively, the structure and function of biological membranes. Their functional characteristics will depend on the nature of structural transitions resulting from surrounding environmental modifications. Thus, interaction of the membrane with different molecules can distort its packing arrangement, as it happens in the case of detergent molecule bindings. It can also result in a stabilizing action on the membrane components inhibiting processes, as in the case of anesthetics or excess of divalent cations. The binding of molecules can also have a triggering action on some normally inactive membrane components. In addition, other structural transformations can be envisaged. It is known that an applied electric or magnetic field can induce orientation of the anisotropic components of liquid-crystalline compounds (Fergason, 1964). This phenomenon deserves attention with reference to this particular biomagnetic study. Incidentally, this hypothesis of interaction between magnetic fields and living systems has been put forward by Labes (1966), but was never verified in any experimental biomagnetic work.

There is some indirect evidence of the liquid-crystalline structure of membranes. Birefringence and light scattering changes during nerve activity have been reported by Cohen et al. (1968, 1971). Equivalent changes have been found in signals emitted by fluorescent probes that were bound to the membrane molecules (Tasaki et al., 1968; Conti et al., 1971; Tasaki, 1974). These findings suggest that reorientation of membrane molecules takes place in the presence of an applied electric field of intrinsic or extrinsic origin. It cannot be excluded that such a phenomenon could also occur if a magnetic field

were used instead.

II.3.3 Ion permeation through membranes

This paragraph mainly concerns passive ion transfer (as opposed to active transfer of metabolic origin) through the axonal membrane as it occurs during nerve excitation and impulse propagation.

It has been stated in section II.2 that there is indisputable evidence that during the course of the action potential the ionic current crossing the membrane is carried by at least two different types of ions in normal physiological conditions. There is an early current accompanied by a net flux of sodium, followed by a late current accompanied by a net flux of potassium. It has also been established that a large number of ions other than sodium are able to carry the early current, and several ions other than potassium can carry the late current. In addition, sodium and potassium current activation kinetics depend on the membrane itself, but sodium inactivation process seems to be related also to the ionic environment. The use of pharmacological agents blocking selectively one of the two ionic currents has demonstrated the independence of the early and the late conductance pathways of the membrane (a concise review is given by Hille, 1972). Additional evidence of the independence of the two pathways is brought by noise measurement experiments (Poussart, 1969; Fishman et al., 1975a, b; Conti et al., 1975).

The two major possibilities for ions to cross the membrane are either by a carrier mechanism or through physical channels. A carrier is a molecule that can combine with ions to form a complex capable of permeating the membrane. A channel is a specific region offering low resistance to ions crossing the membrane. There is strong evidence that passive transport of ions in excitable membranes is accomplished by ion specific pores (Armstrong, 1975). This

evidence relies upon pharmacological and thermodynamical considerations.

Channel properties are basically of two kinds: ionic selectivity and gating ability. The selectivity mechanism has been interpreted in terms of ions interacting with negatively charged sites in the membrane and in terms of the relative importance of ion binding versus ion mobility (Hille, 1975; Mullins, 1975). The gating process is directly related to excitability. The mechanisms accounting for this phenomenon have not yet been completely explained, although important advances have recently been made in the understanding of the gating process (Hille, 1976). It is now established that calcium ions do not act as plugs in the pores, but that the gating process is ascribed to conformational changes of macromolecules in the membrane, each channel possessing a gate displaying an "open" or "closed" state. Internal membrane currents, the so-called gating currents, have been experimentally recorded (Bezanilla et al., 1975; Rojas et al., 1975). They could correspond to the conformational changes of charged macromolecules involved in the gating process.

Several attempts were made to obtain indirect evidence of these conformational changes associated with the gating process. It has been found that heat is associated with nervous activity (Howarth et al., 1968). Infrared emission has been detected from live crab nerves under stimulation (Fraser et al., 1968). Birefringence and light scattering changes have also been observed in relation with nerve impulse (Cohen et al., 1968, 1971; Tasaki et al., 1968). These findings strongly support the view that the nerve impulse originates from macromolecule conformational changes.

Research in excitable membrane biophysics has been extremely fruitful in the recent decade. It has now reached the point where a relatively well defined image of the nerve excitation process

has emerged from both experimental and theoretical studies. Although many questions still remain unsolved, a good fit can be established between nerve function and membrane structure.

II.4 Influence of magnetic fields on the nervous system

Among the biological systems reported to be affected by magnetic fields, the nervous system seems to play an important role. Numerous investigations are concerned by this biomagnetic response which has been experimentally recorded at different levels: entire system or central nervous system, electrocardiogram and electroencephalogram, neuromuscular preparations, isolated nerves or neurons, and membranes. In addition, theories have been put forward that explain or predict actual biomagnetic responses.

II.4.1 Biomagnetic responses of the nervous system

It has been demonstrated that magnetic fields (inhomogeneous and of constant amplitude from 10^{-4} to 0.08 T) have an inhibitory effect on the central nervous system. Studies on human subjects have shown that exposure to the field results in headaches, insommia, tiredness and loss of appetite (Vyalov et al., 1964). Conditioned reflex investigations on various animals (fish, birds and rabbits) have established more precisely an inhibitory action of the magnetic field (Kholodov et al., 1964). Furthermore, the same author has observed that this action seems to persist after the field has been suppressed.

Histological studies on rabbit brains show an increase in oligodendroglial, microglial and astrocyte cells after exposure to magnetic fields (Kholodov et al., 1969). Collagen development in tissue culture is also reported by Israeli et al. (1971).

The electrical response of the brain (electroencephalogram) is modified even when a weak field (a few hundredths of a Tesla) is applied.

An increase in the number of spindles during and after exposure of rabbit brains is reported by Chizhenkova (1966). This is confirmed by Kholodov (1967b), who also experimented on isolated brains. He found an increased reaction of the electroencephalogram to constant magnetic fields.

There is some evidence (Becker, 1965) that in addition to the nerve impulse propagation system, there is a direct current system in living organisms. This steady-state potential system would be of a semi-conducting nature and therefore more sensitive to the action of magnetic fields (Hall effect) than are electronic or ionic conduction processes. Vectorial relationships between the field and the nervous system might also be interpreted with the help of this d.c. neural semi-conducting system.

The electrocardiogram is another indirect neural response that has been studied in detail in biomagnetic experiments. Beischer et al. (1964) exposed squirrel monkeys to inhomogeneous constant fields, ranging from 2 to 7 T. They found a decrease in the heart rate, an increase in the degree of sinus arrhythmia, and an increase of the T-wave amplitude. These biomagnetic effects could originate from the heart or the vagal nerve, since the heads of the monkeys were also located in the field. In another experiment (Reno et al., 1966), isolated hearts of turtles were exposed to homogeneous magnetic fields (0.34 - 1.56T range). The field elicited sudden potential spikes that appeared with some latency, and did not always disappear when the field was turned off. Gonet (1975) has studied the effect of 0.7 T homogeneous fields on the electrocardiograms of mice, rats and hamsters, and could not record any changes in mice and rat ECG's. However, an increase of the T-wave amplitude was recorded in experiments on hamsters. This result is interesting

because it indicates that the electrocardiogram alteration is specific to certain species only.

Chalazonitis et al. (1964) noted a decrease in the spontaneous activity frequency, transitory arrhythmias, a diminution of diastolic activity and a hyperpolarization in the myocardial fibres of Helix Pomatia exposed to a 1.5 T magnetic field. These inhibitory effects were amplified when temperature was higher. Vovk et al. (1971) have investigated the influence of a homogeneous magnetic field of 0.22 T on the isolated sartorius muscle of the frog. They did not detect changes in the stimulation threshold, although the threshold fluctuations did increase during exposure to the field. Experiments were performed both with the field perpendicular and parallel to the specimen. There was no difference in the results.

The investigations mentioned below are all concerned with the effect of magnetic fields on isolated nerve preparations. Erdman (1955) has shown that 0.1 T magnetic fields affect the rheobase and the chronaxy of the frog isolated sciatic nerve. Higher fields (1.7 T) did not block the nerve impulse and the propagation velocity remained unaffected. Similar results are reported by Jonnard (1963) in unpublished measurements on frog nerves that were done in 1933 using a 0.05 T electromagnet. When the field was perpendicular to the nerve, an increase of chronaxy and a simultaneous decrease of rheobase were recorded. The opposite happened when the field was parallel to the preparation. However, Jonnard states that the latter experiment might have little significance due to the technical difficulties encountered. Liberman et al. (1959) failed to confirm Erdman's results. They exposed single fibres of the frog sciatic nerve to a 1 T transversal magnetic field. The excitation threshold strength was measured and it was not influenced by the field. Reno (1969) investigated the conduction

velocity of the frog sciatic nerve exposed to a constant homogeneous magnetic field of 1.16 T. The nerve was bent into a L-shape and placed in the air gap of an electromagnet, thus allowing measurements of the effect of the field in parallel and perpendicular configurations. An increase in conduction velocity was observed, the more pronounced effect being detected when nerve and field were parallel. These effects did not occur immediately after the field was applied and they did not disappear when the field was removed. Russel (1969) recorded the impulses from the subesophageal ganglion of the cockroach placed between the poles of a 0.66 T permanent magnet. He found an inhibitory effect of the field resulting in a decrease of the spontaneous firing rate of the ganglion. Kolta (1973) reports that the effect of a magnetic field of 0.058 T, obtained from a permanent magnet, on the axon-bundle of different biological species (rat, pike, frog) was detectable as a deflection of the nerve. The nerve behaved like a ferromagnetic material. This effect disappeared when phospholipids were dissolved in a methanol-chloroform mixture. No other tissues displayed this behaviour. The same author measured the magnetic susceptibility of the nerve preparation. He obtained a value 10 000 times greater than values reported previously.

Studies have also been carried out at the biological membrane level. Bianchi et al. (1963) reported a 10 to 30% decrease of the sodium transport across frog skin in a magnetic field ranging from 0.025 to 0.065 T. The prevention of this effect by the addition of ouabain indicates that the sodium pump is influenced by the field. Knoll (1962), also working on frog skin, could not detect any effect on sodium transport using a 0.35 T magnetic field. Gualtierotti (1964) investigated the action of stronger fields (up to 1 T) on the membrane potential of the frog. He found that a threshold level of

approximately 0.5 T had to be reached in order to record a sharp depolarization followed by a slower decrease of the membrane potential. Threshold values varied for different parts of the skin of the same animal and for different animals. This effect vanished when the sodium pump was inhibited. Changes in the resting potential of Nitella under magnetic field exposure were investigated by Sachava et al. (1970). Experiments with a 0.1 T magnetic field resulted in a 10 to 20% depolarization of the membrane with almost complete recovery after removal of the field. The same depolarization was noted for higher fields (0.16 and 0.45 T), although recovery was less marked.

From the foregoing, it can be seen that there exist a considerable amount of evidence of an interaction between constant magnetic fields and the nervous system. Experimental results are generally consistent with respect to the biomagnetic response of the whole nervous system or of some of its subsystems such as the brain or the heart. However, there are controversial reports on the influence of magnetic fields on isolated nerves or nerve cells. It seems that the results obtained by some investigators were difficult to reproduce when investigated by others. In many cases, this was due to a lack of detailed description of the experimental procedure, or to variations in conditions that could be critical for detection of small biomagnetic effects. For instance, Erdman (1955) did his experiments on the whole sciatic nerve of the frog, while Liberman et al. (1959), in their attempt to replicate Erdman's results, used an isolated fibre of the sciatic nerve. In other cases, homogeneity of the field was not taken into consideration, nor were the respective orientations of the specimen and the field.

The next part of this section presents a review of the main

theories which have been proposed to predict or explain the biological effects of constant magnetic fields.

II.4.2 Biomagnetic hypotheses and theories

Numerous theories have been advanced by investigators in an attempt to explain or predict the biological effects of constant magnetic fields. However, no one theory has yet been supported satisfactorily by experimental evidence. Theoretical interpretation of biomagnetic experimental results is a very complex problem that involves modern molecular physics as well as biochemistry.

At this stage, it might be useful to describe phenomenologically the action of a constant magnetic field on physical objects (Barnothy, 1964c). Four basic mechanisms can be encountered :

(a) Electromotive forces are generated in moving conductors. This in turn will induce polarization currents if the magnetic field is homogeneous, and conduction currents if it is inhomogeneous. These currents can generate heat, which is an irreversible process, or create electrolytic dissociations that may or may not be reversible.

(b) Forces are exerted on moving charge carriers. These forces can deflect the path followed by the moving carriers in solids and liquids and are at the origin of galvanomagnetic and thermomagnetic effects. They can also modify the ionic concentration in electrolytes.

(c) Torques are generated on permanent magnetic dipoles and non-spherical paramagnetic or diamagnetic particles.

(d) Forces are generated on permanent magnetic dipoles and paramagnetic or diamagnetic particles if the field is not homogeneous. Their amplitude is proportional

to the field gradient for dipoles, and to the product of the field intensity and the field gradient for particles. This effect can lead to the accumulation of certain reaction constituents and to the alteration of diffusion processes.

These magnetic actions can display either a vector character (they reverse when the field is reversed) or a scalar one (heat). If they persist for a certain period of time, the effects are cumulative. In other words, biomagnetic experimental results might be very different for various field intensities, configurations, and exposure times.

It is interesting to note that most biological substances are diamagnetic, a few are also paramagnetic (principally in an activated state) but none is ferromagnetic. The effects of low to moderate fields on such substances are therefore expected to be small as compared to the effects of thermal agitation at normal temperature. In fact, simple calculations show that translational redistribution is almost impossible in gradient fields where $H\frac{dH}{dx}$ is of the order of $10\ T^2/m$, even for larger biological cells and for blood cells that are highly magnetic and mobile (Neurath, 1964). The same author established that a 30 T homogeneous field is necessary to overcome thermal random disorientation and to obtain a rotational alignment of ellipsoidal blood cells.

Heinmets et al. (1961) have suggested that magnetic fields could affect the chemical reactions taking place in biological cells. Synthesis and the rate of enzyme-substrate reactions are known to depend on the local substrate concentrations. Free metabolites in ionic form would migrate under the influence of the magnetic field, and as a consequence of this abnormal distribution, distortion of processes such as synthesis could take place. Abnormal

pH-distribution could also occur if hydrogen ion concentrations are disturbed. This view is shared by Beisher (1963) who states that an inhomogeneous field could affect reactions in which oxygen, which is highly paramagnetic, and enzymes are involved, by displacing chemical equilibria towards the more paramagnetic products.

Valentinuzzi (1965, 1966) presented several theoretical approaches to the problem of the interaction of constant magnetic fields with the nervous system. He showed that simple mechanical action on ions crossing the nervous membrane is meaningless because of the small value of the forces involved. However, if the ionic current loops that occur during excitation are considered, a magnetic effect could take place although it would be very difficult to detect it experimentally. Using an excitation model of the entire nervous system, Valentinuzzi stated that the magnetic field would act through addition and multiplication of small physical effects. Furthermore, during the refractory periods between impulses, the magnetic field would influence the metabolic processes by reducing the rotational diffusion (Brownian rotation) of the paramagnetic free radicals involved. For instance, a field of 0.5 T would, in theory, reduce by 12% the velocity of a reaction in which a free radical with a single unpaired electron participates.

Gross (1964) presented another theory. To explain the experimentally reported inhibitory effects of magnetic fields, he postulated that the bond angle of free radical intermediates involved in biochemical reactions is distorted, thereby preventing a close fit of the enzyme and the reaction products, and slowing down the rates of synthesis of large molecules.

Using a thermodynamic approach of physical chemistry, Ragle (1964) evaluated the amount of energy that is needed to shift

electrochemical cell potentials and the equilibrium constants. He found that a magnetic field of 1 T would produce changes of the same magnitude as those produced by temperature fluctuations of a few microdegrees. He concluded therefore that no biomagnetic effect could exist in biochemical reactions.

Abashin et al. (1975) analyzed the theories of Gross and Valentinuzzi and came to the conclusion that the Gross theory was open to criticism because the existence of electrostatic fields in paramagnetic molecules "extinguishes" the magnetic and mechanical orbital moments. Therefore the bond angle could not be affected by magnetic fields. They also challenged Valentinuzzi's rotational diffusion theory by stating that the spin-orbital bond of molecules breaks in moderate magnetic fields. Therefore no rotational diffusion could take place in fields like those predicted by Valentinuzzi.

Liboff (1965, 1969) considered the action of magnetic fields on the diffusion of charged particles across membranes. He found that a field of 1 T actually influences the diffusion rate only if there exists an electric field parallel to the mean path of the particles. The presence of this electric field in the case of a nerve axon would correspond to a charged axoplasm.

An interesting explanation of biomagnetic effects has been proposed by Labes (1966) who speculated on mechanisms associated with liquid crystals. It has been found that many biological substances are in fact in the mesomorphic phase (also called liquid crystals) and on the other hand that the rod-like molecules of liquid crystals are very easily oriented in magnetic field as weak as 0.1 T. This view is supported by Bresler et al. (1974) who also postulated that membranes have the physical structure of liquid crystals and found

that a reversible change in membrane structure took place when the proximal tubules of frog kidneys were exposed to magnetic fields ranging from 1 to 2.8 T.

From the various theories that have been mentioned in the previous paragraphs, it can be concluded that no theory exists yet that provides a full explanation of the influence of magnetic fields on living systems. At the microscopic level, it seems that only very strong fields have any effect. At the macromolecular level, it is believed that the liquid crystal hypothesis is the most credible, but more has to be known about membrane structure in order to support this hypothesis. At the macroscopic level, chances are small that biomagnetic effects could be detected on isolated physiological entities such as nerve cells, skin, etc. for two main reasons. First, experiments on these specimens are inevitably of a short term nature, and second, the biomagnetic effects are probably small. It seems therefore that interactions between magnetic fields and living systems can only be established at a higher level of functional organization, where additive and multiplicative effects can take place. On the other hand, the complexity of such highly organized systems makes it difficult to determine the exact origin of the measured effects.

CHAPTER III

MATERIALS AND METHODS

CHAPITRE III

DISPOSITIF EXPERIMENTAL ET METHODES

Résumé : ce chapitre comprend quatre parties. La première introduit les critères qui ont servi de guide à l'élaboration de l'appareillage utilisé pour l'étude de l'influence d'un champ magnétique constant sur la réponse électrique de la fibre nerveuse géante du homard, en condition de potentiel imposé. On y trouve aussi la description de l'équipement de mesure de vitesse de propagation du potentiel d'action du nerf péri-oesophageal du homard. La deuxième partie traite de l'équipement de génération et de mesure du champ magnétique. Dans la troisième partie se trouve la description détaillée du dispositif de potentiel imposé à double séparation de saccharose ainsi que l'analyse théorique simplifiée de son fonctionnement. Les montages auxiliaires en rapport avec ce dispositif sont également décrits dans cette troisième partie. La quatrième partie enfin expose le déroulement et la teneur des différentes opérations qui interviennent dans l'expérience biomagnétique qui fait l'objet de cette étude.

CHAPTER III

MATERIALS AND METHODS

III. 1 Introduction

This chapter describes the experimental apparatus that has been designed for investigating the effects of a constant magnetic field on the impulse conduction velocity and the membrane properties of the circumesophageal nerve of the lobster. It also contains a description of the experimental procedure that was used in this investigation.

The design of the velocity measurement apparatus did not cause any particular problem. Two recording chambers were constructed from acrylic plastic with one section at 90^{o} to the other. Dimensions are given in Figure III-1. The basic difference between the two chambers is in electrode design. Both have platinum electrodes, either straight (in chamber No. 1) or V-shaped (in chamber No. 2). Electrodes are silver-soldered to shielded leads. A photograph of the two nerve chambers can be seen in Figure III-2. The nerve chambers have been designed to fit the sliding carrier of the voltage-clamp apparatus that will be described in section III.3, and can therefore be inserted between the pole caps of the electromagnet that will be described in section III.2. The stimulation pulses are delivered to the preparation by a Grass stimulator (S8, Grass Instr.) through a Grass stimulus isolation unit (SIU5, Grass Instr.). The recording is made on a Tektronix R1503N dual-beam storage oscilloscope, with differential amplifier inputs. Oscilloscope traces are triggered by the stimulus pulse.

The voltage-clamp equipment has been designed to meet

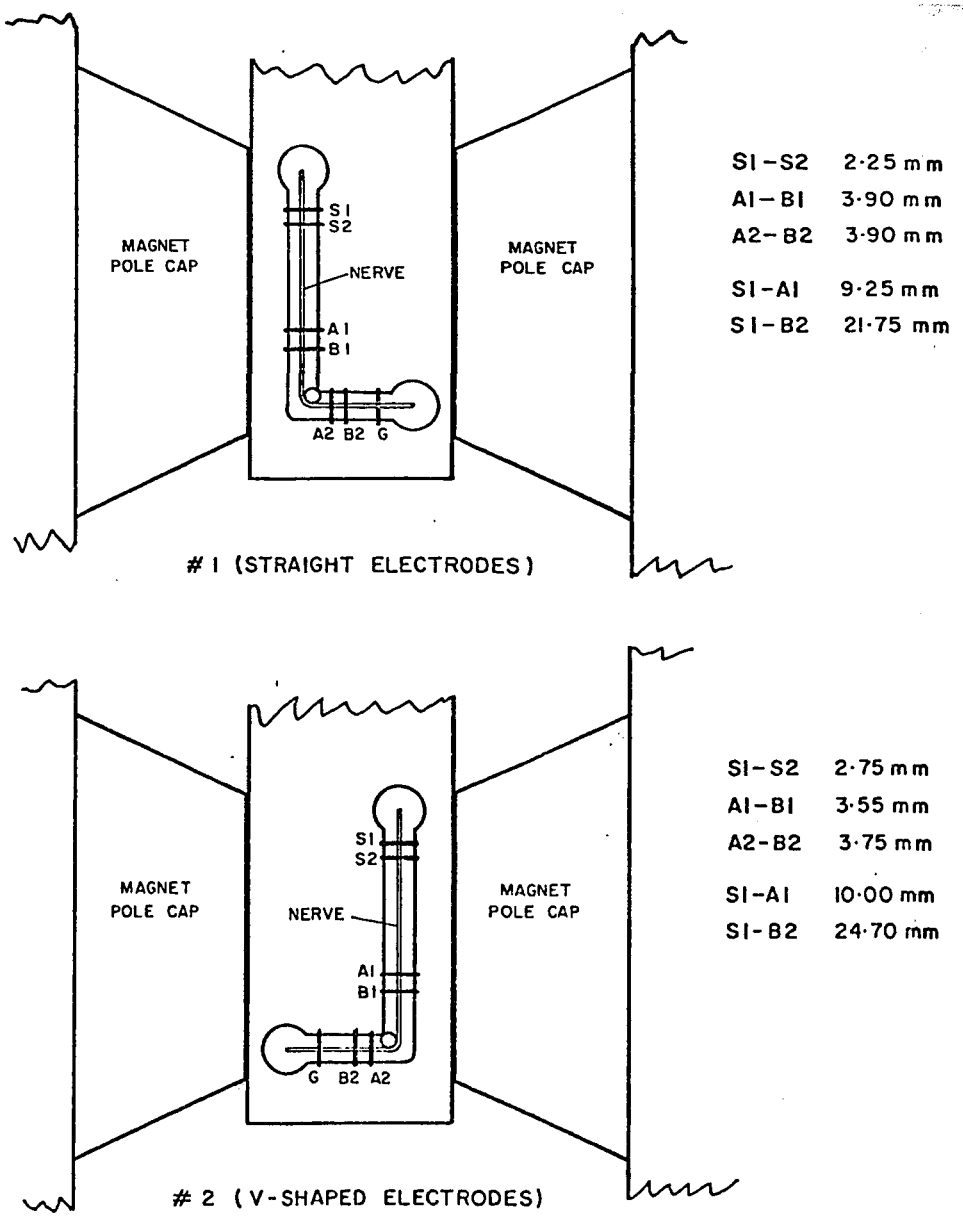

S1,S2 STIMULATION ELECTRODES
A1,B1 TRANSVERSAL RECORDING ELECTRODES
A2,B2 PARALLEL RECORDING ELECTRODES
G GROUND

Fig. III-1. Schematic diagram of velocity measurement nerve chambers

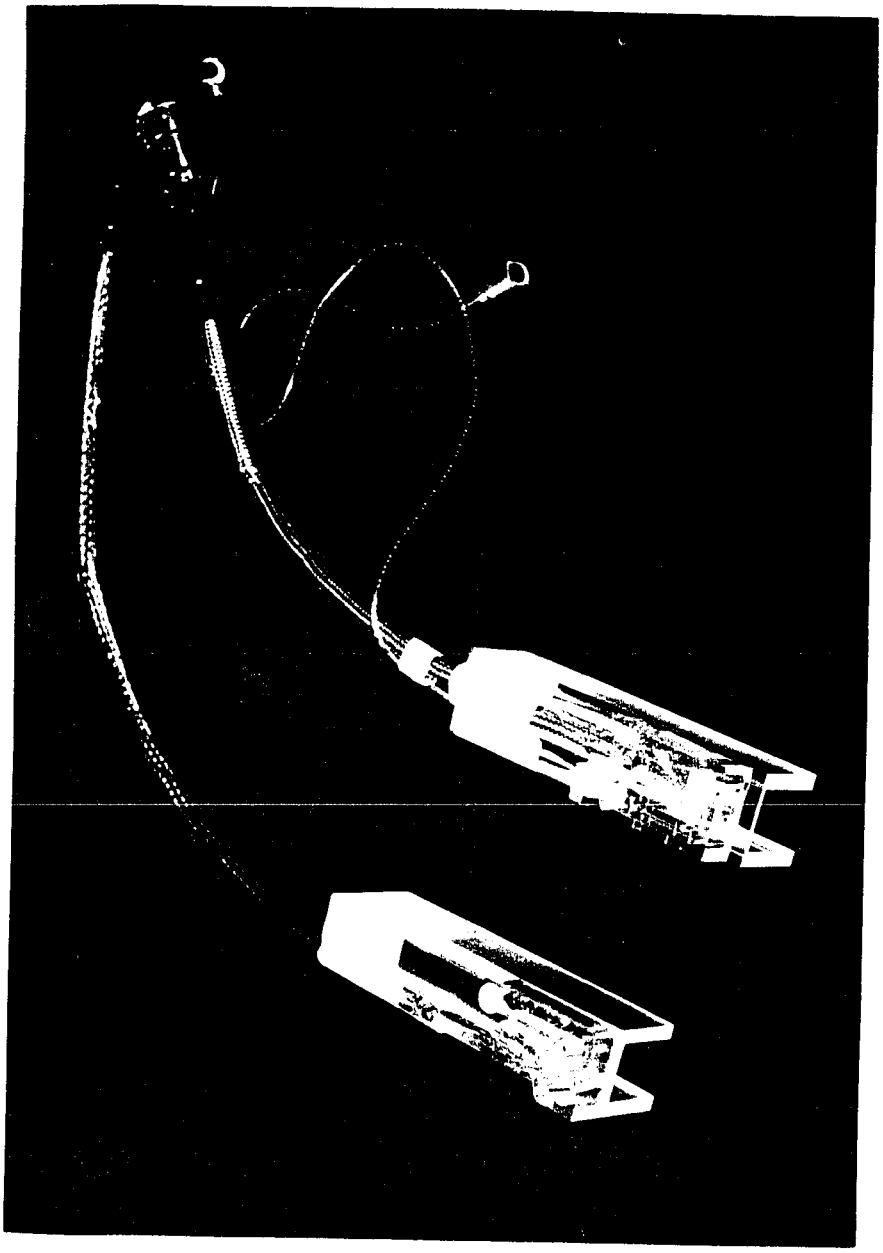

Fig. III-2. Velocity measurement nerve chambers

the strict requirements imposed by the choice of an appropriate methodology, as indicated at the end of Chapter I. The double sucrose gap method that has been selected in this work allows measurements of the currents and the voltages associated with an active patch of nervous membrane. These measurements are meaningless if the patch geometry, the temperature or the chemical composition of the perfusing solutions change in an uncontrolled manner. They are also of very little value if the signal-to-noise ratio is low, or in other words if intrinsic noise is present in the electronic recording and control system, and if extrinsic noise of mechanical or of line interference origin is picked up at the electrode level.

Difficult geometrical constraints were encountered at the design stage of the voltage-clamp experimental apparatus, due to the need to generate a high magnetic field in an air gap that would be reasonably wide enough to accommodate the sample holder and related equipment. Although the use of a permanent magnet arrangement (Dalman et al., 1957) had first been considered because of its simplicity (no power supply, little space occupancy) an available high quality electromagnet offering sufficient space between the magnetizing coils was finally selected together with a highly regulated power supply. This choice made the insertion of the nerve fibre into the experimental chamber difficult to perform, and it was therefore necessary to mount part of the experimental equipment, i.e. the nerve chamber, the electrodes, the preamplifiers and control amplifiers, the cooling system and the temperature and magnetic field measurement system , on a sliding carrier that could be inserted in the field area during the experiments.

The various pieces of equipment are placed in a shielded enclosure and on an instrument stand. In the enclosure, the electromagnet, the experimental chamber on its sliding carrier, the cooling system, most of the electronic circuitry and the bionocular microscope with a battery operated lamp are mounted on a heavy stainless steel anti-vibration base. The enclosure also contains a gaussmeter with its probe and the complete perfusion system. Beside the enclosure is the instrument stand where the various power supplies and signal generators are located, together with the thermoregulation system, the control panel and the recording instruments: oscilloscopes, strip-chart recorder and digital voltmeters.

The next two sections will be devoted to the detailed description of the magnetic field generation and measurement apparatus, and of the equipment used in connection with the voltage-clamp technique.

III.2 Magnetic field generation and measurement

A 4" -water cooled electromagnet (Newport Instrument) is placed in the shielded enclosure. It is equipped with specially designed pole pieces and provides a magnetic field of 1.2 Tesla in a 2 cm wide air gap. The magnet is energized by a d.c. regulated power supply (Sorensen SRL 60-8) with low drift and small ripple (0.3mV p-p). The power supply is kept outside the enclosure. Provision is made for reversing the current in the coils by means of a double pole-double throw switch arrangement mounted on the control panel of the instrument stand.

The amplitude of the magnetic field is measured by a Hall-effect probe connected to a battery-powered gaussmeter

(Bell Inc. 640) located in the enclosure. The readings are repeated by a digital voltmeter (Fluke 8000 A) on the instrument stand. The Hall-effect probe is attached to the sliding carrier that supports the nerve chamber and its related equipment in such a way that the magnetic field can be precisely measured at the exact location where the membrane patch is found when the experiment under magnetic field exposure is performed.

Performances of the magnet have been measured. When velocity measurements are made, the maximum field is 1.2 Tesla with an average gradient of 2 T/m along the part of the nerve parallel to the field, and 15 T/m along the part of the nerve perpendicular to the field. When voltage-clamp experiments are made, in the vicinity where the separation of the sucrose streams by the test solution (nodal area) occurs, the field gradient is less than 0.5 T/m to insure a high homogeneity around the critical experimental area. At 8 cm from the pole cap axis, the amplitude of the field is reduced by nine tenths of its value, and at 15 cm from the axis (at the edges of the magnetizing coils), the field is reduced to one fiftieth of its value.

Tap water circulated through an ice-box is used to cool the magnet. By proper flow adjustment, the temperature increase in the air gap after one hour of full power operation is less than $4^{\circ}C$. The temperature then remains constant.

III.3 Voltage-clamp apparatus

III.3.1 Sliding carrier and nerve chambers

Fig. III-3 represents two photographs of the overall system. The mechanical system basically consists of a fixed stainless steel plate mounted on four rubber low frequency vibration absorbers, that supports the electromagnet and the sliding

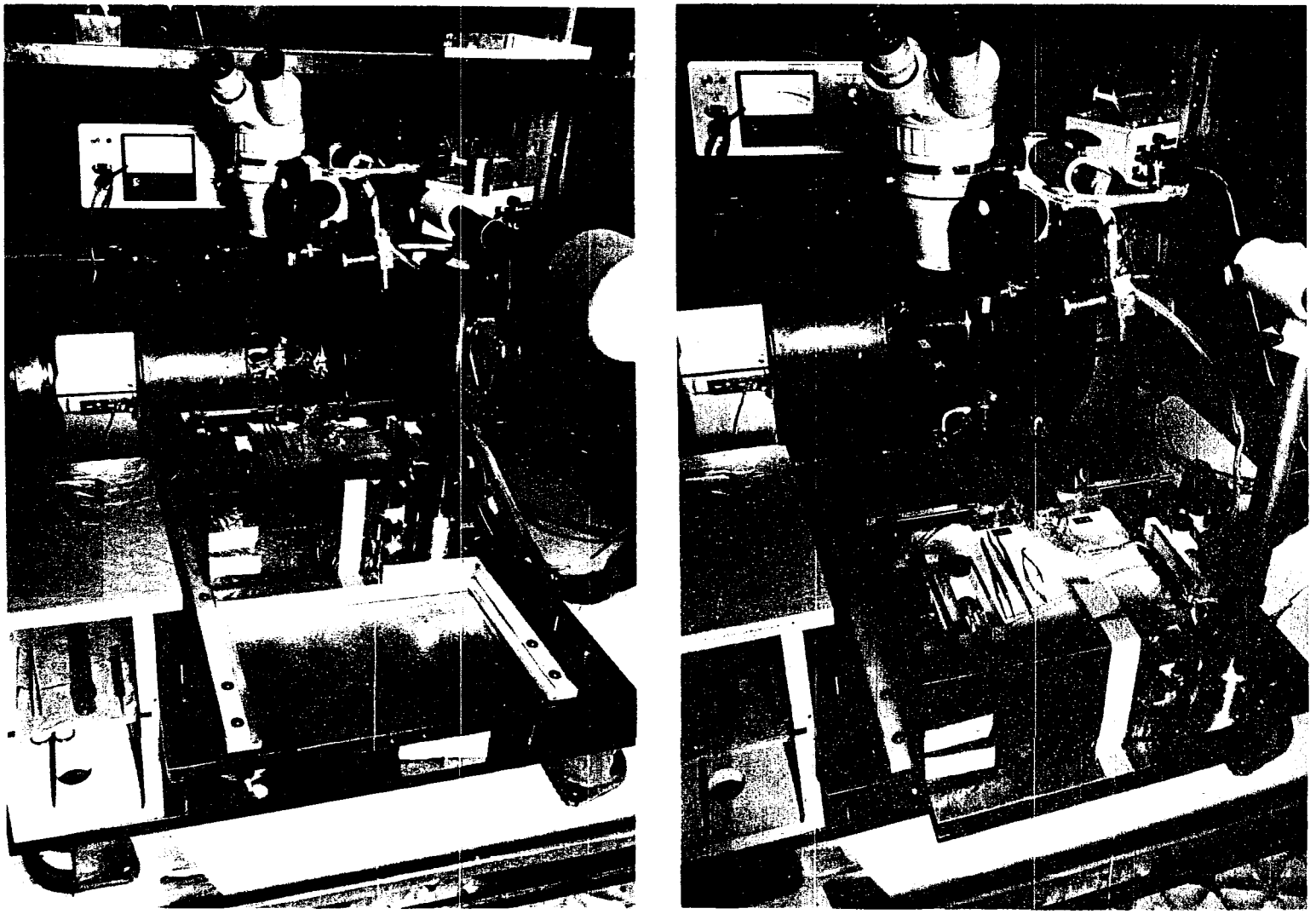

(a) (b)

Fig. III-3. Photographs of the sliding carrier and the parallel field exposure nerve chamber assembly. (a): inside the field area. (b) : outside the field area.

carrier assembly. The latter is composed of fixed nylon rails along which a mobile aluminum and brass carrier slides to facilitate insertion and removal of the nerve chamber in and out of the magnetic field area. This carrier also provides a platform for other parts of the apparatus such as the cooling system, the microscope assembly, the thermistor, the Hall-effect probe and part of the electronic equipment.

Two nerve chambers have been designed to fit the sliding carrier, one for parallel field exposure experiments and the other for perpendicular field exposure experiments. Switching from one to the other requires very little time. Both chambers are made from acrylic plastic, following the basic idea presented by Julian et al. (1962a). However this design differs from their original one due to the small space available between the magnetizing coils of the magnet, which is a little less than 12.5 cm.

As can be seen from Fig. III-4 and Fig. III-5 which are photographs of the parallel and the perpendicular field exposure chambers respectively, the main difference between the two is in the arrangement of the lateral pools. Another difference, which of course cannot be seen from the photographs, is the relative position of the nerve canal and the electromagnet pole axis. Fig. III-6 is a schematic diagram of the critical area where the double sucrose gap is located in the case of the parallel field exposure chamber. Fig. III-7 shows the same for the perpendicular exposure chamber. In both cases, the nerve canal is intersected at right angle in the horizontal plane by the main canal. The vertical sucrose inlets are located in the middle of each side of the nerve canal. A hole in the upstream part of the main canal is provided to receive a glass encapsulated thermistor element. Another hole, located downstream, is used to insert the current electrode. At the bottom of the lateral pools, outlets have

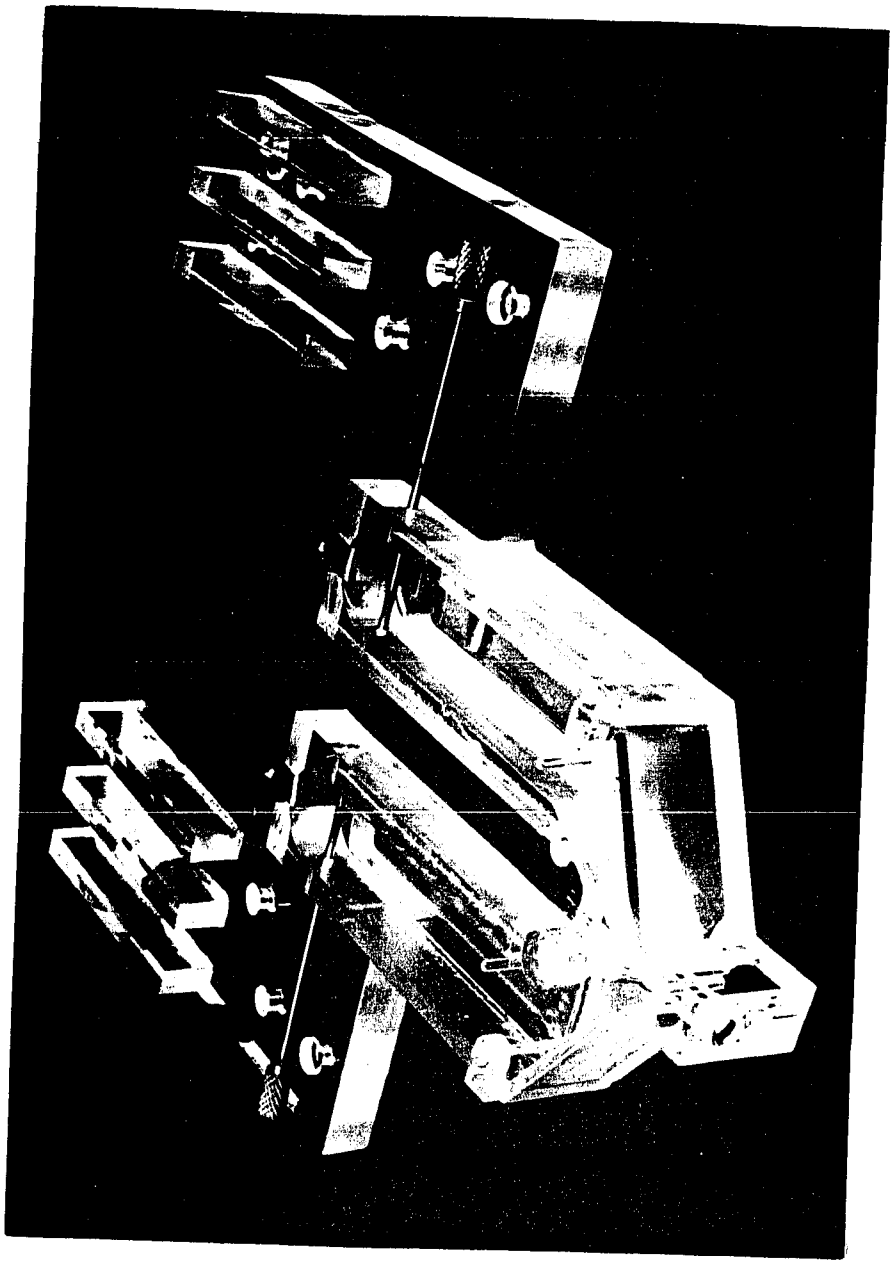

Fig. III-4. Photograph of the parallel field exposure nerve chamber

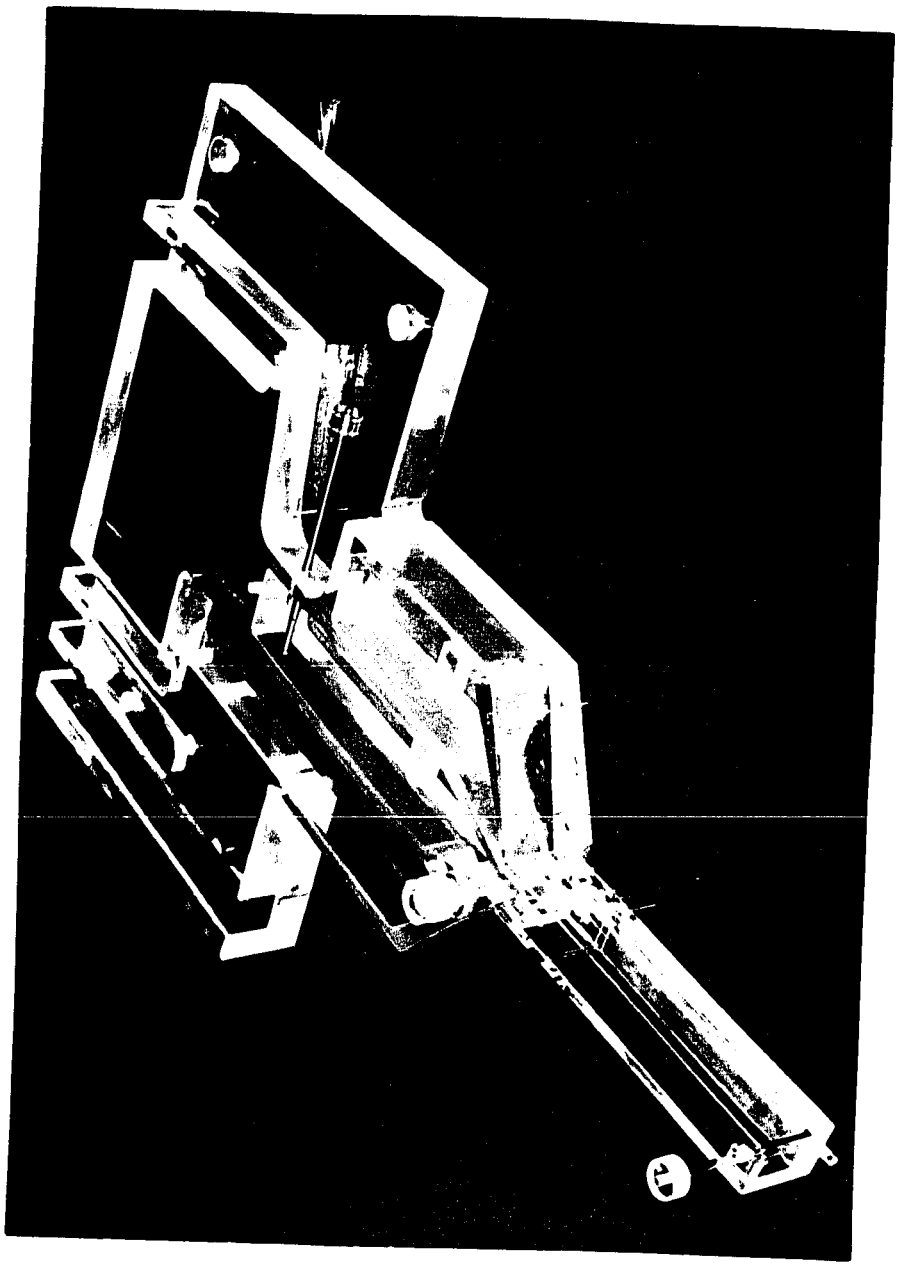

Fig. III-5. Photograph of the perpendicular field exposure nerve chamber

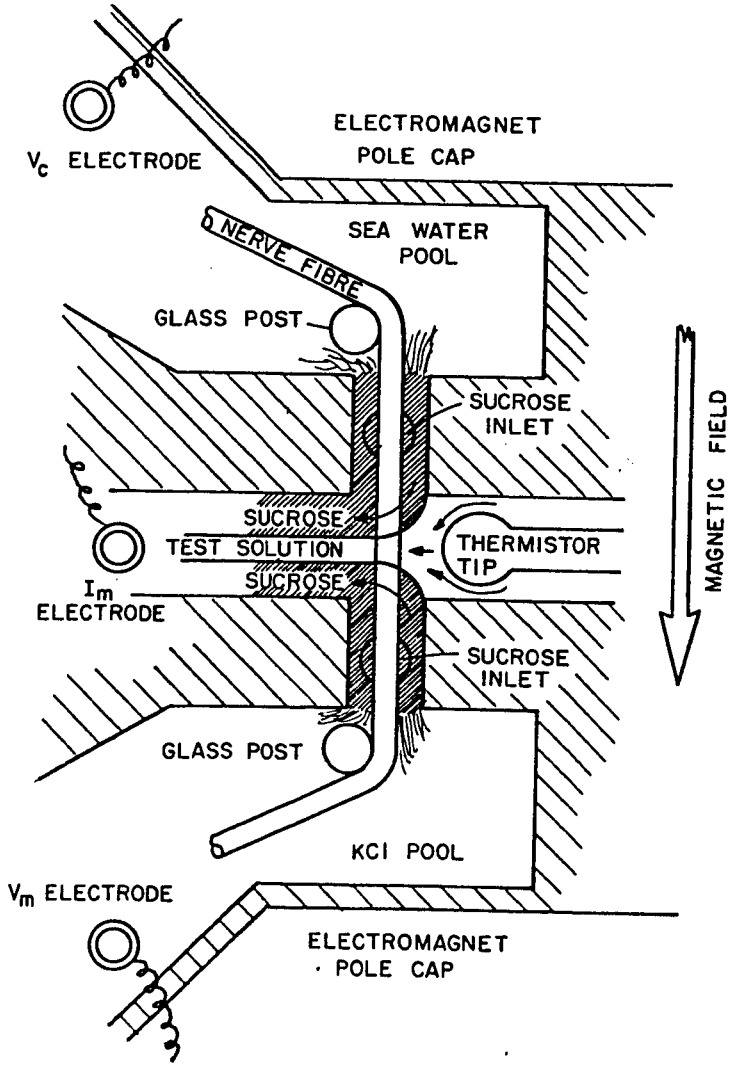

Fig. III-6. Schematic diagram of the critical area of the parallel field exposure nerve chamber (top view)

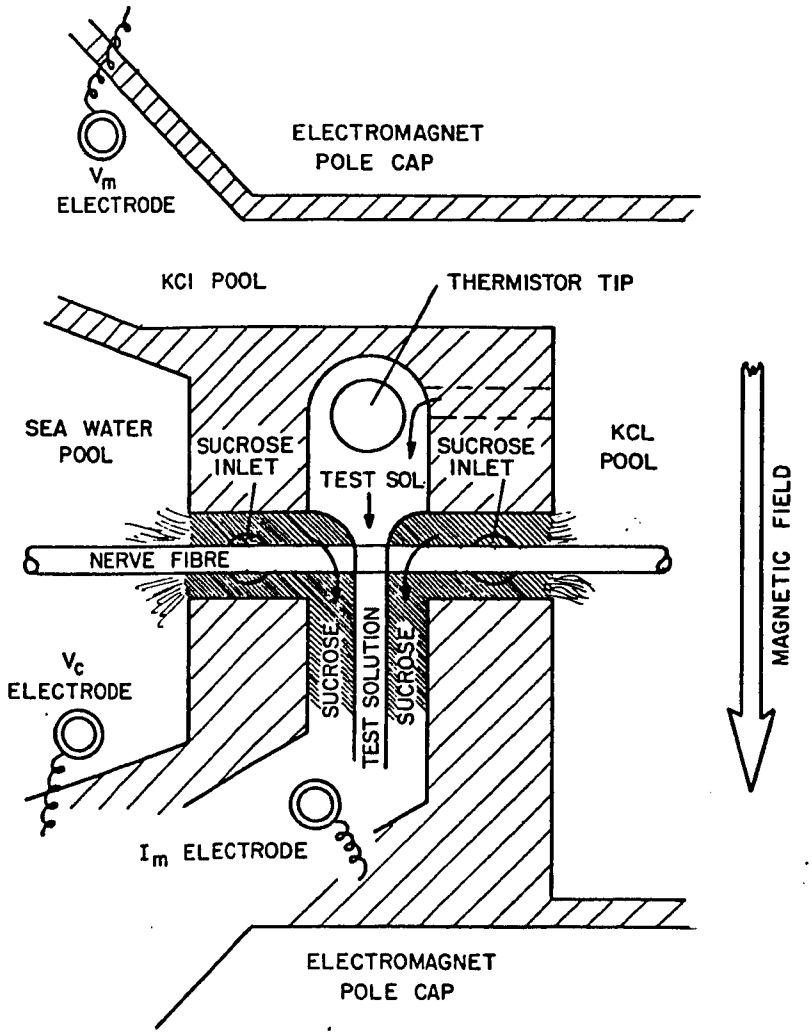

Fig. III-7. Schematic diagram of the critical area of the perpendicular field exposure nerve chamber (top view)

been drilled to provide connection to a siphoning system in order to prevent sucrose accumulation. Nylon threads (9-0) that are wound around stainless steel or plastic shafts attached to the lateral pools are used to pull the nerve fibre in place and to shift to another membrane patch after each experimental run, thus allowing several experiments on the same nerve fibre. In the case of the parallel field exposure chamber, the nerve fibre attached to the nylon threads is bent in a U-shape around two vertical glass posts that are located at both ends of the nerve canal.

Both nerve chambers have attachments for the two other electrodes (control and voltage). These also serve as a support for the mu-metal enclosure containing the preamplifier stages and for the three Teflon miniature needle valves (Manostat) that regulate the flow of the sucrose and test solutions. Provision has also been made for the installation of a three-way Teflon distributing valve (Hamilton) to permit fast switching of test solutions.

The microscope assembly is attached to the sliding carrier by means of a brass stand. It is composed of a binocular microscope (Olympus SZ stereozoom) and a battery operated illumination system. It permits continuous observation under low magnification (x 7.5 to x 30) of the nodal area where the active membrane patch is located, during insertion of the nerve fibre and magnetic exposure.

All electrical and hydraulic connections between the nerve chamber-mobile carrier system and the rest of the equipment are made of flexible electrical leads and Tygon transparent tubing.

III.3.2 Perfusion and thermoregulation systems

The nerve chambers are perfused by gravity. The solutions (composition is given in appendices A.1 and A.2) are contained in

perfusion bottles similar to those that are used for intravenous perfusion. The use of this kind of bottle permits the establishment of a constant pressure head of approximately 80 cm between them and the experimental chamber. The pressure head of approximately 30 cm between the chamber and the discharge tray can be adjusted more precisely by means of a rack-and-pinion assembly that modifies the vertical position of the outlet tube opening. This adjustment and the flow rate adjustments obtained with the help of three Manostat needle valves, one for the test solution and two for the sucrose, are used to set the width and the shape of the nodal area in the main canal where the two sucrose streams are separated by the test solution stream. By proper adjustment, it is also possible to have the sucrose flowing slowly in the lateral pools, thus ensuring good electrical insulation between them and the main canal. Due to the different refraction indexes of the sucrose and the test solution, the nodal area is visible under microscope observation and can be set exactly, measured and checked for stability at periodic intervals during an experiment (Fig. III-8).

Before entering the nerve chamber, the perfusion solutions are passed through a cooling block that is sandwiched between a thermoelectric junction assembly (Cambion 806-1000-01) and a copper block in which ice-cold water is circulated by means of a low noise pump. The thermojunction assembly is part of the thermoregulation system. (A detailed circuit diagram is given in appendix A.8). It consists basically of a sensing and measuring stage, a differential stage and a power stage that drives the thermo-electric junction assembly. The loop is then closed by means of the perfusion solutions to be temperature regulated.

The temperature of the test solution is measured close to the membrane patch by means of a miniature thermistor (Fenwall GP31P2)

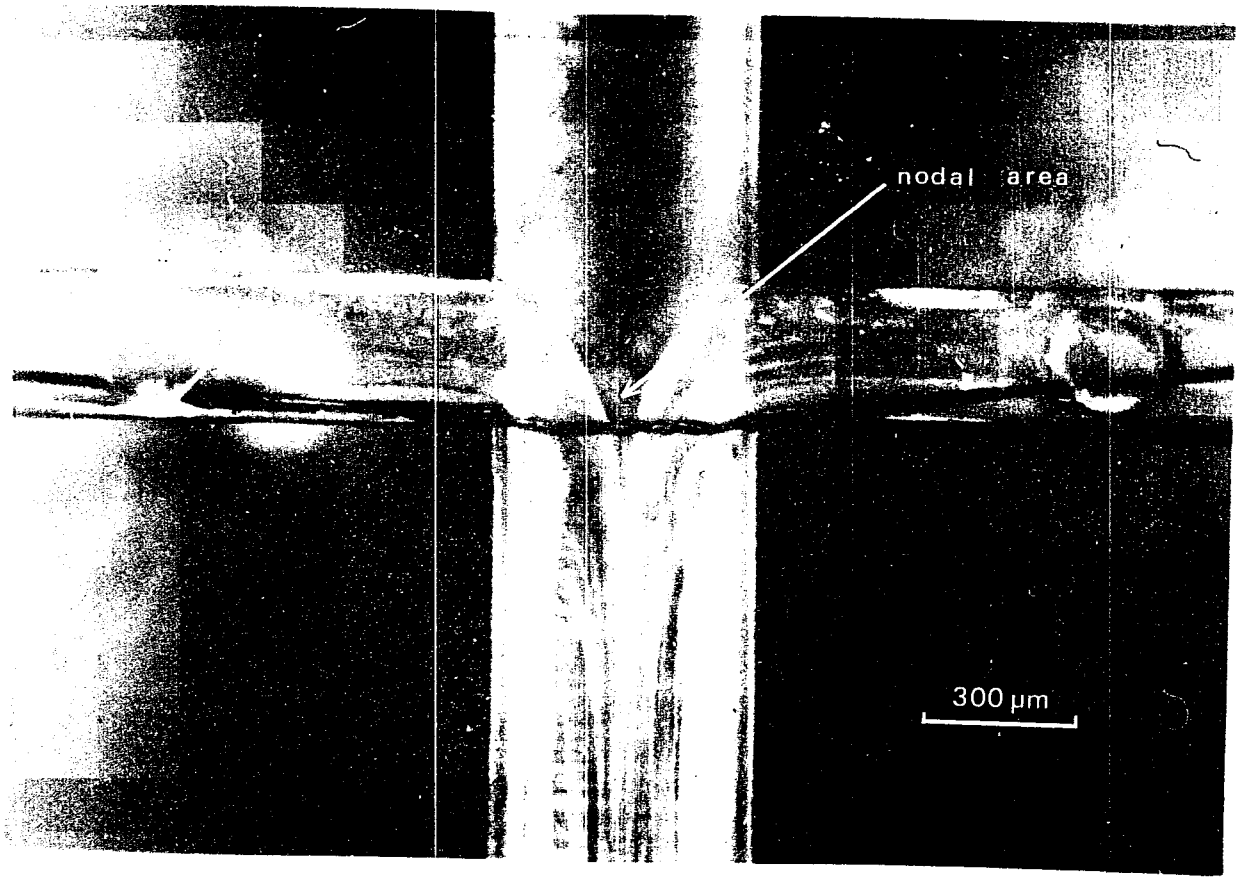

Fig. III-8. Photograph of the double sucrose gap. A black thread is located where the nerve fibre is found under experimental conditions

that sends a signal to the sensing and measuring stage. The output of this stage is compared to the desired temperature, as set by a ten-turn potentiometer, in the differential stage. Any excursion from the set-point activates the power stage which will provide a current with the appropriate polarity to the thermojunction that heats or cools the perfusion liquids until the control point is attained.

This control system, although not very sophisticated, displays a good stability ($\pm 0.1^{\circ}C$) over several hours of continuous operation, provided that the solution flow has been stabilized five minutes before the beginning of the actual experiments.

III.3.3 Electrodes

The double sucrose gap voltage-clamp technique requires only external electrodes that are immersed in the three pools of the nerve chamber: the voltage electrode in the KCl lateral pool, the control electrode in the artificial sea water lateral pool and the current electrode in the test solution flowing in the main canal. Silver-silver chloride electrodes in KCl saturated agar bridges are used in this apparatus. They are prepared as described in Appendix A.3. Their d.c. resistance is about 300Ω and their 1kHz impedance is about 500Ω. The potential difference between any two electrodes, as measured in saline solution, is of the order of 100 μV. If higher values are recorded, it is usually a sign of irregular plating or contamination, and the electrodes are discarded.

The electrode leads are connected to the preamplifier stage and the output of the control amplifier by means of miniature gold-plated connectors.

III.3.4 The electronic measurement and control system: simplified theory of operation

This system is represented in a simplified form in Fig. III-9. It consists essentially of a current measuring device, a voltage measuring device and a control device that keeps the membrane voltage at an assigned value, as chosen by the operator.

A simplified theory of operation and the main results that are derived from it are presented in the following paragraphs. A more detailed treatment is given in Appendix A.7.

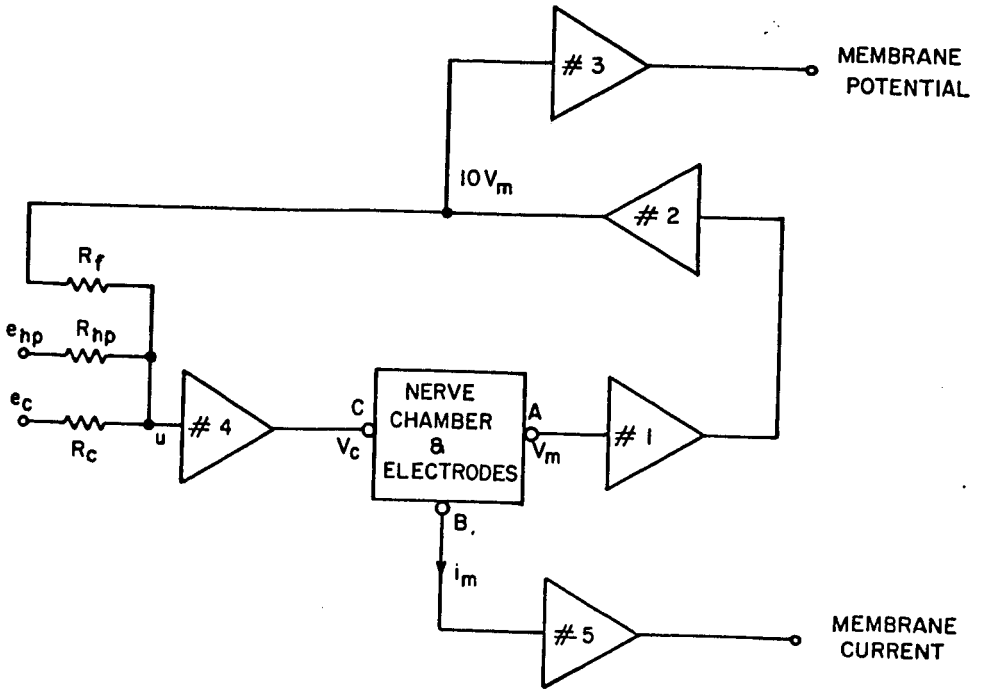

Fig. III-9. Simplified diagram of the measurement and control system (explanations are given in the text)

III.3.4.1 The membrane analogue circuit in the double sucrose gap arrangement.

The Hodgkin-Huxley membrane model, as represented in Fig. II-1 (Chap. II, section II.2.2.2) can be reduced to a two branch model by means of Millman's and Thevenin's theorems. In this model, g_m and E_r are both time and voltage dependent. Fig. III-10 represents the nerve fibre membrane in the double sucrose gap arrangement. The left part represents the control voltage pool. It usually contains artificial sea water. The central part is the so-called nodal area where the gap is located. The right part is the membrane voltage area. It contains potassium chloride which depolarizes the membrane in such a way that the inside and the outside potentials are approximately equal. In other words, KCl plays the role of an electrical short-circuit. These three areas are separated by the outside insulating sucrose solutions. Of course, there exists a conducting path inside the axon, the axoplasm having a relatively low longitudinal resistance.

Referring to Fig. III-10, the following notations are used:

R_{suc} = sucrose longitudinal resistance

R_{ax} = axoplasm longitudinal resistance

R_{asw} = series test solution resistance

A, B and C are the membrane voltage, the current and the control voltage electrode locations respectively

E_r and g_m are the membrane patch e.m.f. and conductance

Assuming that the nodal area has a width of 100 μm and that the axon diameter is 100 μm , it can be shown that, with the physical dimensions of the sucrose gap arrangement being

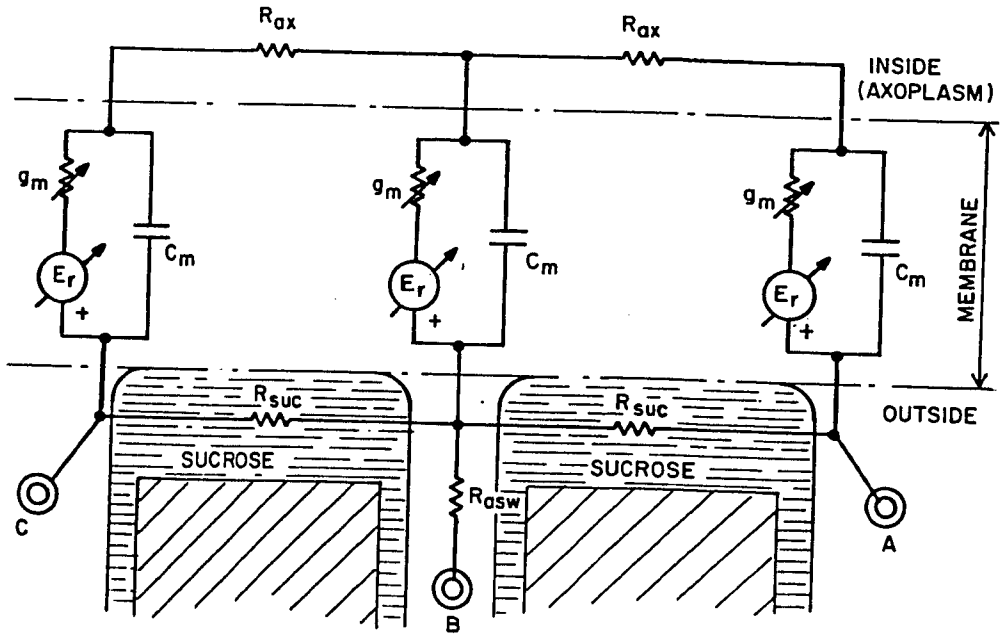

Fig. III-10. Nerve membrane in the double sucrose gap arrangement

2 mm for the sucrose length and 300 μm for the nerve canal diameter, and with typical electrical data for the lobster fibre(*) (Katz, 1966), the following values can be assigned to the components of the model: R_{suc} = 100 MΩ (minimum); R_{ax} = 150 kΩ; R_{asw} = 2 kΩ (maximum); E_r = 100 mV (in the resting state) and g_m = 1 μS (in the resting state). Taking these values into account and assuming that the voltage electrometer preamplifier draws a negligible current from the membrane, the nerve fibre in its sucrose arrangement therefore can, for analytical purposes, be replaced by the simple T-network of Fig. III-11. This is in fact the membrane analogue that is represented by the box labelled "nerve chamber and electrodes" in Fig. III-9. From this analysis is also derived the passive membrane model. The circuit diagram of this model is given in Appendix A.9.

III.3.4.2 Control amplifier equation.

The equation that governs the operation of the control amplifier is given in this section. The complete analysis can be found in Appendix A.7.

The following assumptions will be made (see Fig. III-9):

(i) amplifier No 1 has a very high input impedance and draws therefore a negligible current. Its gain is set at 1.

(ii) amplifier No 2 (gain of 10) and amplifier No 3 (gain of 2.5) are operational amplifiers. Their gains are constant over the frequency range concerned.

(*) membrane resistance : 2000 Ω - cm^2
membrane capacitance: 1 μF/cm^2
axoplasm resistivity : 60 Ω - cm

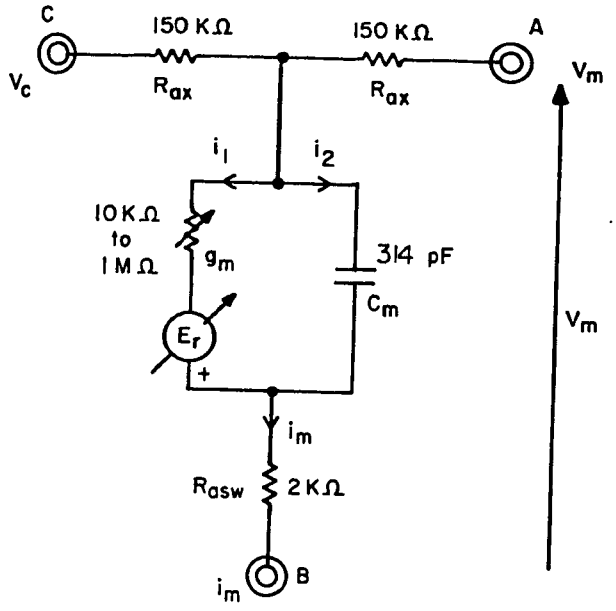

Fig. III-11. Equivalent T-network membrane model in double sucrose gap arrangement

(iii) amplifier No 5 is connected in a current-to-voltage configuration. The input terminal B is therefore at virtual ground.

(iv) the voltage drop across the series resistance R_{asw} is negligible. This assumption in fact introduces a systematic error that can be eliminated in the actual system by substracting electronically from the measured membrane potential a voltage that is proportional to the membrane current (Poindessault et al., 1976).

Using the symbols indicated on Fig. III-9 and Fig. III-11, the control amplifier equation is as follows:

$$\left\{\frac{10}{R_f} + \frac{1}{A_4}\left(\frac{1}{R_f} + \frac{1}{R_c} + \frac{1}{R_{hp}}\right)\left(1 + R_{ax}g_m + sR_{ax}C_m\right)\right\} v_m + \frac{1}{A_4} R_{ax}g_m \left(\frac{1}{R_f} + \frac{1}{R_c} + \frac{1}{R_{hp}}\right) E_r + \frac{e_c}{R_c} + \frac{e_{hp}}{R_{hp}} = 0 \qquad \text{(Equ. 1)}$$

where A_4 is the open-loop gain of amplifier No 4. It should be noted that the $sR_{ax}C_m$ term vanishes as soon as the transient due to the capacitive current in C_m ends.

III.3.4.3 Resting state operation.

When the membrane is at rest, it displays the resting potential E_r^o. The command potential e_c being equal to zero in this case, and assuming that the gain A_4 is large enough, equation (1) simply reduces to :

$$\frac{10}{R_f} E_r^o + \frac{e_{hp}}{R_{hp}} = 0 \qquad \text{(Equ. 2)}$$

This equation shows that a constant d.c. offset voltage must be applied between command pulses at the summing point of the control amplifier.

III.3.4.4 Active state operation .

In the active state, the instantaneous membrane voltage v_m can be expressed as :

$$v_m = E_r^o + \Delta v_m \qquad \text{(Equ. 3)}$$

Substituting in equation (1), taking in account the resting state equation (2) and using typical values for the different components of the circuit, it can be shown that the control amplifier equation becomes :

$$\left\{\frac{10}{R_f} + \frac{1}{A_4}\left(\frac{1}{R_f} + \frac{1}{R_c} + \frac{1}{R_{hp}}\right)(1 + R_{ax}g_m)\right\}\Delta v_m + \frac{e_c}{R_c} = 0 \qquad \text{(Equ. 4)}$$

Choosing R_f = 100 kΩ, $R_c = R_{hp}$ = 500 kΩ, assuming R_{ax} = 150 kΩ and further assuming that we are in the worst case, i.e. that r_m takes its minimum value of about 1 kΩ, a 1% control will be realized if A_4 is greater than 2000, using equation (4). Therefore, if a value of 10 000 or more is taken for the open-loop gain of amplifier No 4, a tight control of v_m will be achieved.

If the requirements of a high gain control amplifier with high value resistors connected to its summing junction are met, and assuming that the resting potential is exactly balanced by means of the holding potential, equation (1) reduces to the following approximate equation that is valid for low frequency operation:

$$\frac{10}{R_f}\Delta v_m + \frac{e_c}{R_c} \simeq 0 \qquad \text{(Equ. 5)}$$

III.3.4.5 Dynamic operation and stability considerations .

The instrumentation system must be able to bring the membrane to its clamp voltage well before the fast sodium current starts in order to maintain the membrane voltage at the assigned value in a very stable manner despite the large variations in current

amplitudes and their sign reversal, and to allow a true and fast recording of the current changes versus time.

A low noise wideband operational amplifier, used as a current-to-voltage converter is used to record the transmembrane current. An output of 1 V corresponds to an input of 1 μA. Its step response must have a time constant not exceeding 10 μs and at least 2 V/μs slew rate is required.

A good dynamic performance of the control system is rendered difficult by the fact that the membrane constitutes an active load that is connected in the feedback branch of the control amplifier. The overall speed is limited by the membrane electrical characteristics, which are those of a low-pass filter with a cut-off frequency of about 20 kHz . In order to efficiently clamp the membrane to the assigned values, it is necessary that the time required to drive the membrane from one value to another be less than 50 μs. Drift has to be kept as low as possible (less than 1 mV in several hours). A chopper stabilized amplifier is used for the control amplifier. This amplifier must have an output current capability allowing it to maintain the membrane potential at the required value and to provide the membrane with the current necessary to bring its voltage back to the assigned value when large current surges occur in the membrane. In addition noise figures must be kept at a low level (a few μV).

Stability is another important condition to be satisfied in this system. It is evident that the membrane potential should not be allowed to oscillate at high frequency. On the other hand, overdamping of the control system would result in an inefficient clamp of the membrane. A correcting network

is therefore inserted in the control circuit, in addition to the usual compensating networks that are found on each individual amplifier for stability purposes. By adjusting its variable capacitors, it is possible to improve the rise time of the response without falling into instability. In particular, it is possible to compensate for the relatively heavy capacitive load of the control amplifier. The closed loop step response of the control system can typically be adjusted to be slightly under-damped with a 5% overshoot and a rise time of less than 50 μs.

III.3.5 The electronic measurement and control system: Description of the actual measuring and control system

Fig. III-12 represents the functional block-diagram of the measuring and control system implemented to study the biomagnetic response of the lobster nerve fibre.

The detailed circuit diagrams are given in Appendix A.4.

The numbers in the following paragraphs refer to the blocks of Fig. III-12.

a) Clock (block No 1). It consists simply of an integrated circuit timer (Signetics 555) used as an astable multivibrator with a suitable frequency determined by an external R-C network.
It is used to pretrigger the pulse generator of block No 2 and the Kymograph camera control circuit (block No 13).

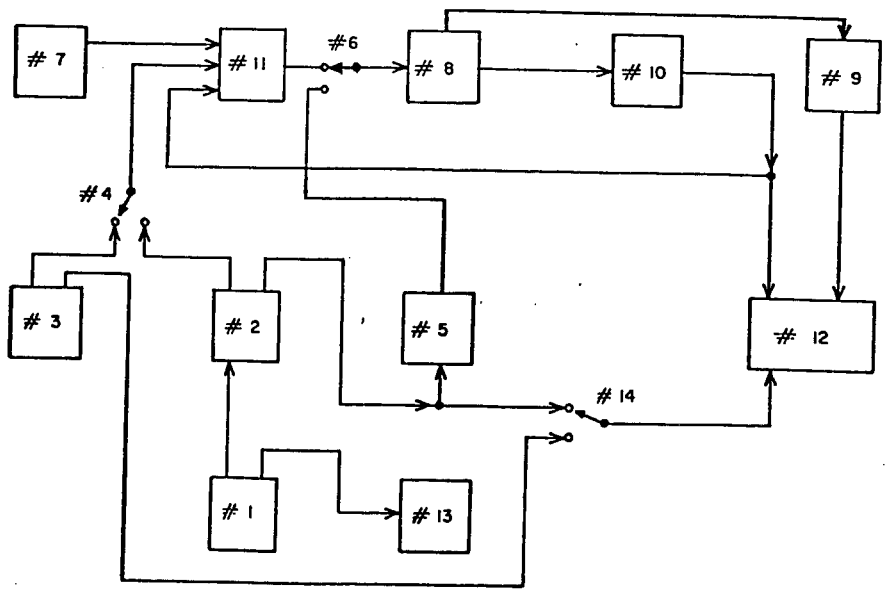

1. CLOCK
2. COMMAND SIGNAL GENERATION (MANUAL MODE)
3. COMMAND SIGNAL GENERATION (AUTOMATIC MODE)
4. AUTOMATIC / MANUAL MODE SWITCH
5. STIMULATION UNIT
6. STIMULATION / VOLTAGE-CLAMP MODE SWITCH
7. HOLDING POTENTIAL UNIT
8. NERVE CHAMBER AND ELECTRODES
9. CURRENT-TO-VOLTAGE CONVERTER
10. VOLTAGE PREAMPLIFIER AND BUFFER AMPLIFIER
11. CONTROL AMPLIFIER AND TIGHTENING NETWORK
12. RECORDING AND DISPLAY APPARATUS
13. KYMOGRAPH CONTROL UNIT AND CAMERA
14. AUTOMATIC / MANUAL SYNCHRONIZATION SWITCH

Fig. III-12. Measuring and control system block-diagram

b) Command signal generation for manual operation (block No 2).

It consists of two units: a pulse generator and a rotating switch to set the command pulse levels.

The pulse generator (Tektronix 2101) provides positive and negative pulses of 10 V amplitude and variable duration. The maximum pulse period being 400 ms, which is too fast for manual operation, it is set by the external triggering circuit described as block No 1 before. Time intervals up to 2 s can be chosen between command pulses. The output of the pulse generator is delayed in order to provide sufficient time for the Kymograph camera film to move to the next frame between successive stimulus or voltage-clamp pulses. It is also used as a synchronizing signal for the rest of the equipment in the manual mode of operation.

The 4 pole-24 position rotating switch serves a double purpose. It sets the depolarizing and hyperpolarizing command pulse levels, acting as a step potentiometer for the pulses from the pulse generator. Suitable resistance values have been chosen in order to obtain a sequence of command pulses that scans the whole range of membrane potentials, as used in typical clamp experiments. The same switch is part of the transistor circuit that activates two pilot lights (light emitting diodes) in such a way that the red one is on with any depolarizing pulse, while the green one goes on with hyperpolarizing pulses only. This sytem permits identification of the type of signal being

applied to the nerve, and allows switching from one value to another between pulses, thus avoiding transients which affect the biological specimen adversely.

c) Command signal generation for automatic operation (block No 3).

In order to make the voltage-clamp procedure faster, an automatic sequence generator has been designed (see Appendix A.5) and is inserted in the overall system, together with the Mode switch (No 4) and the synchronization switch (No 14).

d) Stimulation unit (block No 5).

Stimulation (or current clamp) of the membrane is achieved by means of another pulse generator (Tektronix 2101) used to generate the command pulses in the manual mode. The STIM-VOLTCLAMP switch(No 6) is simply switched to the STIM position, thus connecting the pulses from this pulse generator to the command electrode of the biological sample through a 10 MΩ resistor. Repetition rate and pulse duration are independently set on the pulse generator itself. One shot stimulation is also possible.

e) Holding potential unit (block No 7).

The d.c. voltage that is used to hold the potential of the membrane at its resting value or at a small hyperpolarization value between command pulses to prevent Na inactivation (Hodgkin et al., 1952b) is simply taken from the regulated power supply (Powertec 2K15D-1.3) through a ten-turn potentiometer and connected to the holding potential input of the control amplifier.

f) Current-to-voltage converter (block No 9).

The current amplifier (Analog Devices 506L) is connected in the current-to-voltage converter configuration, with a 1 MΩ resistor in parallel with 10 pF as feedback impedance. It provides an output voltage equal to $-10^6 I_m$, where I_m is the membrane current collected by the current silver-silver chloride electrode (nerve chamber No 8) connected to the inverting input of the operational amplifier by a short stiff wire to reduce input capacitance. A current offset nulling network is also connected to the same input of the amplifier. This amplifier displays a good frequency response (100 kHz full power response) and a sufficient slew rate (3 to 6 V/μs) that allows a reliable recording of the fast current variations.

g) Voltage preamplifier and buffer amplifier (block No 10).

The membrane voltage is obtained from the membrane potential silver-silver chloride electrode connected by a short stiff wire to the non-inverting input of an electrometer amplifier (Analog Devices 523L) in a cathode follower configuration. This is an integrated circuit J-FET operational amplifier with less than 0.25 pA bias current and a very high input impedance (10^{12} Ω differential). The noise figure is very low (15 μV rms) and the drift is negligible. In order to minimize stray capacitance effects, the input is guarded by a guard ring connected to the inverting input. The output of the electrometer amplifier is then connected to the non-inverting input of the buffer amplifier (National Semiconductors LH 0022CD) which is a low drift, FET-input, high accuracy operational amplifier in a non-inverting configuration with a gain of 10.

h) Control amplifier and tightening network (block No 11).

This circuit is represented in Fig. III-13. It consists basically of a summing network connected to the non-inverting input of the control amplifier (Analog Devices 231K), a capacitive minor loop for stability, and a tightening network that has two functions: it permits progressive application of the clamping voltage to the membrane and it sets the amplifier to a fixed low gain when it is not in use, in other words when the membrane is not voltage-clamped.

Relatively high value resistors have been chosen for the summing network as a compromise between acceptable noise level and high input resistance for the amplifier. The inputs are: 10 V_m (the membrane potential) connected to a high frequency accentuation network (100 kΩ, in parallel with 1 kΩ in series with a variable capacitor); the holding potential connected to a 500 kΩ resistor; the hyperpolarizing command pulse connected to a 500 kΩ resistor; the depolarizing command pulse connected to a 500 kΩ resistor(*); a 100 kΩ resistor that is normally connected to ground in the voltage-clamp mode, while it is part of the feedback loop that fixes the gain of the amplifier when the tightening network is open; and a 200 kΩ resistor that can be used to add a supplementary signal, such as a sine wave for instance. All resistors are high quality metal film 1% resistors.

(*) The command pulses have distinct input resistors because it has been found in certain instances that a small capacitor was required in parallel with the hyperpolarizing command input resistor in order to improve the frequency response.

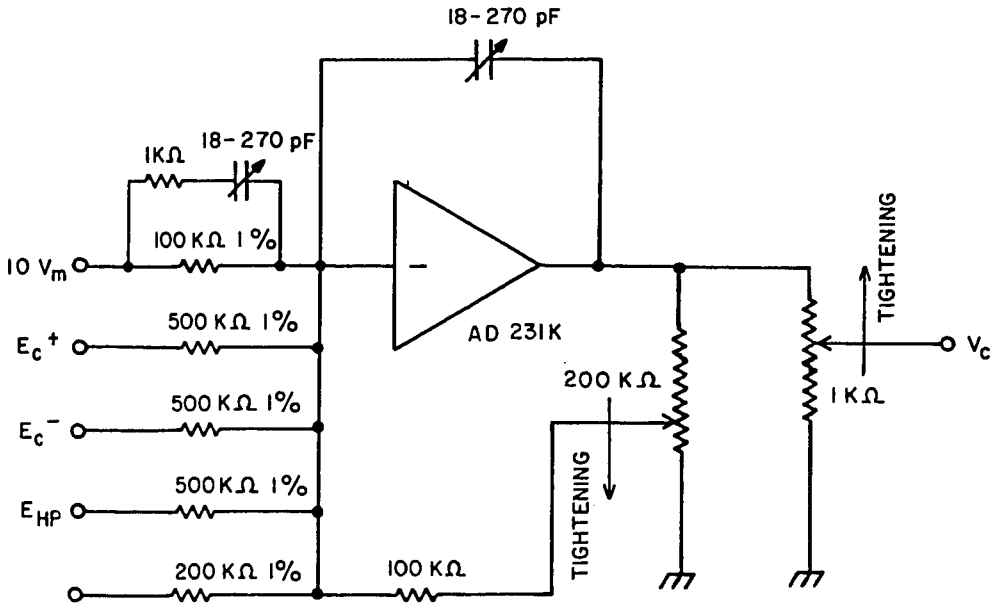

Fig. III-13. Control amplifier and tightening network

The AD 231K amplifier is a chopper stabilized operational amplifier with a built-in MOSFET chopper circuit. The drift is negligible, the offset voltage and current staying within 5 μV and 5 pA over a 120 day period. The open loop low frequency gain is 150 dB. The frequency response at full power is 3 kHz minimum. The rated output current is 25 mA. The noise figure is also very low (less than 5 μV rms). This amplifier offers the double advantage of having a small size and no alternating current supply requirement for the chopper circuit. It can therefore be located close to the nerve chamber inside the shielded enclosure.

The tightening network is a double potentiometer whose sliders move in opposite directions. In the voltage-clamp mode the slider of the 1 kΩ potentiometer is high, thus the output of the amplifier is directly connected to the control silver-silver chloride electrode, while at the same time the slider of the 200 kΩ potentiometer is low, thus connecting the corresponding input resistor to ground. When the clamp is removed (stimulation mode), the situation is reversed and the amplifier gain is fixed to a low value by the feedback network constituted by the 200 kΩ resistance of the potentiometer in series with the 100 kΩ resistor.

The capacitive minor loop, which simply consists of a variable capacitor (18 to 270 pF) connected between the output and the non-inverting input (summing point) of the control amplifier, provides, in conjunction with the high frequency accentuation network described above, stability and good frequency response for the control amplifier.

i) Power supplies, shielding and grounding. It has been mentioned in section III. 1 that the preamplifiers and the control amplifier are located in a shielded enclosure into which no a. c. line is permitted to enter. The d. c. power supplies (Powertec 2K15D-1.3 for the linear electronics, Standard Power Supplies + 5 V for the digital electronics) are therefore mounted on the instrument stand and capacitive filters are connected across the supply terminals of each amplifier. The supply lines that run from the instrument stand to the enclosure are double-shielded, as are the signal leads between the nerve chamber electrodes and the control panel on the instrument stand.

The shielded enclosure, the shields around the leads, the large metallic equipment bodies, namely the magnet, the supporting base, the sliding carrier, the microscope, and the instruments of the stand are all connected in a tree-like configuration to avoid ground loops, to a single grounding point that is attached by a heavy copper strap to a waterpipe of the laboratory.

III.3.6 Recording and display apparatus

The membrane currents and voltages are displayed on a dual-beam storage oscilloscope (Tektronix R 5103N) on which a Polaroid camera (Tektronix C5 camera) can be mounted for permanent records of the traces. A Kymograph camera (Grass Medical Instruments, C4N camera) is mounted in front of a slave dual-beam oscilloscope (Tektronix 561 B) that records on Kodak 2495 RAR film either the voltage or the current on the upper trace and a coded signal from an auxiliary signal generator (IEC F-34 Function generator) on the

lower trace. The resting membrane potential, or the holding potential in the voltage-clamp mode, is continuously recorded on chart paper by one pen of a dual-pen strip-chart recorder (Honeywell Electronik 196), the other pen being used to record the temperature sensed near the nodal area in the nerve chamber.

An I vs V processor has also been designed (see Appendix A.6) to permit the direct display of the voltage vs current graphs on the screen of a dual-beam storage oscilloscope (Tektronix 564 RM) used in the X-Y mode with proper intensity modulation.

III.4 Equipment tests and calibrations

The magnetic field is calibrated against a permanent magnet standard (Hirst Electronic Industries, UK., 998 $\pm$7Gauss). A calibration graph of the magnet is established by plotting the magnetic field versus the supply voltage. This graph shows good linearity over the entire range of use (0 - 1.2 Tesla) and permits the exact determination of the reverse polarity voltage to be applied in order to cancel the remanent field.

The electronic voltage-clamp equipment is checked at regular intervals for calibration and linearity by means of calibrated pulses applied at the command potential input of the control amplifier to a T-network passive membrane model (see appendix A.9). The dynamic behaviour of the measurement and control apparatus is tested using a modified version of the Neurofet active membrane model (Roy, 1972) that displays the features of an actual excitable nervous membrane, the circuit of which is also given in Appendix A.9. The tests are performed under magnetic exposure ranging from 0 to 1.2 Tesla and no electronic artifacts are detected. There is also no evidence of response transients when the field is switched on or off.

Sucrose insulation between the lateral pools and the main canal of the nerve chambers is measured by passing a 1.7 nA calibrated current from one lateral electrode to the central electrode and recording the corresponding voltage drop by means of the voltage measurement circuit.

The thermoregulation system is calibrated by comparison with copper-constantan thermocouple readings.

III.5 Experimental procedure

III.5.1 Double sucrose gap experiments

The following steps are taken routinely:

a) all electronic equipment and instruments are switched on to warm up and stabilize. The ice-box is filled with crushed ice. Circulating water flow is checked for proper cooling of the electromagnet and the thermoelectric assembly.

b) the pH value of the test solution is adjusted (Fisher Accumet 210 pH-meter) to be between 7.3 and 7.5 with a few drops of either 0.1N HCl or 0.05N Tris and the electrical conductivity of the sucrose solution is measured (Barnstead PM-6 purity meter). Both solutions are then put in the perfusion bottles and kept refrigerated.

c) the dissection of the lobster(*) is performed next, following the procedure described by Wright et al. (1958). To prepare for the dissection, the extremities are amputated (tail, claws, walking legs and antennae) using large surgical scissors. Using a dorsal approach, the

(*) The lobsters (Homarus Americanus) are obtained from a local fishmarket and placed in a tank of artificial sea water (Instant Ocean, Aquarium Systems) kept refrigerated (8-12°C) and aerated. The average weight of the lobsters is 600 to 900 grammes.

exosqueleton is cut along the sides and the dorsal part of the head. It is then removed and the cephalothorax cavity is emptied of viscera using sharp pointed surgical scissors. It is then immersed in cold artificial sea water.

The two nerve bundles of the ventral cord are then visible. They emerge from the cerebral ganglion, pass on either side of the esophagus and then disappear under a bony plate where they connect to the subesophageal ganglion. The bony plate is cut at the level of this ganglion in order to permit the removal of both circum-esophageal connectives with the cerebral and the first ganglion. The preparation is then transferred to a Petri dish filled with lobster physiological solution at 2-3°C, where it is held by thin tungsten needles inserted through the ganglions which are placed on two rubber pads glued to a glass microscope slide.

The Petri dish is then placed on a dark-field illumination dissecting stage under a binocular stereozoom microscope (Olympus SZ). The microdissection is best performed under a magnification of 25 to 60. Firmly holding one of the connectives by the stump of a cut nerve branching from the cord (Dumont No. 5 tweezers), a slit is made in the epineurium (No. 7 scalpel, No. 11 blade) in which iridectomy scissors (Irex 66-straight) are introduced. The sheath is then cut from one ganglion to the other, and using a glass dissecting needle and the tweezers, the nerve bundles are teased out. It is recommended that the slit be made on the external side of the connective to avoid damaging the giant fibres that lie along the dorsal surface of the nerve, just below the sheath. There are three

giant axons in each circumesophageal connective, two of them running together and possessing a tapered part, and the third one separate and closer to the median plane of the lobster. This one is the best to use, because it is plainly visible and presents a regular cylindrical shape. A gradual removal of the neighbouring fibres with the help of the glass dissecting needle permits isolation of this giant axon still attached to its two ganglions. It is then carefully cleaned of any connective tissue that is still attached to it, and carefully checked along its full length for the presence of mechanical damage. A very clean fibre is obtained using this dissection technique (Fig. III-14). Diameters range between 90 and 130 μm and the average length is about 3.5 cm . The Petri dish is then placed in the refrigerator.

d) The perfusion bottles are then installed in the shielded enclosure and the flow is started. KCl is poured into the lateral pool where voltage measurements are made and artificial sea water is poured into the other pool. The air bubbles are bled out of the whole perfusion system and the thermoregulation system is put in operation to the set temperature. The node (sucrose separation) is then established under microscope observation.

e) The electrodes are then checked by measuring the potential difference between any two, and are inserted in the nerve chamber. Care has to be taken to prevent air being trapped under the current electrode in the main canal, which would be a source of electrical noise

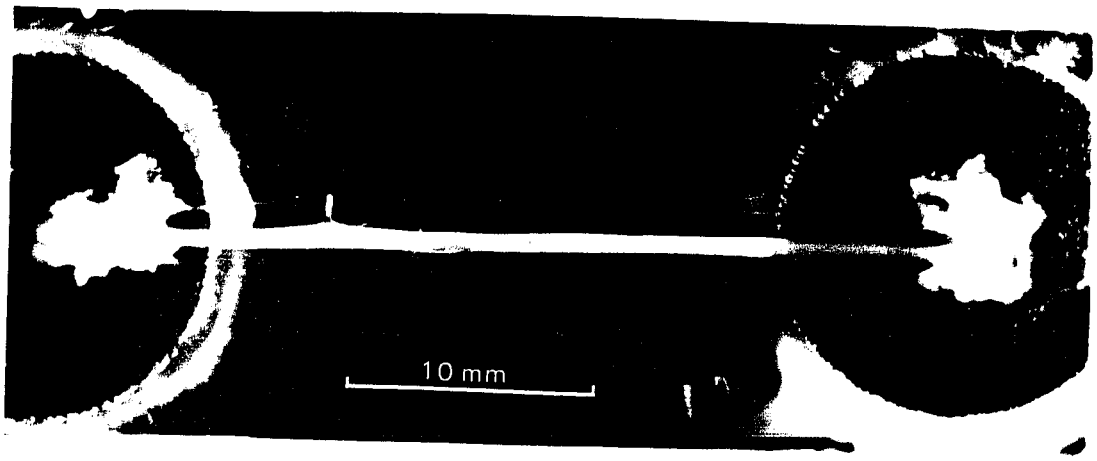

Fig. III-14. Photograph of the lobster nerve preparation. Lower part: undissected right connective. Upper part: dissected giant axon from left connective

and the cause of a rapid decay of the biological sample.

f) The preparation is then ready to be transferred by means of a small acrylic transfer pool to the nerve chamber where the isolated axon is cut and attached by two knots to the 9-0 nylon threads that serve to position it in the nerve canal(*). The attached fibre is then slowly pulled in the nerve canal until one end is extending at least 5 mm in the KCl pool. The node is readjusted if necessary.

g) The resting potential is monitored. When it has reached a stable level, a few stimulation pulses are applied to the specimen to check for its excitability and healthy condition.

h) The sliding carrier is then carefully pushed in position between the electromagnet coils and the biomagnetic experiment can start. It is not necessary to remove the sliding carrier from the exposure area in order to use another patch of membrane. The axon is simply moved along its axis by pulling on the nylon threads.

i) After termination of the experiment, the axon is brought back to the sea water pool in order to have the nylon threads ready for the next experiment. The perfusion solutions are replaced by distilled water to rinse the equipment, and the nerve chamber is cleaned. At regular intervals the electronic equipment is checked and recalibrated when necessary.

(*) The undissected connective is sometimes brought back to the Petri dish and kept refrigerated. It is still possible to isolate an excitable giant axon from it several hours later.

III.5.2 Conduction velocity experiments

In this case the experiments are simpler to plan and to carry out. The procedure follows the steps a), b) and c) of section III.5.1, but the connectives are not dissected. One of them is transferred into the oil-filled nerve chamber and its biomagnetic response is recorded. The second connective is kept refrigerated. It can be used for an other experiment several hours later.

CHAPTER IV

EXPERIMENTAL RESULTS

CHAPITRE IV

RESULTATS EXPERIMENTAUX

Résumé : dans ce chapite, on expose les résultats de nos expériences biomagnétiques:

1) influence du champ magnétique continu de 1.2T sur la vitesse de conduction du nerf péri-oesophageal du homard en configuration parallèle et perpendiculaire pour des durées d'exposition allant jusqu'à 30 minutes.

2) influence du champ magnétique continu de 1.2T sur l'axone géant du homard aux niveaux du potentiel de repos, du potentiel de membrane et du courant transmembranaire en condition de potentiel imposé en double séparation de saccharose dans les cas suivants :

   a) configuration parallèle

   b) configuration perpendiculaire

   c) exposition brève (quelques minutes)

   d) exposition prolongée (plus de 15 min.)

On insiste aussi sur les difficultés rencontrées, particulièrement au niveau de la survie du spécimen.

CHAPTER IV

EXPERIMENTAL RESULTS

IV.1 Introduction

This chapter contains the results of the experiments that have been carried out in order to investigate the influence of a constant magnetic field upon the nervous system, with special reference to the circumesophageal connective nerve of the lobster.

Two different sets of experiments have been performed. In the first series, the nerve trunk was taken as a whole and exposed to the magnetic field in such a way that impulse propagation velocities could be recorded, one section of the nerve being parallel to the field vector while the other section was perpendicular to it. Although easy to perform, these experiments were not so easy to interpret due to the complicated pattern that the compound action potential takes. This is why a large number of experiments were done in order to allow a statistical analysis to be made.

In the second series, the experiments were made on the isolated giant axon using the double sucrose gap technique that has been described in Chapter III. The experimental procedure was far more complicated in this case, and due to the many difficulties that will be mentioned in Section IV.3, emphasis was put on performing a few optimally controlled experiments from which conclusions could be drawn with a reasonable degree of confidence. In this set of experiments, results were obtained for the resting potential, for the membrane action potential (non-propagated action potential) and for the transmembrane currents under voltage-

clamp conditions, using the giant axon of the lobster in parallel and in perpendicular configurations with respect to the magnetic field, under both short and long exposure durations.

IV.2 Conduction velocity experiments

Fifteen experiments have been performed on the lobster circumesophageal nerve in order to investigate the influence of the 1.2 T magnetic field on the impulse conduction velocity. The nerve was placed in either experimental chamber described in Chapter III (see Fig. III-2), and immersed in oil. It was first stimulated in the absence of magnetic field (pre-exposure control period), the magnet was then turned on (exposure period), and stimulation was continued after the magnet had been turned off (post-exposure control period). Each nerve, therefore, served as its own control.

IV.2.1 Control experiments and data acquisition

Control experiments were made on the lobster nerve in oil to establish how time affects the response under normal physiological conditions. Deterioration of the preparation with time corresponded to a gradual decrease in amplitude of the action potential and in conduction velocity, and to a gradual increase in the latency period between stimulation and firing. Experiments were also conducted to detect the presence of induced electrical artifacts. No evidence of switching transient was observed when the magnet was turned on or off.

In general, diphasic recordings were made with the nerve immersed in oil. However, a few monophasic recordings were made with KCl in the end compartment of the nerve chamber and, by using the differential inputs of the oscilloscope, the corresponding diphasic pattern was recorded on the same photograph as the two monophasic traces for the same direction. From a comparison of

these monophasic and diphasic recordings it was found that diphasic recordings could be used for measurements of relative changes in velocity. Due to the phase difference between signals from the two electrodes for this electrode configuration, the peaks and troughs of the diphasic recordings were farther apart than the peaks in the two monophasic recordings, and therefore the velocities calculated from the diphasic pattern were about 30% smaller than the values calculated from the monophasic traces. However, the ratio of the velocities obtained using the two methods was consistent at this lower value as time elapsed (within the limits of the experimental error in the calculation). Thus, relative measurements of the velocity from diphasic recordings are valid. The velocity of impulse in nerves immersed in oil is less than that of nerves in physiological solutions (Hodgkin, 1939), and this together with the diphasic measurement reduction accounts for the values of the absolute velocities (in the range of 3 to 13 m/s, see Fig. IV-3 at the end of Section IV.2) being lower than those published in the literature (Hoekman et al., 1971).

It was also observed that the absolute velocities were generally larger when recorded at the proximal set of electrodes (A1,B1) than those obtained at the distal set of electrodes (A2, B2). This difference can be explained by the fact that the stump of a nerve branching off from the circumesophageal connective was usually located between the two sets of recording electrodes. Therefore, the number of individual fibre action potentials participating to the compound action potential is different at electrodes A1-B1 and at electrodes A2-B2. The recorded potential shape is modified and so are the relative positions of peaks and troughs, thus leading to different velocities. This phenomenon can be seen in Fig. IV-2 at the end of Section IV.2, where one observes that

the velocity baselines are lower in the case of the field parallel to the nerve (electrodes A2-B2) compared to those in the case of the field perpendicular to the nerve (electrodes A1-B1). This baseline difference does not affect the results of this study, because only the velocity variations with respect to the baseline are considered.

The traces of the propagated action potentials were recorded on Polaroid film. Recordings were taken at intervals during the pre-exposure period of stimulation to ensure that the velocity of the impulse was not changing with time. The period of exposure to the magnetic field varied from 20 to 30 min, but for the majority of the experiments was 30 min. Recordings were taken at 5 or 10 min intervals after the magnetic field was turned on. Several recordings were taken at these same intervals after the field was turned off to detect any "recovery" response of the nerve.

IV.2.2 Data processing

A serious problem in data interpretation arises because the circumesophageal nerve contains many fibres of various diameters. As a result, the response pattern to supramaximal stimulation often displays many peaks corresponding to different groups of fibres. Therefore, care must be taken when measuring velocity on the recordings to make sure that the distance measured is that between peaks corresponding to the same group of fibres, and the following approach was used. Fig. IV-1 shows the labelling of the peaks and troughs of the traces recorded in a typical experiment in which the compound action potential displayed a rather complicated pattern. The upper trace (A1-B1 corresponds to the electrodes located in the area where the field is perpendicular to the nerve.

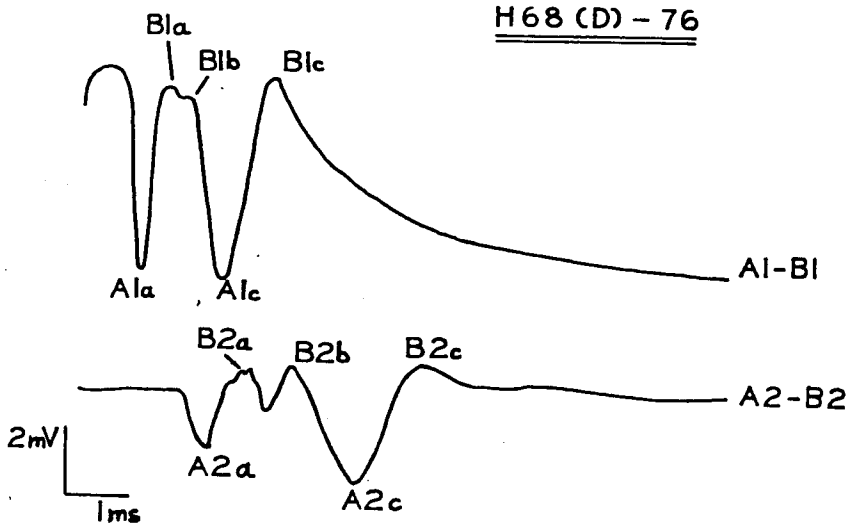

Fig. IV-1. Lobster nerve velocity measurements. Labelling of peaks and troughs on diphasic recordings. Upper trace: differential recording of compound action potential measured at electrodes A1 and B1 (Field perpendicular to nerve). Lower trace: differential recording of the same event at electrodes A2 and B2 (field parallel to nerve) . See also Fig. III-1

The lower trace (A2-B2) corresponds to the recording in the area where the field is parallel to the nerve (see also Fig. III-1, chapt. III). The A1 and A2 troughs are single (except for a small subpeak on A2a) whereas the B1 and B2 fast peaks are multiple. By observing the traces on each photograph taken at regular interval during the course of the experiment, the peak labelled B1a was determined to be the true fast B1 peak , and B1b was discarded as an unreliable sub-peak. Close observation of the traces on successive photographs showed that among the three small subpeaks in the first fast B2 peak, the middle one was the one which became and remained the highest one. It was taken as the B2a peak. The second last B2 peak, B2b, was discarded as an unreliable sub-peak. The photos for the other experiments were analyzed in a similar way. In general, the second or third sub-peaks which occasionally appeared on major peaks were rejected as unreliable. Also, if the peak-trough ceased to appear or changed significantly in shape with time, such data were discarded.

The distance on photographs between action potential peak and trough detected at the A and B electrodes were measured. After applying a correction to account for the photographic reduction of the oscilloscope image, the velocity of the nerve impulse was calculated from these distances by using the measured separation of the electrodes and the time base setting of the oscilloscope. Thus, in the case of Fig. IV-1, the velocity of the fast fibres at electrodes A1 and B1 is obtained by dividing the interelectrode distance by the distance measured between the trough A1a and the peak B1a. The velocity of the slow fibres at the same electrodes is obtained by dividing the interelectrode distance by the distance

measured between the trough A1c and the peak B1c. The same procedure is used to determine the velocities at electrodes A2 and B2.

From these data, values for the velocity 5, 10, 15, ... min after the field was turned on then off, were obtained. When required, linear interpolation between the actual points was applied to obtain values at the desired times. Once the velocity during the pre-exposure stimulation period had stabilized, this velocity just before the field was turned on was taken as the base velocity v_B.

Error analysis in data acquisition was made in the following manner. The main error in velocity measurement was due to the broadness of the peaks and to the width of the oscilloscope trace, both limiting the accuracy with which the positions of the peaks could be determined. The t=0 left vertical line on the oscilloscope was taken as having an accurately-known position, and an absolute error was associated with the distance between this line and the peaks. This error increased as the broadness of the peaks increased. The absolute errors in the distance to corresponding peaks were combined by the probable error root-of-sum-of-squares formula to find the absolute error in the distance between the peaks. This gave relative errors which were usually in the range of 5 to 15%. The error in the measured separation of the pairs of electrodes was approximately 1% and the error in the photographic reduction correction factor was less than 1%, so these errors were considered negligible compared to the time error. The relative error in the calculated velocity was taken as equal to the relative error in the distance between the peaks.

Because the temperature of the tap water used to cool the magnet warmed up during the course of the experiment, the temperature of the experimental chamber in the magnet gap also increased by as much as 3.5°C/h . Experiments were therefore done with tap water circulated through a heat exchanger in an ice-box in order to minimize such temperature variations. A temperature/time gradient of less than 1.5°C/h was attained in these conditions. During control experiments in which the magnet was energized for the same time as in normal experiments, temperature measurements in the gap were made with a Cu-Constantan thermocouple and a Speedomax (Leeds and Northrup) temperature recorder.

Velocities obtained from the recordings following the method described above were corrected for temperature in the following manner. Using the dimensional analysis of Huxley (1959) and the parameters of Huxley (1959), Easton et al. (1957) and Dalton et al. (1962), for squid and lobster, a Q_{10} of 1.5 was calculated for the data. This Q_{10} value was used to correct the data for the temperature in the gap just before the magnet was turned on. For some of the experiments the variation of temperature with respect to time was less well-known than for others, but the temperature correction was never more than 8%. The errors in the corrections were less than this and were not added to the experimental errors in the velocity because they were much smaller than the errors in time measurements and not precisely known.

Data from each experiment were normalized by calculating the relative velocities $v(t)/v_B$ at the desired times, to allow comparisons to be made of velocities recorded in the different

experiments, for each configuration (parallel and perpendicular), during and after exposure to the magnetic field. For each time and for each configuration a weighted mean was calculated. With the values from each experiment weighted according to the probable experimental error in each, the root-of-sum-of-squares of the errors in v(t) and v_B were calculated.

IV.2.3 Statistical analysis

The following statistical analysis was performed (Meyer, 1975). The variance for each configuration (parallel or perpendicular) was calculated for the corresponding data at each time, using the weighted mean of the points. Comparisons were made at each time point between (i) the slower and faster fibres for a particular direction, and (ii) the parallel and perpendicular directions, where the results of fast and slow fibres for a direction were combined to give a mean weighted according to the errors in the velocity ratios(*).

For each comparison a two-tailed Fisher F-test was applied to determine whether or not the variances for the pair were homogeneous. The appropriate Student t-test, for homogeneous or inhomogeneous variances, was then used to determine whether the difference between the pair of weighted means was significant.

(*) For the complete set of lobster data, comparing the slow and fast fibres, for the perpendicular field the difference between the points was statistically significant at no time, and for the parallel field the difference between the two points 5 min after the field was turned off was significant at only 10%, and all other differences were insignificant. Therefore, the speed at which the fibre conducts impulses (which is related mainly to the size of the fibre when one is talking about only one species) has no relationship to its response to a magnetic field, and the results for the fast and slow fibres were averaged (by the weighted mean method) for each direction.

In the case of inhomogeneous variances, the degree of freedom was estimated as $n_i - 1$, where n_i was the degree of freedom in the set of data with the larger variance. The t-test was also applied to determine whether the difference between the combined parallel or perpendicular data was significantly different from the 100% (i.e. no velocity change) value at each time point.

IV.2.4 Results

Fig. IV-2 represents the tracings from Polaroid photographs taken before, during and after exposure of the nerve to the magnetic field in a typical experiment.

Results from a representative experiment are shown in Fig. IV-3. Absolute velocities have been plotted for slow and fast fibres, in parallel and in perpendicular configurations. The error bars represent the probable experimental error, based on errors in the distance measurement as described in Section IV.2.2. One can observe on this graph that velocities in the same fibre group (fast or slow) before exposure are different, depending on orientation of the nerve with respect to the magnetic field. This phenomenon has been explained above (Section IV.2.1.). For the parallel field, the fast fibres shows an upward trend while the field is on and the slow ones have a downward trend, but for the perpendicular field, the response to the field is not consistent. The maximum observed change in velocity in this experiment was an increase of 25% for the fast perpendicular fibres and a decrease of 25% for the slow parallel ones.

Fig. IV-4 shows the velocity graph for the overall set of data, as a percentage of the control velocity v_B before exposure.

H 73 (D) - 76

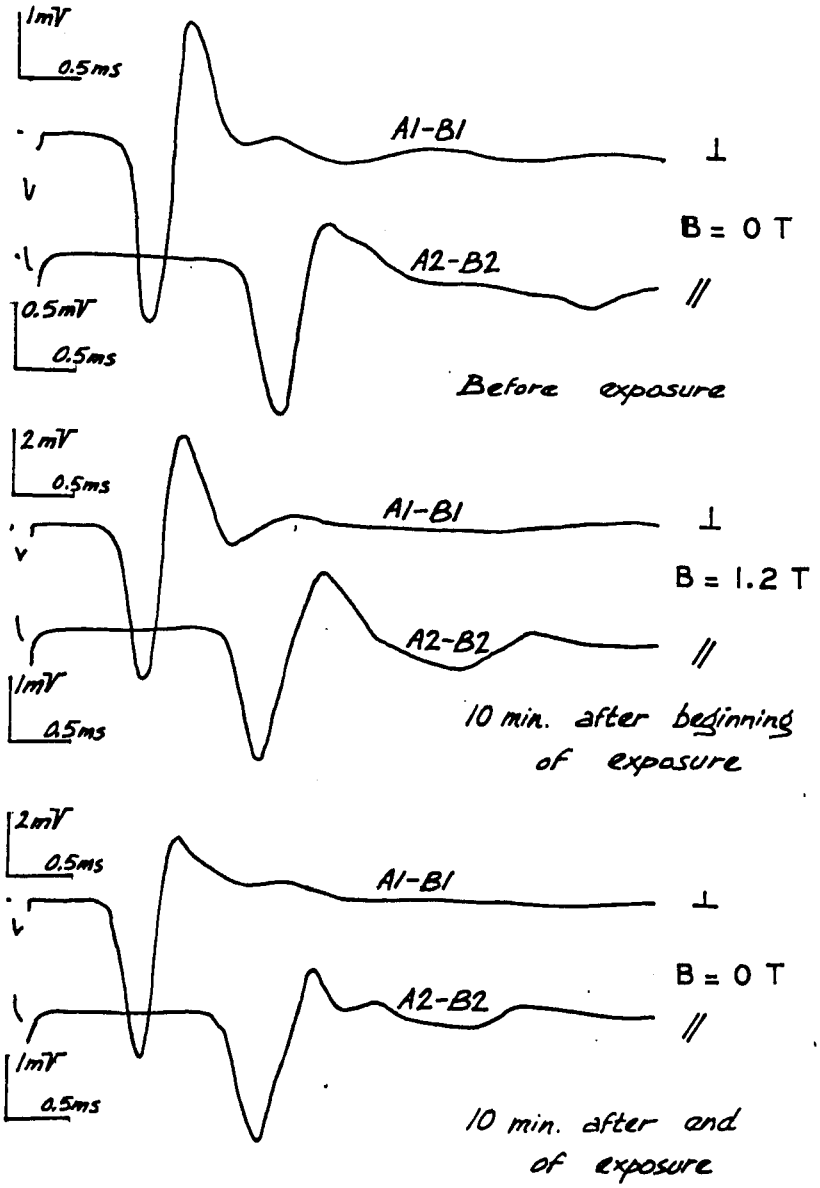

Fig. IV-2. Compound action potentials of lobster nerve recorded differentially before, during and after exposure to a 1.2 T magnetic field perpendicular (A1-B1) and parallel (A2-B2) to the nerve. See also Fig. III-1

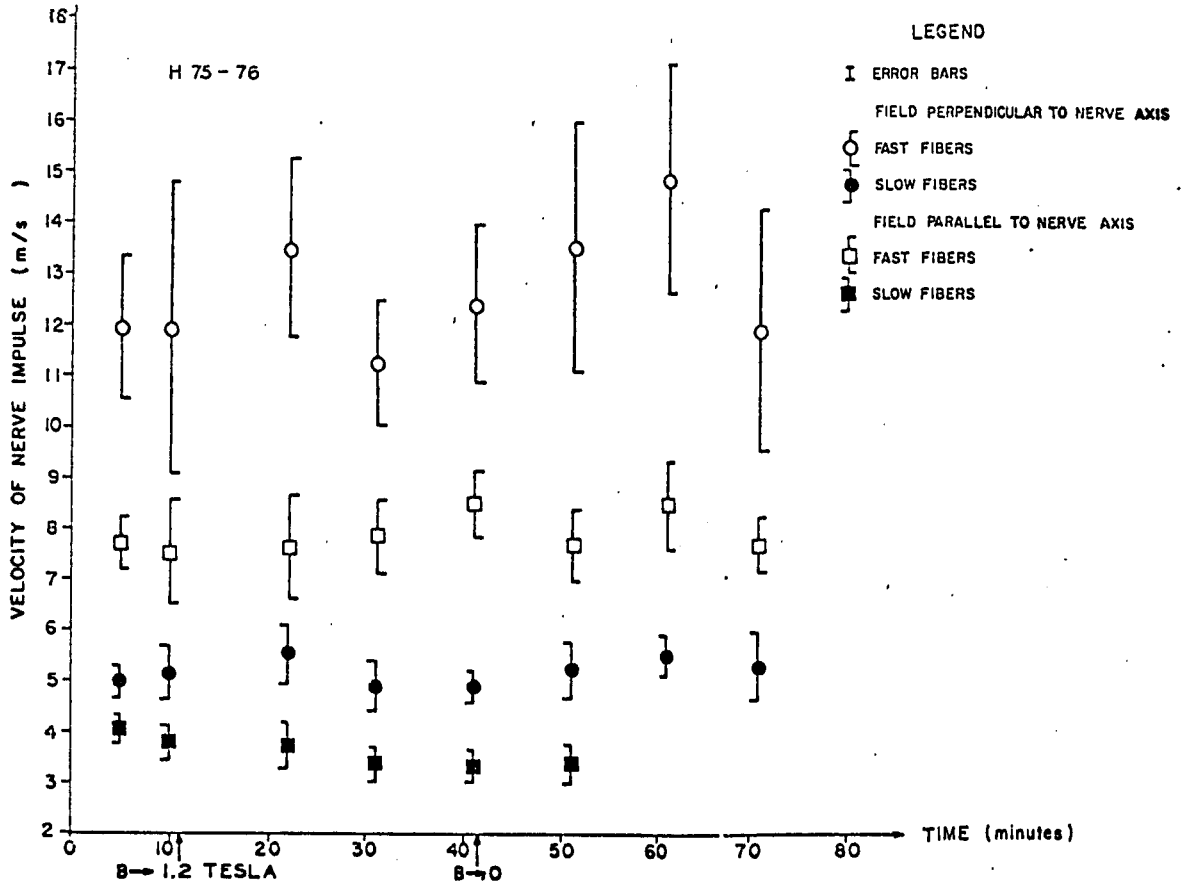

Fig. IV-3. Nerve conduction velocity with and without magnetic field exposure. Typical lobster data

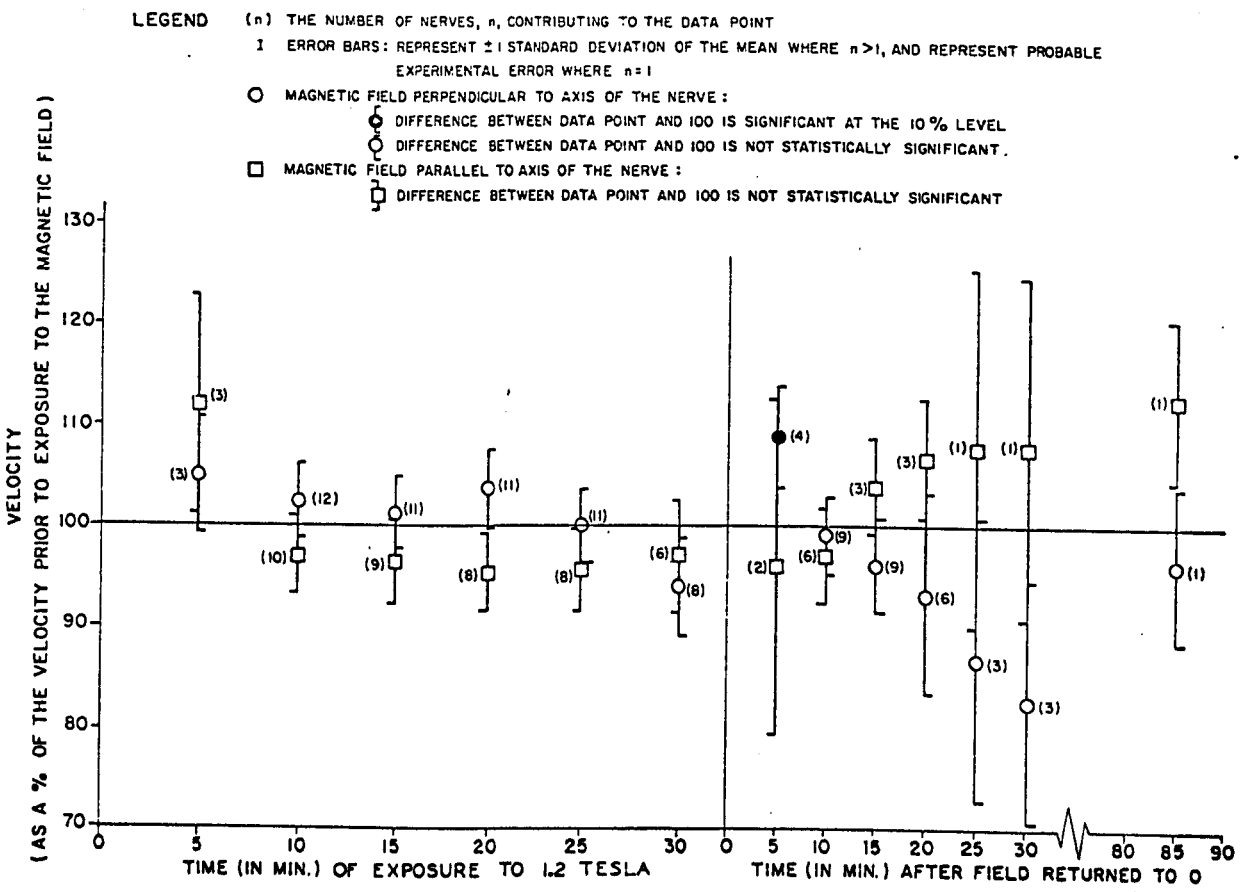

Fig. IV-4. Nerve conduction velocity with and without magnetic field exposure. Results for all data

As can be seen from the graph, only the point for the perpendicular field five minutes after the field was returned to zero is significantly different from the no-change 100% value, and this difference is significant only at the 10% level.

In summary, it has been established that within the experimental limitations of these conduction velocity measurements, a constant magnetic field of 1.2 T has no significant influence on the propagation velocity of the impulse along the circumesophageal nerve of the lobster in either parallel or perpendicular configuration with respect to the magnetic field vector direction.

IV.3 Biomagnetic experiments on the membrane potentials and the transmembrane currents of the lobster giant axon

IV.3.1 Preliminary experiments

Several preliminary experiments were made to (i) evaluate the quality of the experimental double sucrose gap apparatus that has been specially developed for this work and compare the results to the data published in the original work by Julian et al. (1962a, b) and (ii) get at least a rough idea of the biomagnetic response of the axonal membrane in order to establish a set of meaningful figures for the amplitude of the magnetic field and the exposure duration to be used.

IV.3.1.1 Control expériments. Fig. IV-5 represents the tracings from Polaroid photographs of a typical membrane action potential (lower trace) and the corresponding action current (upper trace). The amplitude and the time course of the action potential correspond closely to those reported by Julian et al. (1962a), and so does the resting potential, which shows the same amount of hyperpolarization due to the use of the sucrose gap technique (Blaustein et al., 1966b). Fig. IV-6 shows the tracings

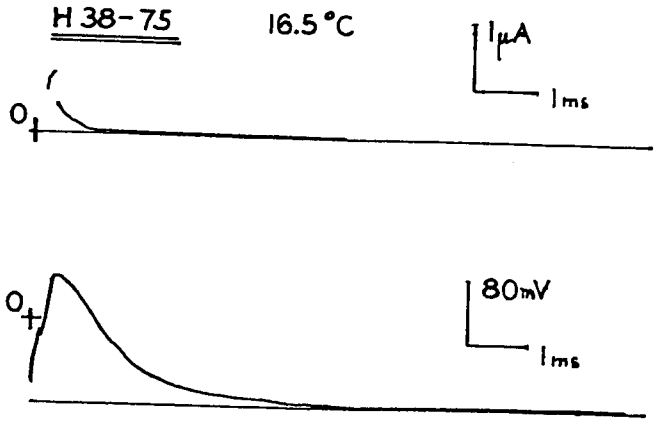

Fig. IV-5. Membrane action current (upper trace) and action potential (lower trace) of lobster giant axon in double sucrose gap

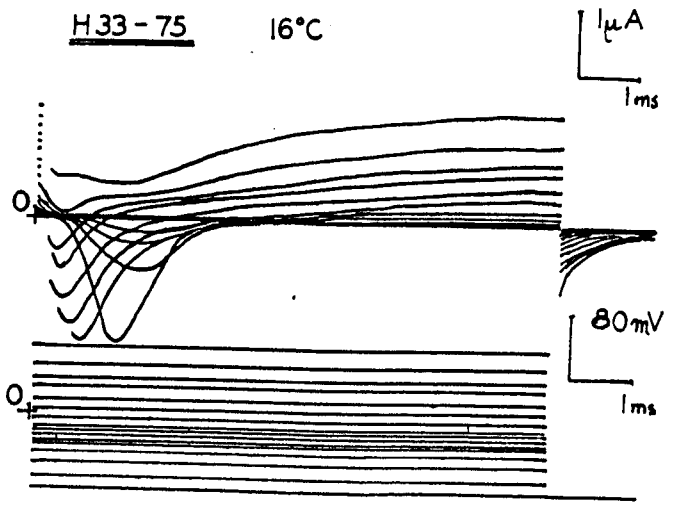

Fig. IV-6. Transmembrane currents (upper trace) and corresponding membrane voltages (lower trace) of lobster giant axon under voltage-clamp conditions in double sucrose gap

of the transmembrane currents (upper trace) and the corresponding membrane voltages (lower trace) as obtained from the lobster giant axon under voltage-clamp conditions. For this particular axon, the membrane area in the gap was approximately 2.5×10^{-4} cm^2. The current-voltage relation graph corresponding to the data of Fig. IV-6 is represented in Fig. IV-7. The upper curve represents the late current (10 ms after the beginning of the command pulse) and the lower curve refers to the early transient current that appears after the initial capacity transient current. This graph is very similar to the one that can be found in Julian et al. (1962b), except that in our case the transient current density is a little higher and the negative slope part of the transient current curve is steeper.

Other experiments were performed in order to investigate the behaviour of the nerve preparation when it was left in the sucrose gap for different lengths of time. It was found that the resting potential, after an initial phase lasting around 5 min, was usually decreasing at a rate of 1 to 5 mV/min. Although the action potential overshoot did not change very much, excitability was reduced and after 15 to 20 min in most cases the membrane had lost its ability to respond to stimulation. This process was accompanied by an increase in the latency time between stimulus and response. It was in general very difficult to keep a healthy axon for more than 30 min in the nerve chamber. Another phenomenon that happened quite often was a sharp and sudden depolarization of the membrane by 25 to 40%. We could not discover any specific reason for this highly undesirable behaviour that usually resulted in an unexcitable axon. However, we found that this phenomenon usually took place after the membrane had been driven by successive sets of voltage-clamping pulses. In such

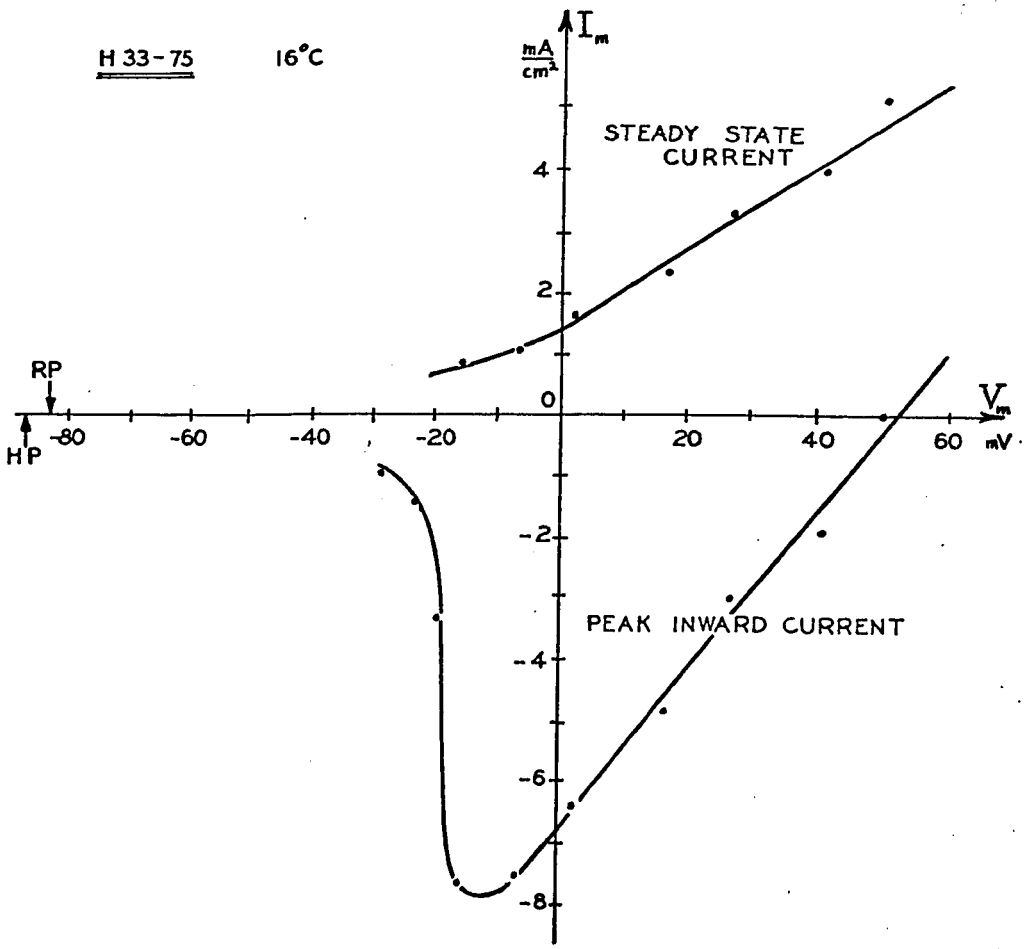

Fig. IV-7. Current-voltage relation of lobster giant axon. Points taken from data presented in Fig. IV-5. HP = holding potential. RP = resting potential of the unclamped membrane patch

cases leakage current increased noticeably. Reduction of the amplitude and of the duration of the voltage pulses did not improve the situation. These two aspects of the lobster axon behaviour in the double sucrose gap arrangement, i.e. its unstable resting potential and its tendency to refuse to be voltage-clamped more than once have also been reported by Pooler (1968)(*). Therefore, due to the relatively short functional time of the lobster membrane patch in the nodal area, problems in long term biomagnetic experiments were expected to be encountered. However, these control experiments showed that the measurement and control apparatus that had been built by the author could be used with a reasonable degree of confidence to undertake the exploratory experimental investigation of the influence of a constant magnetic field on the axonal membrane of the lobster, provided that relatively short exposures to magnetic fields were used and an adequate set of criteria established to show that any observed effects could not be attributed to degeneration of the axon or to any other time dependent effects that may go on in the absence of a magnetic field.

IV.3.1.2 Biomagnetic test experiments.

At this stage it was important to carry a few test experiments to determine roughly the magnetic field amplitude range for which the biomagnetic effect could occur. Fig. IV-8 and Fig. IV-9 show the tracings of action and resting potentials recorded from an axon located in the parallel field nerve chamber and exposed to a magnetic field of various intensities. It is seen from these recordings that there are no detectable variations in the

(*) In a recent paper, Oxford et al. (1975a) suggest to "dope" the sucrose with 10^{-4} M $CaCl_2$. This is supposed to enhance the stability of the resting potential. It has not been tried in this study.

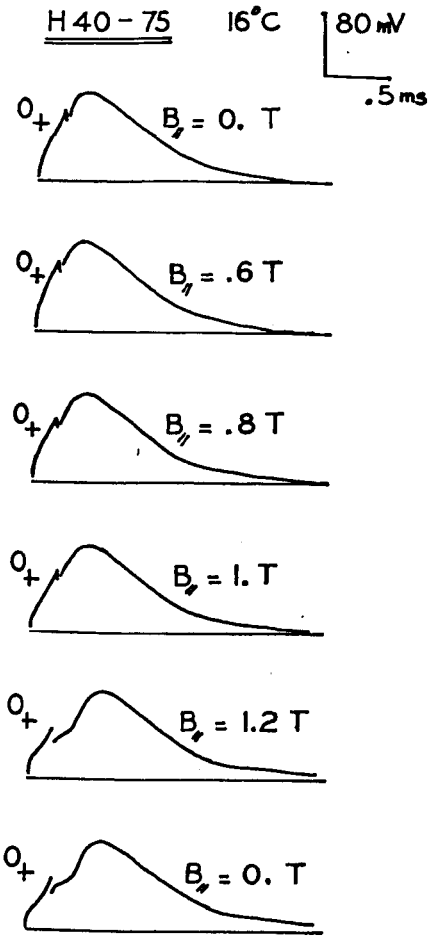

Fig. IV-8. Membrane action potential of lobster giant axon exposed to a magnetic field of various amplitudes. $B_{//}$ = field parallel to axon

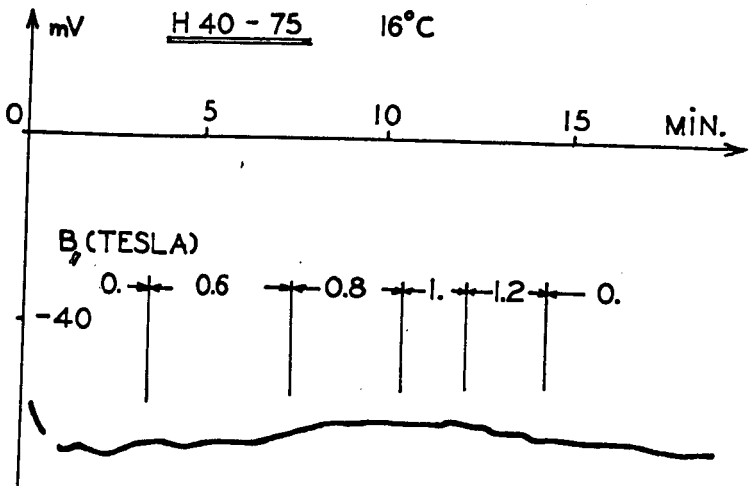

Fig. IV-9. Resting potential of lobster giant axon exposed to a magnetic field of various amplitudes. $B_{//}$ = field parallel to axon

time course of either the action potential or the resting potential in relation to the intensity of the applied magnetic field. The increase of the latency time of the axon is most probably imputable to fatigue, as this phenomenon had been already recorded in the absence of any magnetic field. It was therefore decided to set the magnetic field intensity to 1.2 T, which corresponds to the maximum power of the available electromagnet, with the hope that the highest value of the field would have the largest biomagnetic effect. It was assumed that these considerations were also valid in the case of the perpendicular field exposure experiments and therefore no tests were made on the axon exposed to incremental fields in the perpendicular exposure nerve chamber.

IV.3.1.3 Evaluation of the experiments.

In view of the relative instability of the biological specimen in the double sucrose gap arrangement, particularly under voltage-clamp conditions, and because of the large number of factors that contribute to the adequate survival of the excitable membrane, it was found necessary to establish a set of criteria in order to decide which experiments could be accepted with a reasonable degree of confidence. In addition to the standard electrophysiological criteria for rejecting experiments, like a low resting potential (less than 60 mV), a low amplitude action potential (less than 100 mV) or a total absence of excitability, other ways of judging the quality of the experiments had to be considered. In fact, there was the risk that an experiment would not be accepted on the grounds that a particular physiological parameter, used as a standard quality indicator, would have changed in such a way that the experiment should normally be rejected. This variation, however, could well be due to the influence of the magnetic field itself, in which case the experiment should be retained as proof of a biomagnetic

effect. In other words, care had to be taken when deciding whether an experiment had to be rejected or not. Fortunately, the magnetic field has no detectable effect on the resting potential and on the amplitude of the action potential, as it has been established in the biomagnetic test experiments (paragraph IV.3.1.2) and as it will be verified in the following sections. Therefore, the following criteria were used for selecting the acceptable voltage-clamp experiments:

(i) for short term exposure experiments, the resting potential remains stable within 5% of its normal physiological value;

(ii) for short term exposure experiments, the action potential amplitude remains stable within 5% of its normal physiological value;

(iii) for long term exposure experiments, the decay of the preparation is accounted for by accepting experiments in which the resting potential does not drop by more than 2 mV/min ;

(iv) for long term exposure experiments, the action potential overshoot remains stable within 5% of its amplitude at the beginning of the experiment;

(v) under voltage-clamp conditions, the baseline corresponding to the current at holding potential between successive clamping pulses does not drift by more than 5% of the maximum amplitude of the inward current;

(vi) under voltage-clamp conditions, no notches indicating a poor voltage control of the membrane are observed in the recorded currents.

Table IV-1 lists the thirty-two experiments that were made in order to study the biomagnetic response of the axon membrane

	Magnetic field parallel to axon	Magnetic field perpendicular to axon
Short term exposure	H124-77*	H101-76 H130-77*
	H125-77*	H127-77 H131-77*
	H126-77*	H128-77 H132-77*
		H129-77*
Long term exposure	H46-76 H50-76* H82-76*	H93-76 H104-76* H112-76
	H47-76 H51-76* H86-76	H94-76* H109-76 H113-76
	H48-76 H52-76* H116-76	H100-76* H110-76
	H49-76* H81-76* H117-76	H103-76 H111-76

Table IV-1. Double sucrose gap biomagnetic experiments. Numbers with asterisks refer to voltage-clamp experiments. Underlined numbers correspond to the experiments selected according to the criteria exposed in Sect. IV.3.1.3.

of the lobster under different exposure conditions. Experiments in which transmembrane currents under voltage-clamp conditions were measured are marked with an asterisk. The underlined numbers correspond to the experiments that were selected using the criteria stated above. As can be seen from this table, more than half of the experiments had to be rejected under these conditions, and the toll is particularly severe in the case of the long term exposure voltage-clamp experiments.

IV.3.2 Short exposure time experiments

Experiments have been performed on the lobster axon in order to investigate the influence of the 1.2 T magnetic field on the resting potential, the membrane action potentials and the transmembrane currents under voltage-clamp conditions for short term (less than 5 min) exposure times. The giant axon was placed in either experimental chamber, sucrose and test solution streams were started and the artificial node between the two sucrose streams was established, its width being set under microscopic observation around 70 to 90 μm. Three to four minutes were allowed for the temperature of the flowing solutions to stabilize, and for the resting potential to reach a steady-state value. In some experiments, the resting potential was continuously monitored on the strip-chart recorder while stimulation of the fibre through the control pool electrode elicited non propagated membrane action potentials that were recorded by the voltage electrode located in the other lateral pool. In other experiments, the axon transmembrane voltage was controlled by the voltage-clamp electronic apparatus. After the stimulation had elicited an action potential that indicated the good condition of the axon patch under investigation, the control loop was progressively closed and the

membrane potential brought to a slightly (5 to 10 mV) hyperpolarizing voltage. A set of command pulses were applied to the fibre through the control pool electrode and the corresponding transmembrane currents were recorded by the central pool electrode. The magnetic field was then turned on, and the same procedure was used. The field was then turned off again, and the same procedure was used, followed by a progressive release of the clamping of the membrane. The resting potential and a control membrane action potential were then recorded.

Records were taken on Polaroid and 35 mm films. A set of pictures was taken before, during and after exposure to the magnetic field. The same node (membrane patch in the double sucrose gap) served therefore as its own control. Exposure to the field was usually less than 5 min in these experiments.

Fig. IV-10 and Fig. IV-11 represent the tracings of the recordings obtained in a typical experiment with the magnetic field parallel to the nerve fibre. Tracings made from the recordings in the case of the field perpendicular to the nerve fibre are shown in Fig. IV-12 and Fig. IV-13.

In the case of the parallel field exposure, the membrane resting and action potentials are identical before, during and after exposure to the magnetic field, except for a slight delay of the firing time, which is attributable to the progressive decay of the preparation (Fig. IV-10). The tracings of the transmembrane currents, as represented on Fig. IV-11, were made from 35 mm film. The actual traces obtained before, during and after exposure to the field can be exactly superposed for every

depolarizing voltage level. It is therefore concluded that a magnetic field of 1.2 T, applied during 5 min or less to the giant axon of the lobster in such a way that the axon and the field are parallel, does not affect the normal excitation process of the axonal membrane.

In the case of the perpendicular field exposure, the situation was almost the same. As can be seen on Fig. IV-12, the amplitude and the rising phase of the action potential are unaffected by the magnetic field. There is a slight increase of the resting potential (about 4 mV) and the repolarization phase of the action potential is faster during exposure. However, this situation remains unchanged when the field is suppressed. It is thought that this faster repolarization is not ascribable to the field influence but rather to the larger resting potential in this particular case. The transmembrane current tracings display the same kinetics, although superposition of the traces on 35 mm film shows a progressive decrease in the amplitude of the currents. However if the pre-and post-exposure traces are averaged in order to account for fatigue (Hodgkin et al., 1952b), the resulting traces correspond exactly to the exposure traces for every depolarizing step. It should be noted here that the recordings of Fig. IV-12 and Fig. IV-13 were made on different patches of the same axon, and that in the latter case the resting potential after exposure was slightly less than before. These results support the evidence that a perpendicular magnetic field of 1.2 T applied during 5 min or less to the lobster axon does not interfere with its normal function.

IV.3.3 Long term exposure experiments

Experiments have been performed on the lobster axon in order to investigate the influence of the 1.2 T magnetic field on the resting and action potentials and the transmembrane currents under

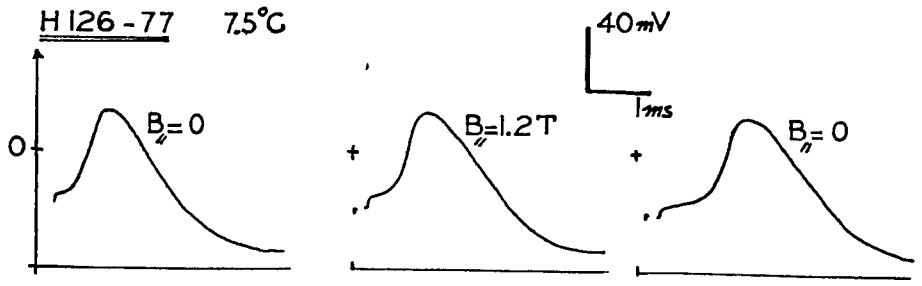

Fig. IV-10. Influence of a constant magnetic field on the action potential of the lobster giant axon (short exposure).
$B_{//}$ = field parallel to axon

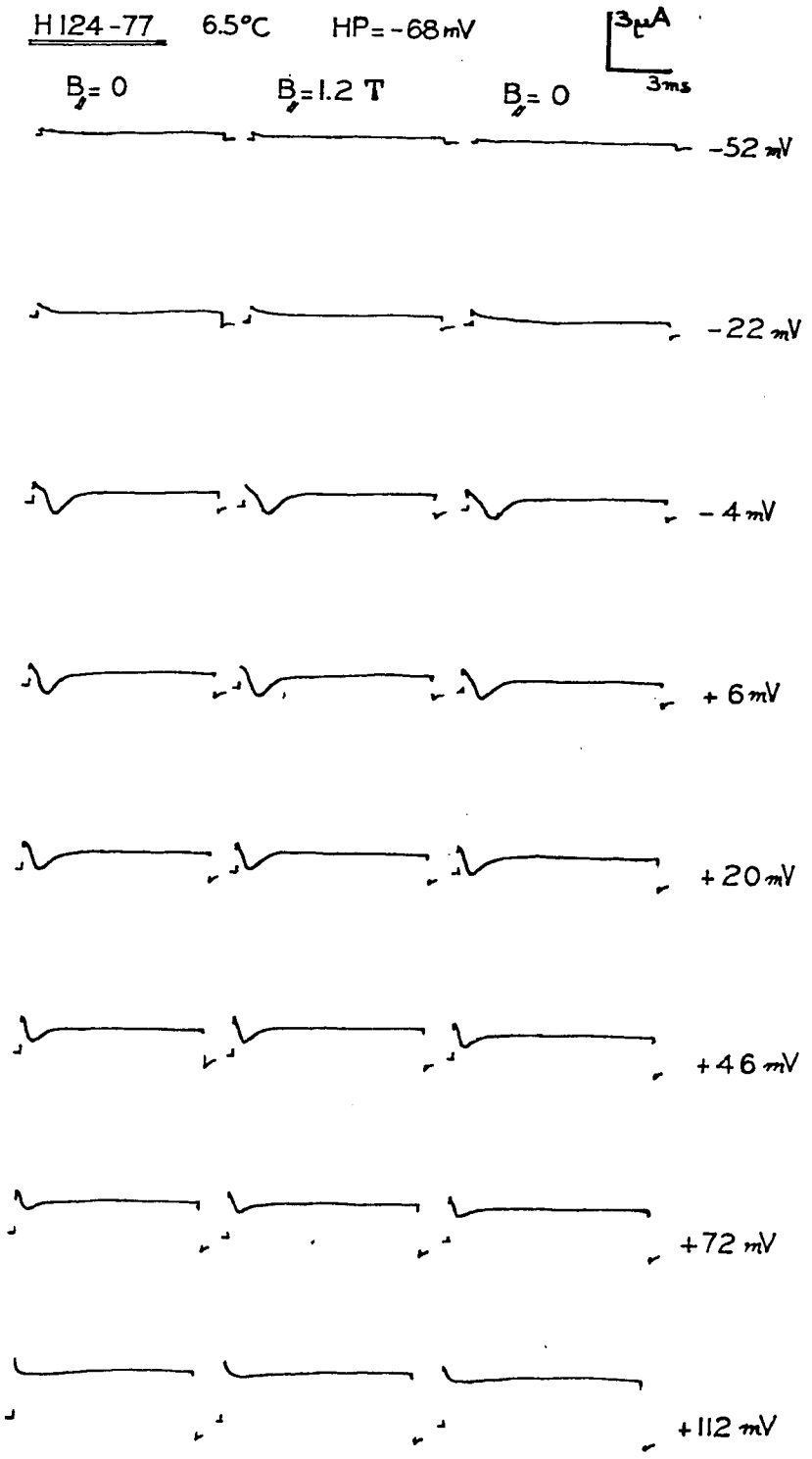

Fig. IV-11. Influence of a constant magnetic field on the transmembrane current of the lobster giant axon (short exposure). $B_{//}$ = field parallel to axon. Number at right of each set of records gives clamping voltage with respect to ground

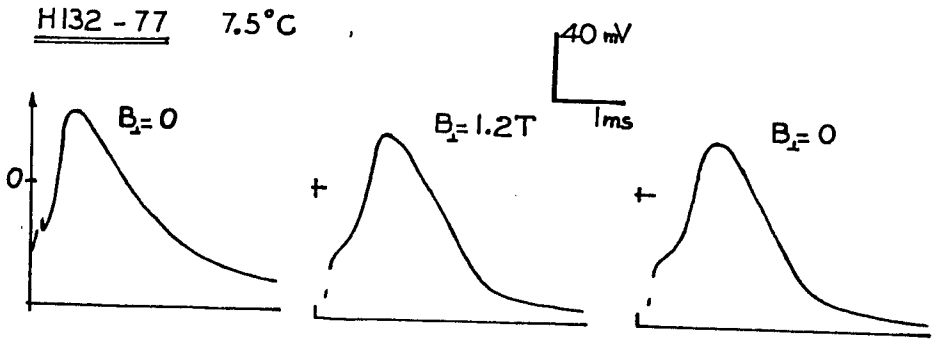

Fig. IV-12. Influence of a constant magnetic field on the action potential of the lobster giant axon (short exposure). $B_{\perp}$ = field perpendicular to axon

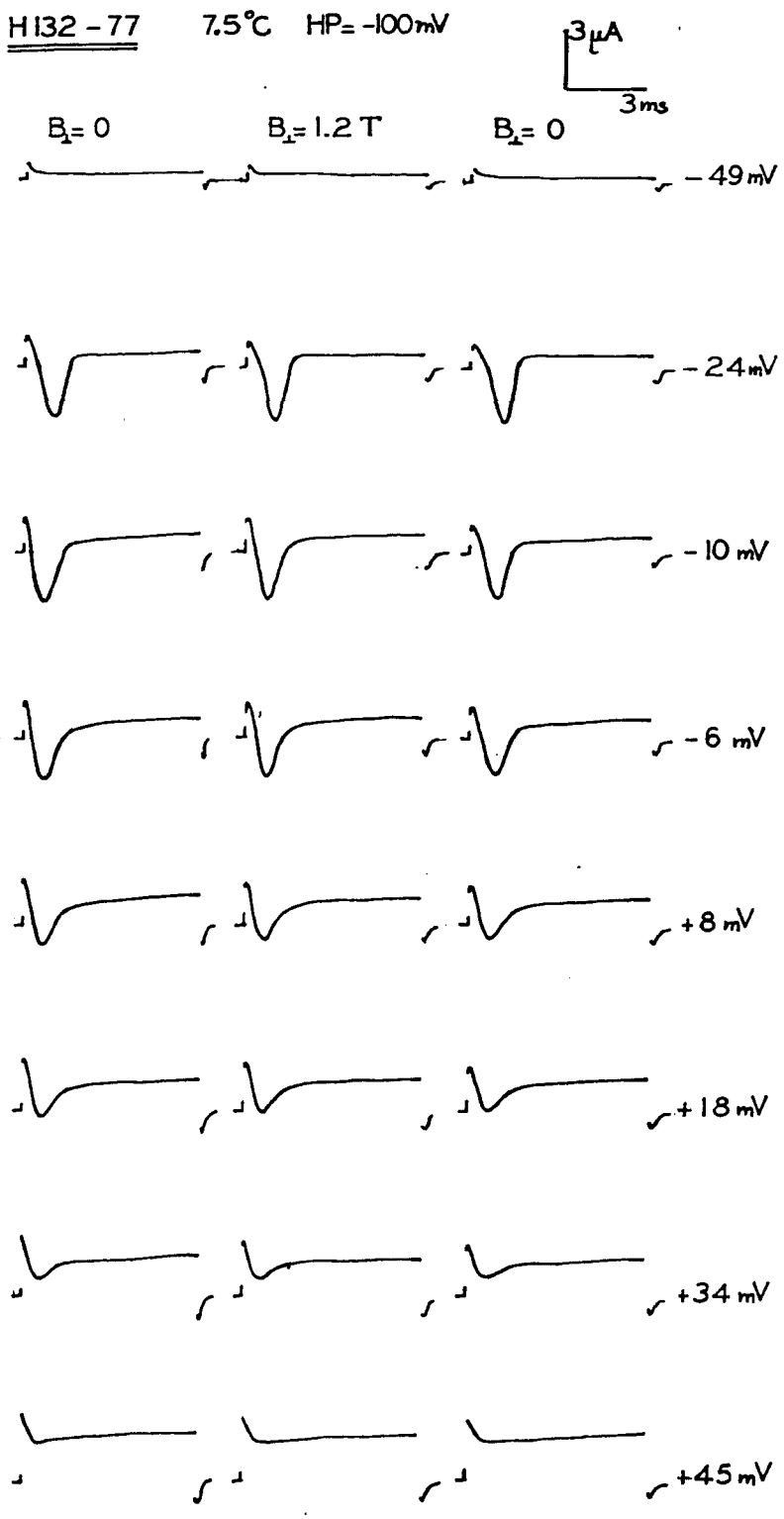

Fig. IV-13. Influence of a constant magnetic field on the transmembrane current of the lobster giant axon (short exposure). $B_{\perp}$ = field perpendicular to axon. Number at right of each set of records gives clamping voltage with respect to ground

voltage-clamp conditions for long term exposure times. The deterioration of the axon in the nodal area was a major problem, and it proved difficult to carry experiments of a duration exceeding 25 to 30 min . In fact, under voltage-clamp conditions, large leakage currents often developed as early as 15 min after the beginning of the experiment.

The experimental procedure followed the same lines as described in the short term exposure experiment section (Section IV.3.2) with the exception that there was no need for pre-exposure control experiment, for it had been established that the normal nerve membrane behaviour is not immediately affected by the field (see Section IV.3.2).

Experiments were made to study the biomagnetic response of the resting and the action potentials in either geometrical configuration. Results are shown on Fig. IV-14 and Fig. IV-15. As can be seen from the tracings, there is no marked change of the action potential amplitude and rising phases. In the case of the perpendicular field exposure (Fig. IV-15), the resting potential remains remarkably stable during the course of the experiment, and so does the action potential. In the case of the parallel field exposure (Fig. IV-14), traces A, B, C, D and E are almost superposable (except for an increase in excitation threshold and in the slope of the repolarization phase as time elapses). A corresponding decrease in the resting potential can also be seen.

Voltage-clamp experiments were also made, and the data used to establish current-voltage relation graphs. The peaks of the transient currents and the steady-state values of the late currents were plotted for each depolarizing step of every voltage-clamp experiment. These I vs V graphs were difficult to interpret due to the large leakage currents that were present in most experiments. It was therefore necessary to correct the plotted currents for leakage.

To make this correction, the following approach was used

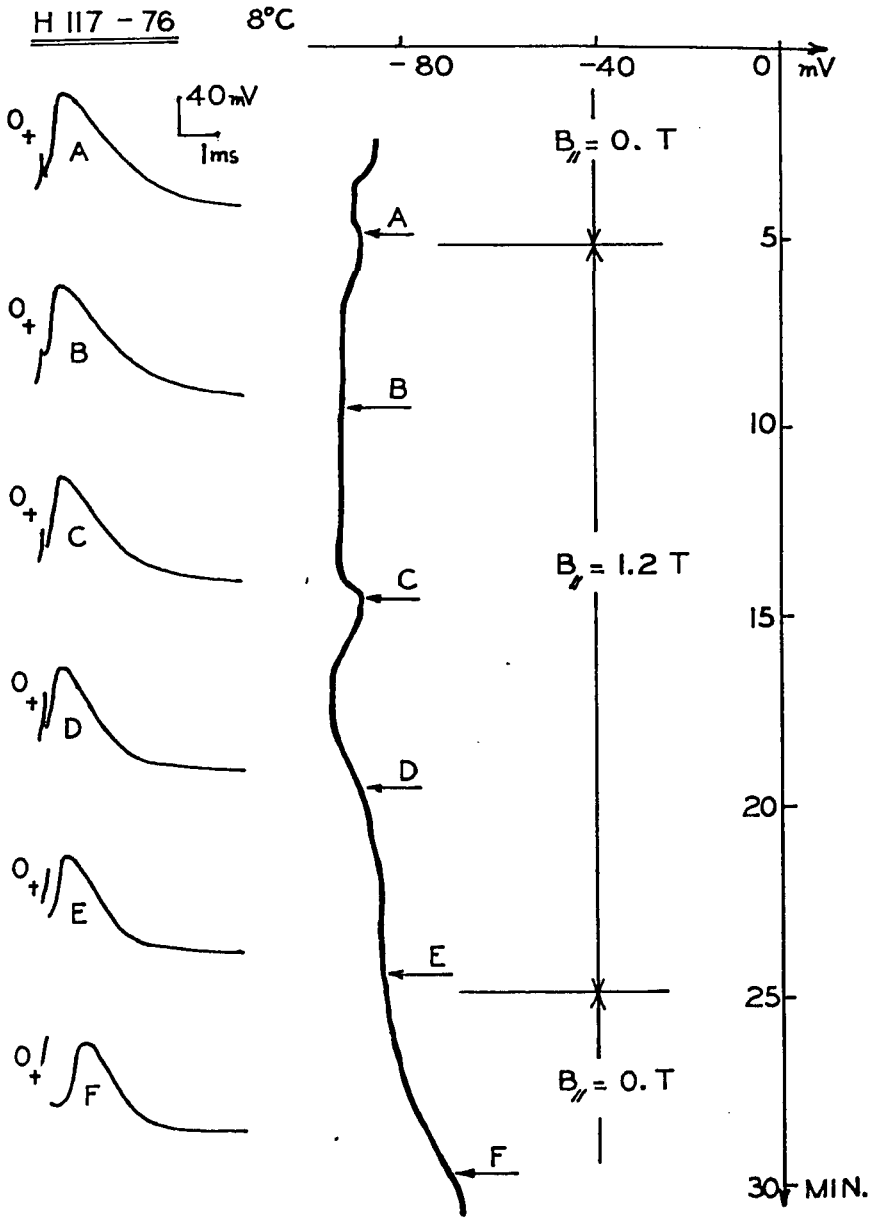

Fig. IV-14. Influence of a constant magnetic field on the resting and action potentials of the lobster giant axon (long exposure) $B_{//}$ = field parallel to axon

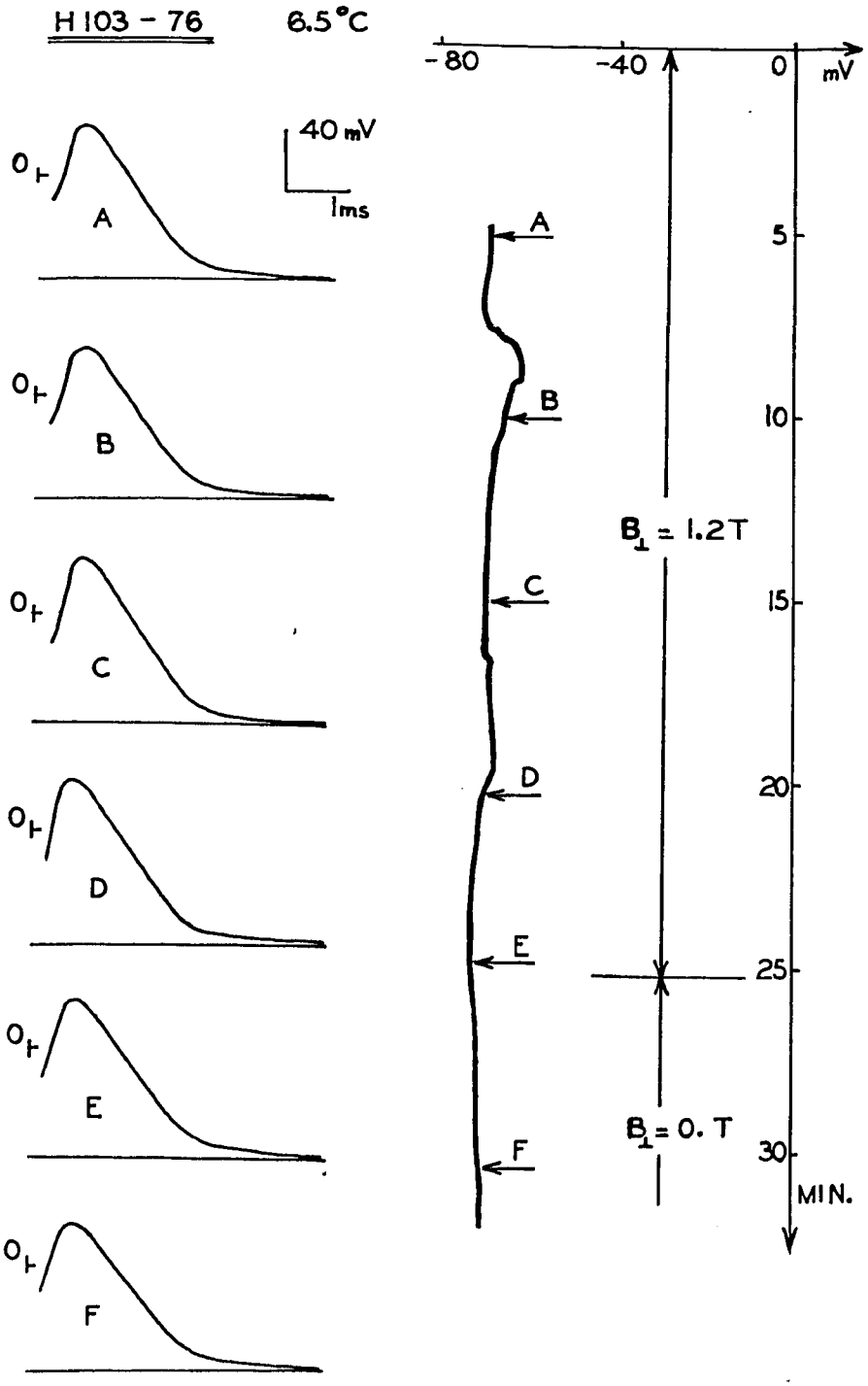

Fig. IV-15. Influence of a constant magnetic field on the resting and action potentials of the lobster giant axon (long exposure) $B_\perp$ = field perpendicular to axon

(see Fig. IV-16). Leakage current was assumed to be proportional to the applied voltage steps, i.e. the leakage conductance was assumed to be constant with respect to voltage and was taken as the slope of the line that joins the zero-current holding potential point (labelled HP on the I vs V graph) to the value of the late steady-state current for small depolarization steps. This leakage current I_ℓ (dash-dotted line on Fig. IV-16) was then substracted for each depolarizing clamp voltage from the corresponding steady-state current I_{ss} (continuous line) in order to get the potassium current I_K (dashed line), and from the corresponding peak transient current I_{pt} (continuous line) in order to get the sodium current I_{Na} (dashed line). This correction procedure is a simplification of more elaborate approaches that account for some non-linear characters of the lobster axon leakage conductance (Blaustein et al., 1966a; Moore et al., 1966; Takata et al., 1966). It was considered to be sufficient for the present exploratory investigation.

Fig. IV-17 represents the peak sodium current and the steady-state potassium current characteristics at different times during a long term biomagnetic experiment in which the field was parallel to the axon. It is obvious from the graph that the magnetic field does not exert a dramatic influence upon the axon conductances. The general aspect of the I vs V curves remains the same, even after 15 min of exposure. The sodium conductances (the slopes of the linear part of the sodium current characteristics) are identical in the 1 min, 5 min and 9 min exposure cases, and so are the maximum inward currents. The situation then deteriorates, and a possible interpretation of the 15 min curve flattening could be the fatigue of the preparation. In the case of the potassium conductance, there is a progressive decrease of the conductance with time, that could also be imputable to fatigue. However, the potassium current amplitude

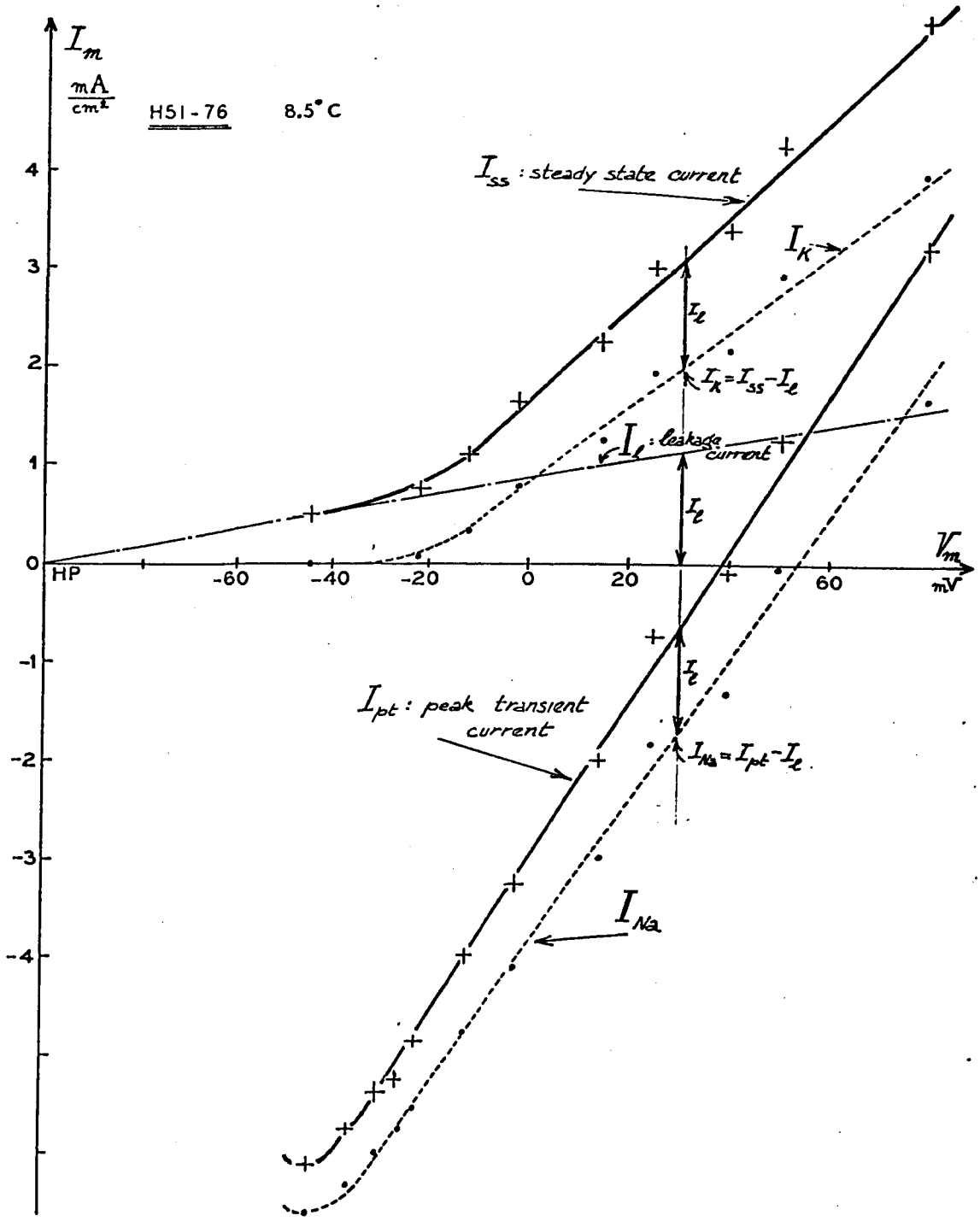

Fig. IV-16. Leakage current correction on the current-voltage relation of the lobster giant axon

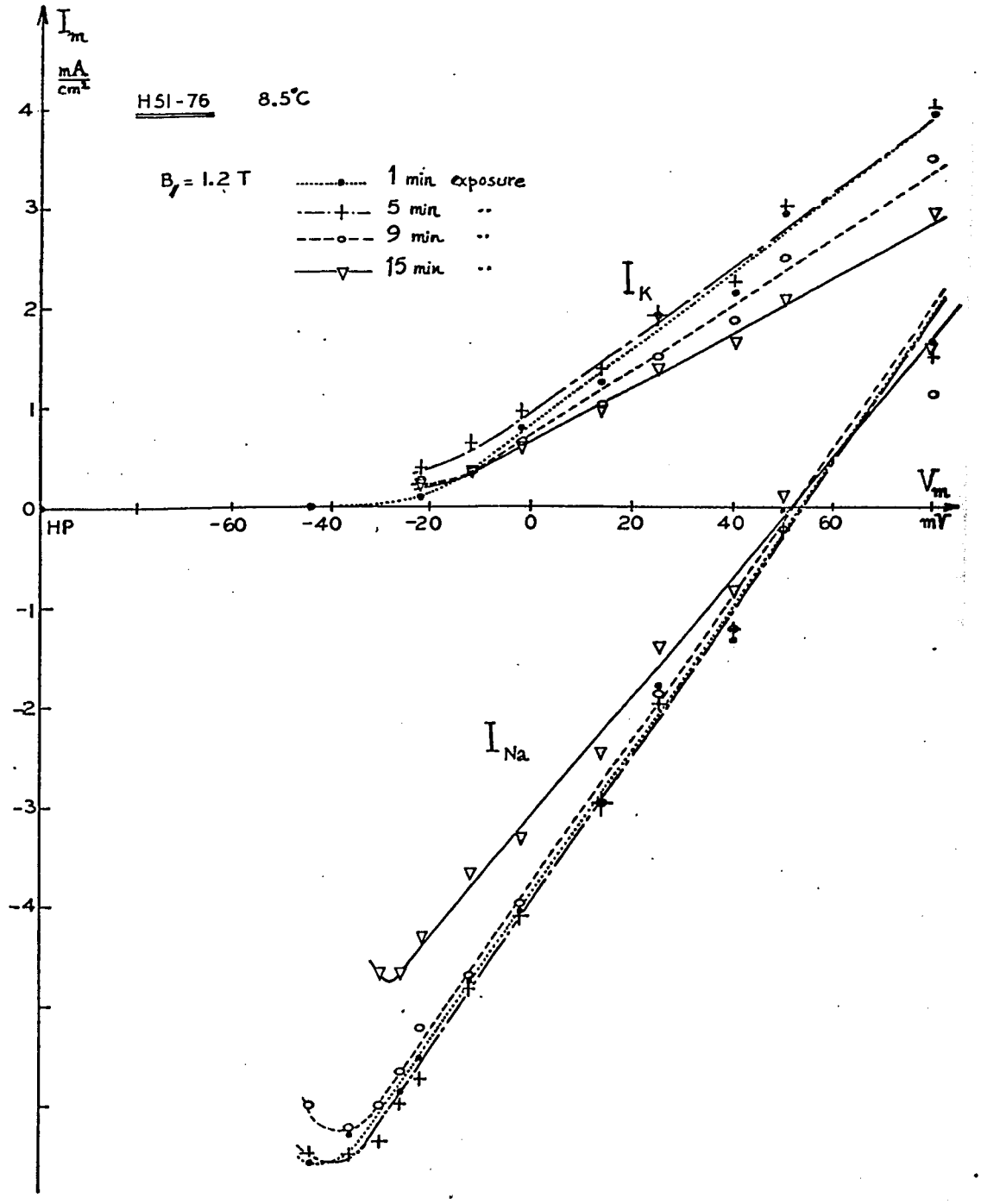

Fig. IV-17. Influence of a constant magnetic field on the current-voltage relation of the lobster giant axon (long exposure). $B_{//}$ = field parallel to axon

5 min after the beginning of exposure is higher than it was 1 min after the magnet was switched on. This corresponds to a faster repolarization of the membrane in current-clamp conditions (Julian et al., 1962b), a phenomenon that has been often recorded in this study . In fact, it was found that even during short period of time the falling phase of the action potential does not generally display a stable slope, as does the rising phase. In view of this fact, it is not possible to draw a meaningful conclusion from this potassium current amplitude change in relation to the magnetic field.

Fig. IV-18 shows the peak sodium current and the steady-state potassium current characteristics of an axon under voltage-clamp conditions at different times during a biomagnetic experiment in the perpendicular field exposure nerve chamber. Here again, there is no striking evidence of any long term biomagnetic effects. The sodium current amplitude increases with time, while the sodium conductance remains approximately constant. These variations are within the range of experimental and data processing errors. The potassium current curves are reasonably well grouped and identical in shape. Here again, it is not possible to decide whether the magnetic field is responsible for the small slope variations or not.

The long term exposure voltage-clamp experiments establish that a constant magnetic field does not influence some of the normal functions of the lobster axon membrane in a detectable manner. If any biomagnetic response is present, it might be hidden by other purely physiological phenomena, among which the relatively fast decay of the axon plays probably a predominant role.

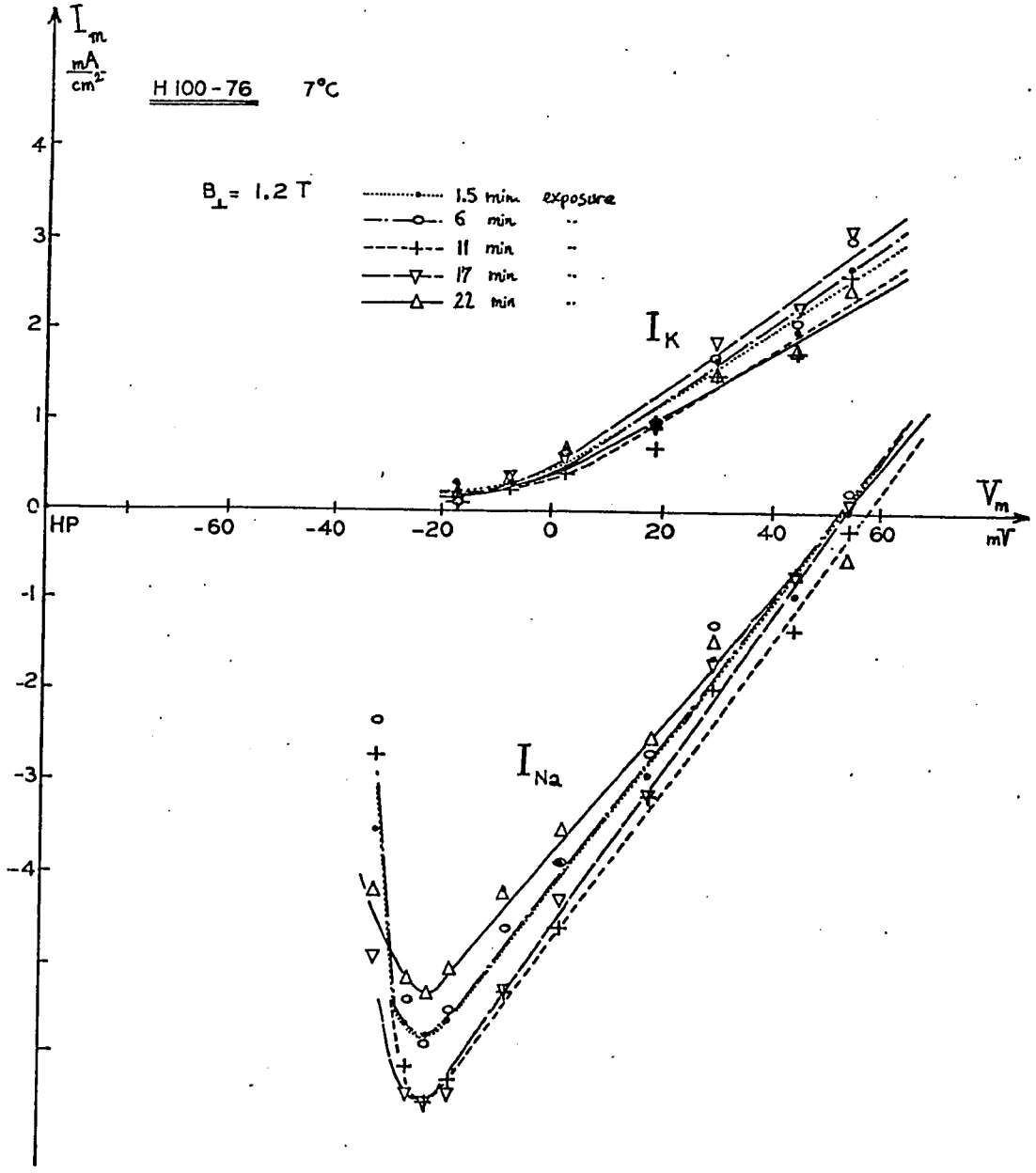

Fig. IV-18. Influence of a constant magnetic field on the current-voltage relation of the lobster giant axon (long exposure). $B_\perp$ = field perpendicular to axon

IV.4 Conclusions

From the results presented in this chapter it is apparent that no measurable interaction between a constant 1.2 T magnetic field and the lobster circumesophageal connective could be found. Neither impulse velocities nor membrane conductances were affected by the field in either exposure configuration.

These rather negative results will be discussed in Chapter V.

CHAPTER V

DISCUSSION

CHAPITRE V

DISCUSSION

Résumé : les résultats concernant les mesures de vitesse de conduction sont comparés à ceux obtenus par d'autres investigateurs. Une tentative d'interprétation des différences observées est faite et certaines hypothèses sont avancées. On fournit une analyse de la fiabilité de la méthode choisie pour ces expériences de biomagnétisme en potentiel imposé, en particulier pour ce qui concerne les expositions prolongées au champ magnétique. Les résultats obtenus quant au potentiel membranaire, au potentiel de repos et au courant transmembranaire sont reliés à ceux obtenus lors des mesures de vitesse de conduction. Cette relation permet d'une part de vérifier l'accord entre les résultats obtenus dans les différentes mesures, et d'autre part d'avancer certaines hypothèses quant aux paramètres qui pourraient être influencés par le champ magnétique.

CHAPTER V

DISCUSSION

The negative results reported in the "Results" chapter are very intriguing. A strong magnetic field such as the one used in the present work could have been expected to affect the normal nerve behaviour. Furthermore, it should have been possible to (i) confirm the results established by other authors and (ii) get a deeper insight of the underlying membrane phenomena by the use of a powerful electrophysiological tool such as the voltage-clamp technique. Unfortunately, this has not been the case. It is therefore important to discuss the validity of the results obtained, the adequacy of the approach selected for this work, and to relate the findings to the published material.

V.1 Conduction velocity measurements

Difficulties in performing reliable velocity measurements on nerve trunks are inherent to the method of extracellular recording. The relative positions of the external recording electrodes, the nerve, and the active fibres within the nerve affect the shape and the amplitude of the action potential of the nerve, even under supramaximal stimulation conditions (Brown, 1968). Diphasic recordings are difficult to interpret, particularly if the distance between consecutive electrodes is of the same order of magnitude as the length constant of the fastest fibres. In the experiments recorded here, seven electrodes were used on a 3.5 cm length of nerve. These might have caused some recording problems.

Although temperature regulation could have been more

accurate, this did not lead to serious problems because temperature corrections never exceeding 8% were made which were generally of lesser amplitude than the systematic errors taken into account when collecting data from the recording photographs. The validity of these temperature corrections may be debatable, because there is no evidence that Huxley's dimensional analysis (Huxley, 1959) can be used with a nerve exposed to a magnetic field, or even that the Hodgkin-Huxley nerve model (Hodgkin et al., 1952b) is valid in this case.

Notwithstanding the difficulties mentioned above, the findings of the experiments described here contrast with the results reported by Reno (1969) who found that a magnetic field of comparable intensity (1.16 T) significantly increased the conduction velocity of the frog sciatic nerve , particularly in the parallel configuration. His findings were the followings. A velocity increase was observed after a 5 to 6 min delay consecutive to switching on the magnetic field. Impulse velocity in the parallel configuration increased progressively, to reach about 130% of its value before exposure. Very little change was observed in the perpendicular configuration. After the magnetic field had been turned off, the velocity in the parallel configuration continued to increase, to reach values as high as 160% of those recorded before exposure. This after-effect lasted for 16 to 18 min after the end of the exposure period.

Reno's results could not be reproduced here. According to our conduction velocity experiments on the lobster nerve under magnetic exposure (refer to Section IV.2.4, Chapter IV), the maximum velocity change recorded was under 15% of the pre-exposure velocity value; the corresponding error was approximately 10%. There was no evidence of orientation dependence,

delayed action or after-effects on conduction velocity.

In addition to the fact that the experiments were conducted on lobster nerves instead of frog sciatic nerves, other differences between Reno's work and the investigation reported appear here: Reno used a more homogeneous magnetic field (0.1 T/m and 0.2 T/m vs 15 T/m and 2 T/m for perpendicular and parallel exposure, respectively), and he also achieved a better temperature regulation (0.3^{o}C variations vs 1.5^{o}C in this study).

One explanation to the differences between Reno's results and those reported in the present investigation could be the structural difference between the frog sciatic nerve and the lobster connective. The former is surrounded by a regular spiral wrapping of myelin interrupted at regular intervals along the nerve at places called nodes of Ranvier, while the latter possesses a loose and unorganized surrounding layer of Schwann cells (see Chapter II, Section II.1). In order to check this hypothesis, three experiments on frog sciatic nerves were conducted,but here again no statistically significant changes in conduction velocity could be detected. These experiments, however, might have little significance, because they were carried out in the lobster nerve chambers and, the interelectrode distance being relatively short, the stimulus artifact was rather large. Consequently, these few frog velocity measurements might not be as reliable as those reported by Reno. More experimental work will be needed on the frog nerve in order to reproduce Reno's results and assess the value of the hypothesis explaining the difference between lobster and frog nerve biomagnetic responses by the possible action of the magnetic field on the myelin wrapping of frog nerves. It should also be noted that differences in magnetic field homogeneity might account

for the discrepancies between Reno's findings and those reported in this study.

However, this work confirms some of the results reported by Erdman (1955) in the case of the frog sciatic nerve exposed to a transversal constant magnetic field. He has established that a 10 min exposure to 1.7 T did not affect nerve impulse velocity. Unfortunately, his report lacks details on temperature regulation and field homogeneity, and there are no results in the case of longer exposure and parallel exposure experiments.

V.2. Sucrose-gap experiments.

V.2.1. Confidence in result interpretation

Short exposure experiments usually provided reliable results. When the axon patch under investigation was kept for less than 5 min in the nodal area between the two sucrose streams, it usually displayed reproductible responses under normal physiological conditions, i.e with no magnetic field. This was verified by the good superposition of traces on the storage oscilloscope screen, although the reading of superposed traces on this instrument is rather imprecise (between 5 and 10%). In order to increase precision, the traces were also recorded on 35 mm film and projected on a screen. With this enlargement procedure, it was possible to reduce reading errors to less than the 5% figure corresponding to instrumentation errors. It was therefore assumed that if recordings of the membrane voltages and currents before, during and after exposure to the magnetic field superpose evenly, or if the average between pre- and post-exposure recordings corresponds to the traces obtained during exposure, this provides enough evidence for the absence of any biomagnetic effect in either

orientation of the field with respect to the axon.

The results of long exposure experiments are more difficult to assess. The experiments were difficult to perform because nerve fibres tend to decay rapidly after 10 to 15 min spent in the sucrose gap arrangement. Only a few experiments can be considered acceptable, thus preventing any attempt to perform a statistical analysis (see Table IV-1, Chapter IV). Current-voltage relations were derived as the best way of interpreting data variations, because successive recordings did not generally superpose, due to the progressive aging of the preparation. In addition to the fatigue phenomenon, the potassium currents appeared to be rather variable in these long term experiments, both with and without magnetic field exposure. This could be observed on the I vs V graphs and also on the action potential recordings where the repolarizing phase often showed a variable slope. This instability of unknown origin could lead to further investigation.

Care has to be taken when drawing conclusions from these long term exposure experiments. The experimental error on membrane potentials and transmembrane currents is estimated to be between 10 and 15%, due to the strict criteria adopted to select the experiments (Section IV.3.1.3, Chapter IV). In other words, the influence of a constant magnetic field on membrane parameters cannot be assessed if their changes are less than 15% in these long term exposure experiments.

V.2.2 Interpretation

The negative results obtained in these exploratory experiments can be interpreted at the phenomenological level. They establish that within the limits of experimental errors magnetic

fields do not interfere with normal kinetics of ionic currents crossing the nerve membrane during the excitation process. In other words, the transmembrane conductances, as defined by Hodgkin et al. (1952b), can be described by the same voltage and time dependent relations as they are in normal conditions. This is true for the sodium and potassium conductances, assuming that the leakage conductance itself remains unaffected by the magnetic field. This assumption was implicitly made in Section IV.3.3 of Chapter IV, when leakage current corrections were made. Although the leakage current behaviour has not been fully investigated, it seems reasonable to think that leakage current variations, almost inexistent in the short term exposure experiments, are simply related to fatigue when longer exposure periods are used. However, an interaction between constant magnetic fields and leakage conductance cannot be ruled out. This particular aspect of the problem could lead to further research.

An interpretation of the results can also be attempted at the molecular level, although it is highly speculative, because of the still unknown character of the membrane structure (Chapt. II, Sect. II.3). Three different aspects must be analyzed in relation with the absence of biomagnetic response from the nerve membrane: the ion-field interaction, the effect of the field on membrane structure, and its effect on the gating mechanisms.

The results obtained here confirm the theoretical speculations showing that magnetic fields in the one Tesla range cannot deflect ion trajectories across biological membranes in a detectable manner (Valentinuzzi, 1965). On the other hand, Liboff's hypothesis (Liboff, 1969) explaining the possible effect of fields on charged particle diffusion in the presence of an electric field (corresponding

to a charged axoplasm) parallel to the particle trajectory, does not appear to be verified by the present study.

Considering now the membrane itself, the results of voltage-clamp experiments do not bring additional evidence of its liquid-crystalline structure (Labes, 1966). If reorientation of anisotropic components occurs under magnetic field exposure, the amplitude of this phenomenon is probably too small to be detected by standard voltage-clamp procedure. However, it cannot be excluded that a more refined technique could lead to interesting results. The fact remains that if physical pores or channels exist in the membrane, their number and size are not markedly affected by the hypothetical re-orientation of the membrane components, otherwise a dramatic change in amplitude and time course of the transmembrane currents would have been recorded.

The evidence of macromolecule conformational changes associated with gating has been reviewed in Chapter II, Section II.3.3. If torques of magnetic origin were to act on the non-spherical diamagnetic macromolecules, this might contribute to the gating process, and this would indirectly modify the detected electrical response of the membrane. However, the results of the present investigation do not provide any evidence of a magnetic effect on the gating process.

V.3 General discussion of the results

It is now important to relate the results obtained in velocity and in membrane experiments and to evaluate their consistency. From this, additional conclusions might be drawn.

Velocity and membrane parameters are not independent. Pickard (1966) established a mathematical expression relating the impulse velocity to some of the membrane parameters in the case

of the unmedullated axon:

$$\theta = \frac{4}{3} \left\{ \frac{G_o}{C^3 (r_1 + r_2)^2} \left(\frac{V_T}{2V_R - V_T} \right)^3 \right\}^{\frac{1}{4}} \qquad \text{(Equ. 6)}$$

with

θ = impulse velocity (m/s)

G_o = average maximum rate of rise of the sodium conductance (S/ms)

C = membrane capacity (F/m)

r_1 = axoplasmic resistance (Ω/m)

r_2 = external medium resistance (Ω/m)

V_T = threshold voltage (10^{-3} x V)

V_R = resting potential (10^{-3} x V)

This relation has been established for the squid axon. It is also believed to be valid for other invertebrate unmyelinated fibres (Pickard, 1966).

The sensitivity of velocity to parameter changes can then be derived:

$$\frac{\Delta\theta}{\theta} = \frac{1}{4}\frac{\Delta G_o}{G_o} - \frac{3}{4}\frac{\Delta C}{C} - \frac{1}{2}\frac{\Delta(r_1+r_2)}{r_1+r_2} + \frac{3}{2}\frac{V_R}{2V_R - V_T}\left(\frac{\Delta V_T}{V_T} - \frac{\Delta V_R}{V_R}\right)$$

(Equ. 7)

Fig. V-1 represents the velocity changes associated with each individual parameter variation in Equation 7, assuming the others to be constant. The $\pm$ 10% horizontal lines represent the experimental range for which it was concluded that there is no velocity change under magnetic exposure. As can be seen from the graph, assuming that G_o has been measured with a 5% precision

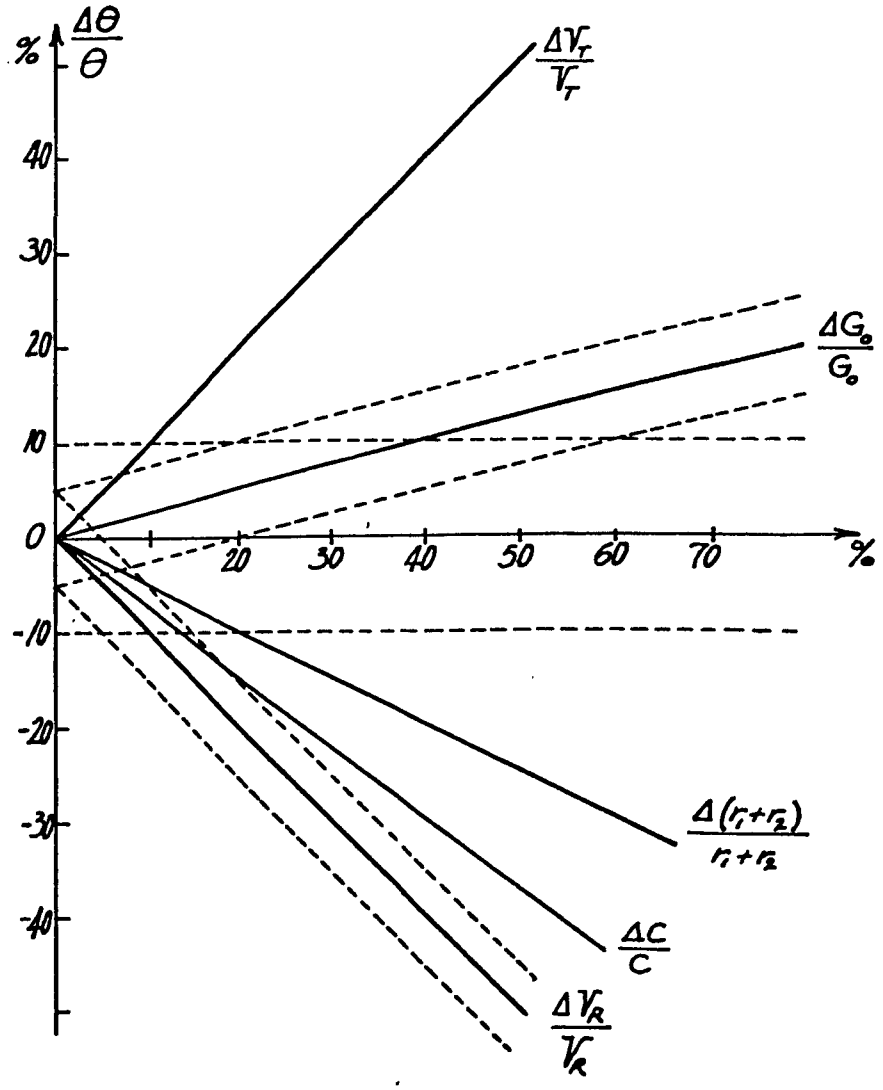

Fig. V-1. Impulse velocity variation as a function of individual electrophysiological parameter variations (V_T, V_R, G_o, C and $r_1 + r_2$). Dashed lines represent the limits in which these variations are measured

(represented by the dotted lines parallel to the G_o line), no velocity change should be detected as long as G_o varies by less than 60%. This simple analysis confirms the consistency of the results obtained with the velocity and sucrose gap experiments reported here: no velocity changes (within 15% maximum and 10% most of the time) and no conductance changes (within 5% for short exposure experiments) could be recorded by independent measurements under magnetic exposure conditions. The same argument can be used to show the consistency between velocity and resting potential measured during this investigation.

No biomagnetic measurements were made on the membrane capacity, the threshold voltage and the longitudinal resistances of the intra- and extracellular media. Observation of the graph (Fig. V-1) shows that velocity is quite sensitive to threshold voltage variations, but less to capacity changes, and even less to longitudinal resistance changes. It would nevertheless be interesting to investigate the influence of a constant magnetic field upon these four parameters.

Assuming that θ, V_R and G_o remain absolutely unaffected by magnetic fields, the following relation, derived from Equation 7, should hold:

$$3\frac{\Delta C}{C} + 2\frac{\Delta(r_1+r_2)}{r_1+r_2} = 6\frac{V_R}{2V_R-V_T} \times \frac{\Delta V_T}{V_T} \qquad \text{(Equ. 8)}$$

This result is interesting and could lead to a relatively simple experimental verification.

To summarize, the results of the present investigation do not establish the firm evidence that magnetic fields have absolutely no effect on nerve fibres. However, they do establish with a reasonable degree of confidence and within an acceptable experimental

error range that the resting potential, the sodium and potassium conductances, and the nerve impulse velocity are unaffected by a constant magnetic field exposure. Furthermore, with the help of equation 8, the study of biomagnetic responses of nerve axons can now be reduced to the investigation of the interaction of magnetic fields with membrane capacity, threshold voltage and longitudinal resistances.

V.4 Assessment of methods

Considerable effort has been put in attempting to develop an appropriate tool for biomagnetic research. It was also hoped that this tool might be used in membrane biophysics. In view of the present results, it is necessary to evaluate the approach, the tool and its use in relation to biomagnetic and biophysical research.

As stated in Chapter I, the experimental approach to the investigation of the influence of magnetic fields on living systems should be as rigorous as possible, even in the case of pilot studies. This involves using well-established techniques and suitable corresponding modifications to adapt them to biomagnetic work. In the case of the nervous system, the voltage-clamp technique is most probably the tool to use. Velocity measurements on whole nerve trunks are not as good, because data interpretation is difficult and brings very little information regarding the underlying phenomena. However, they are easier to make and, in exploratory work, they can provide some hints for planning more sophisticated experiments. In addition, they might be less detrimental to the nerve than the voltage-clamp method in long term exposure experiments.

One can argue about the choice of the lobster circumesophageal connective for this study. It was found that velocity measurements on this sample did not provide such clean diphasic compound action potentials as those recorded from other well-known preparations. This of course was the source of the many data processing difficulties already mentioned (Chapt. IV, Sect. IV.2.2). It is expected that conduction velocity would be better and more reliably measured on single nerve fibres, using micro-electrodes or the technique developed by Jacob (1973), where the extracellular resistance is increased by electronic means. Monophasic recording could be performed on a single lobster axon perfused by temperature controlled sea water.

The velocity studies were planned to be performed in conjunction with voltage-clamp studies. There is limited choice of specimens offering a reasonable length of nerve and easily dissected giant axons, particularly for the inland laboratory investigator. The lobster nerve is probably the best available preparation for the present work: the connective is about 3.5 cm long and axon diameters can be as wide as 135 μm, which is at least 4 times larger than the frog sciatic axon. In addition, it was thought that an unmedullated nerve would be more adequate for this study, because of its simpler anatomical structure.

The double sucrose gap method was selected for different reasons. It has been developed for the lobster giant axon and results using this method under normal physiological conditions are well established (Julian et al., 1962a,b). It has been used successfully in biophysical research involving the influence of ultraviolet rays on the axonal membrane (Oxford et al., 1975b). It does not require the use of internal longitudinal electrodes or microelectrodes, which saves considerable space. In fact, the bulky

micromanipulators that are always associated with microelectrodes would have been impossible to use in the restricted area between the coils of the electromagnet.

However, the double sucrose gap method is far from being satisfactory in many respects. The main problem is the short life of the axon when placed in this apparatus, and its rather unreliable behaviour after a couple of minutes: unsteady resting potentials, variable repolarization after stimulation, high leakage currents are often recorded. Calcium depletion around the axon in the sucrose area is probably responsible for many of these difficulties. An additional explanation could be found in the rather high mechanical stress to which the axon is subjected. Actually, although the dissection can be made as delicately as possible, it is followed by the difficult step of inserting the axon into the nerve canal of the experimental chamber. Due to the special geometry of this chamber that has to fit between the coils of the magnet, there is quite a large distance between the lateral pool where the axon is tied to the pulling nylon thread, and the nerve canal. Thus, pulling the nerve is a lengthy, and possibly damaging procedure. Finally, the part of the axon located in the nodal area of the nerve chamber tends to be pushed by the flowing solutions against the edges corresponding to the intersection between the nerve canal and the test solution canal. These edges have been carefully polished under microscopic observation, but it cannot be excluded that micropuncture of the membrane could occur in certain instances: this would accelerate the axon decay.

In any case, it is believed that the double sucrose gap method is probably reliable enough for these preliminary experiments.

Recent advances (see Chapter II, Section II.2.4) have been made which might improve this technique in order to achieve more reliable measurements.

The methods chosen for carrying the present biomagnetic investigation provide acceptable results for such an exploratory study. A careful approach should be used when interpreting these results, but conclusions about magnetic effects can be drawn with a reasonable degree of confidence. In addition, velocity and sucrose gap measurements allow a reduction of the size of the biomagnetic problem under scrutiny. However, there is no immediate evidence of the usefulness of the chosen biomagnetic approach as an investigation tool in membrane biophysics.

CHAPTER VI

CONCLUSIONS

CHAPITRE VI

CONCLUSIONS

Résumé : Ce dernier chapitre contient un sommaire des résultats obtenus dans cette étude et suggère quelques projets de recherche pour le futur.

Les principales conclusions sont les suivantes:

a) Un champ magnétique continu de 1.2 T ne produit pas d'effets détectables sur la vitesse de propagation de l'influx nerveux du nerf péri-oesophageal du homard. Il n'influe pas sur les potentiels et les courants de la membrane de l'axone géant du homard lorsque le temps d'exposition est inférieur à cinq minutes. Pour des expositions plus longues, les résultats sont identiques, quoique à un moindre degré de certitude dans le cas des mesures en potentiel imposé.

b) Les méthodes adoptées constituent une amélioration des différentes approches expérimentales utilisées en biomagnétisme, dans le sens d'une rigueur plus grande. Par contre, il n'est pas prouvé que l'approche biomagnétique des problèmes de biophysique membranaire donne des résultats intéressants sur le plan des relations structuro-fonctionnelles des membranes excitables.

On propose ensuite d'étudier la capacité, les courants longitudinaux et le potentiel de seuil d'excitation sous influence du champ magnétique continu intense, ainsi que les

courants transmembranaires de fuite. On indique aussi qu'il serait intéressant d'étudier la réponse biomagnétique d'autres tissus nerveux, d'entreprendre des expériences de plus longue durée sur une cellule nerveuse provenant d'un animal pré-exposé au champ magnétique in vivo, et d'utiliser des méthodes de mesure plus raffinées afin de déceler d'éventuelles faibles variations des paramètres mesurés au cours des expériences pilotes décrites dans cette thèse. On pourrait aussi faire des expériences biomagnétiques en champ lentement modulé. Enfin, on envisage la possibilité d'un traitement théorique du problème de l'interaction d'un champ magnétique et d'un conducteur volumique possédant les propriétés de l'axone nerveux.

CHAPTER VI
CONCLUSIONS

This concluding chapter presents a summary of the work that has been done, and suggestions for further research.

VI.1 Summary

The following conclusions can be drawn from the investigation described in this thesis:

1) A 1.2 T constant magnetic field has no detectable influence upon the conduction velocity of the circumesophageal connective of the lobster. This is true when the field is applied either perpendicularly or parallel to the nerve.

2) A 1.2 T constant magnetic field has no detectable influence upon the resting potential, the membrane action potential and the transmembrane current of the giant axon of the lobster. This is true for parallel and perpendicular field orientation with respect to the axon, and short exposure experiments (less than 5 min).

3) Long exposure experiments (more than 5 min) are not totally conclusive at membrane level. However, it seems that the resting potential, the membrane action potential, and the sodium and potassium conductances of the lobster giant axon are not affected by long exposure to a 1.2 T constant magnetic field.

4) The study reported here is the first biomagnetic investigation using the voltage-clamp technique. The exploratory experiments reported in the present work confirm the value of this powerful technique as a useful tool for more rigorous biomagnetic investigations.

5) No supporting evidence has been found for the possible use of biomagnetic investigations in the field of membrane biophysics, with special reference to the elucidation of structure-function relationships of membranes.

VI.2 Suggestions for further research

In the "Discussion" part (Chapt. V, Sect. V.3), it has been mentioned that the influence of a magnetic field on the capacity, on the longitudinal resistances and on the threshold of the nerve fibre also need to be investigated, in order to reach a final conclusion regarding the biomagnetic response of nerves.

Improvements in the present voltage-clamp technique could increase the lifetime of the preparation. These could include the addition of calcium ions to the sucrose solution, a modified system for insertion of the axon into the nerve canal, and possibly the use of slow voltage-clamp command signals, like ramps or sine waves (Fishman, 1969; Palti et al., 1969), which are less detrimental to the axon. A finer sweep of the clamp voltages around threshold would yield more information about the descending part of the sodium conductance. It might also be interesting to undertake a separate study of the leakage conductance. And

finally, a more refined data processing system could be implemented with on-line data processing in both time and frequency domains.

At this stage, it does not seem that more research should be made in order to establish if magnetic fields influence the gating mechanisms or the channels themselves, because the voltage-clamp apparatus used for the present study would have to be adapted to membrane current noise measurements and gating current recording. However results from this kind of investigations might be interesting in relation with small biomagnetic effects. They could also bring a better understanding of the phenomena underlying nerve excitation.

It would also be of interest to study the biomagnetic response of other biological membranes, such as the frog nerve membrane. The hypothesis proposed here (Section IV. 1, Chapter IV) regarding the role of myelin in the interaction between a magnetic field and the nerve could therefore be tested experimentally.

Different biomagnetic experiments could also be tried. Live lobsters kept restrained in an aquarium between the pole pieces of a large magnet could be pre-exposed to the magnetic field for several days or weeks, and then the above mentioned experiments could be performed. This would bring information about nervous response following very long exposure periods in a constant magnetic field.

The use of very low frequency modulation of the magnetic field amplitude is possible with the experimental equipment and sample similar to those described in this work. Low frequency magnetic fields have been shown to have an influence on excitable structures (Bittman-Coros et al., 1969; Irwin et al., 1970).

It might be interesting to test this biomagnetic response with the present equipment.

Finally, a theoretical study of the active nerve fibre in a magnetic field might be undertaken, using a modified version of the approach proposed by Plonsey (1974). Such an analysis could lead to interesting predictions, that in turn might be verified experimentally.

LISTE DES ANNEXES

APPENDIX A.1

PERFUSION SOLUTIONS

The lobster physiological solution is prepared with the following salts in bidistilled water (Dalton, 1958; Julian et al., 1962a):

Sodium chloride	27.20 g/l
Potassium chloride	0.74 g/l
Calcium chloride (anhydrous)	2.77 g/l
Magnesium chloride (anhydrous)	0.38 g/l
Magnesium sulfate	0.48 g/l

The pH value is determined before each experiment and adjusted between 7.3 and 7.5 with a few drops of hydrochloric acid (0.1N) or Tris (hydroxy-methyl-amino-methane, 0.05N).

The membrane depolarizing agent is obtained as follows:

Potassium chloride	37.30 g/l
Calcium chloride	2.77 g/l

in bidistilled water.

The insulating sucrose solution (248.17 g/l) is prepared as described in Appendix A.2.

APPENDIX A.2

PREPARATION OF AN ION-FREE SUCROSE SOLUTION BY MEANS OF AN ION-EXCHANGE COLUMN

The starting solution, with sucrose concentration of 725/ mM/l (or 248.17 g/l) is prepared from Analar sucrose (BDH Chemicals) and demineralized water. This solution is passed through a mixed bed column filled with a cation exchanger (Amberlite resin IRC-50(H), BDH Chemicals) and an anion exchanger (Amberlite resin IRA-410, BDH Chemicals) mixed in a 1.5: 1 ratio. The resistivity of this purified solution is greater than 2-3 MΩ-cm , which proved to be sufficient for our experimental purposes. Even when kept refrigerated, this solution has to be used within a week, otherwise contamination causes a drop in the resistivity.

Preparing the column

The ion exchange column is shown in Figure A.2-1. The solution to be purified is simply fed through the column by gravity, and the flow rate is controlled by means of the stopcock and/or by varying the elevation of the feeding flask. For particles of 16-50 mesh (our case), a flow rate of approximately 0.1 to 0.2 "bed volume"/minute proved to be optimum. Thus with a column having a "bed volume" of about 250cm^3, the flow rate is approximately 40 cm^3/min .

The resin bed is prepared as follows :

a) Mixing and conditioning. 104 g of IRC-50 and 71 g of IRA-410 are mixed together (this amount gives an approximate wet "bed volume" of 250cm^3). Distilled water is added and the mixture is allowed to stand for approximately two hours, thus letting the resins expand to their wet volume.

b) Filling the column. The column is then half filled with the wet resins. Because of their slightly different densities, the components of the resin bed show a tendency to separate, and care must be taken while filling the column to keep the mixture homogeneous. The resin bed is held in place by two fiberglass plugs.

c) Regeneration and rinsing. An upward flow of demineralized water is used to rinse the bed volume and to evacuate the foreign particles that might be found in the resin bed (the upper plug being removed). The anion exchanger IRA-410 cannot be used in its delivered form. It must be first regenerated by passing a solution of sodium hydroxyde (1 N) through the resin bed, at a flow rate of $10\,cm^3/min$. One liter of NaOH is sufficient. An upward flow is then used to backwash the resin bed in order to eliminate air bubbles and to rinse completely the regenerating solution. This backwash flow rate is adjusted so that the bed volume height approximately doubles, and rinsing is continued until the pH of the rinse water reaches a value of about 7.3. The water level must never fall below the upper surface of the bed volume, otherwise "channeling" could occur.

d) Column exhaustion. When the column is exhausted, which can be detected by the lesser resistance of the purified solution, resins are simply replaced using the procedure described in the previous paragraphs. Regenerating a mixed bed exchanging column is difficult and requires special techniques (Samuelson, 1952).

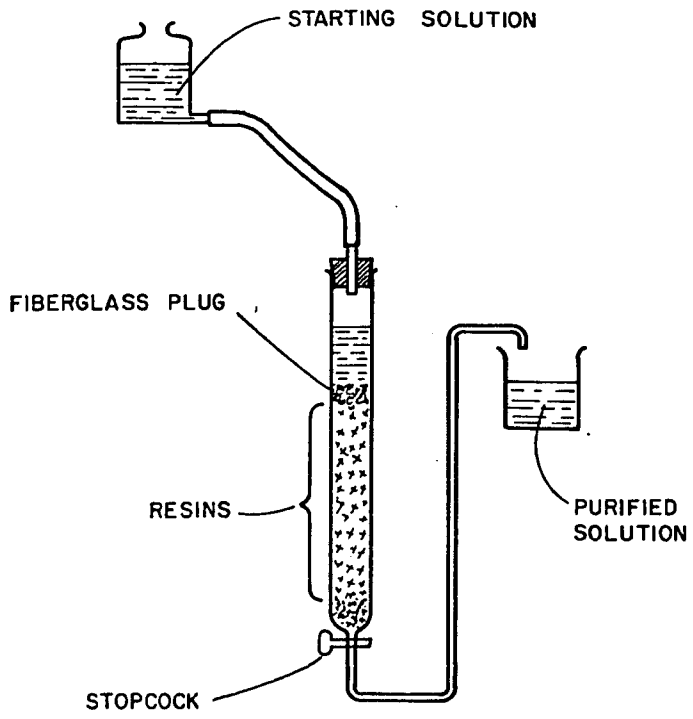

Fig. A.2-1. Ion exchange column

APPENDIX A.3

PREPARATION OF SILVER-SILVER CHLORIDE ELECTRODES

Electrodes were prepared in the following manner. Pure silver wire (1 mm in diameter), carefully cleaned in ether and hand polished, was coiled in order to be inserted in 6 mm (internal diameter) glass tubes. The surface of each coil was approximately 3 cm^2. Before insertion, the coils were cleaned in hot nitric acid and electroplated following a modified version (Fig. A.3-1) of the method described by Getzel et al. (1976). Plating took about 6 min , the current being approximately 10 mA. Usually, coils became plum coloured at the end of the silver-silver chloride deposition. They were rinsed twice in bidistilled water and inserted in the clean glass tubes. Each electrode was then placed in a stoppered test tube filled with a mixture of saturated potassium chloride (224 g/l) and agar powder (40 g/l). The mixture was slowly brought to boiling point in a double-boiler. The KCl-agar mixture became almost transparent at this stage. Test tubes were kept at 100°C for 5 min , and left to cool overnight before being broken. Electrodes were removed from the agar mass with a scalpel and carefully rinsed in saturated KCl. Connecting wires were then soldered to the unplated ends of the coils. The connections, together with the orifices through which the silver wires enter the glass tubes, were sealed with water resistant epoxy resin.

The three electrodes were prepared in the same manner. Impedance measurements made on several samples have shown that their d.c. resistance is about 300 Ω , and their 1 kHz impedance is about 500 Ω . They were immersed in artificial sea water in a dark container and stored in a refrigerator.

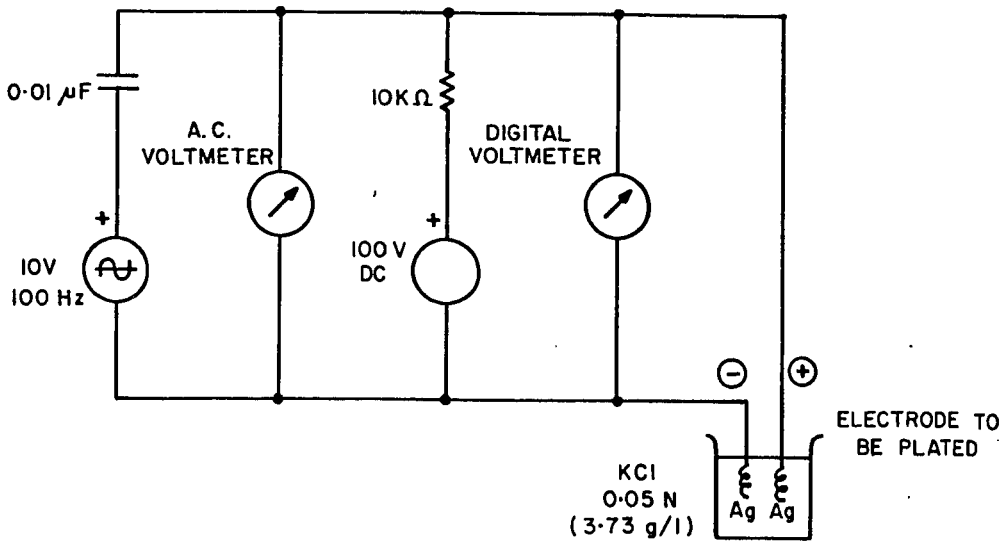

Fig. A.3-1. Plating and measuring circuit

APPENDIX A.4

CIRCUIT DIAGRAMS OF THE VOLTAGE-CLAMP CONTROL AND MEASURING SYSTEM

This appendix contains the following circuit diagrams:

Fig. A.4-1	Clock and Kymograph camera control
Fig. A.4-2	Voltage preamplifier and current-to-voltage converter
Fig. A.4-3	Buffer and control amplifiers
Fig. A.4-4	Control panel
Fig. A.4-5	Rotating command switch and pilot light control
Fig. A.4-6	Automatic command signal sequence generator (circuit diagram)
Fig. A.4-7	I vs V processor (circuit diagram)

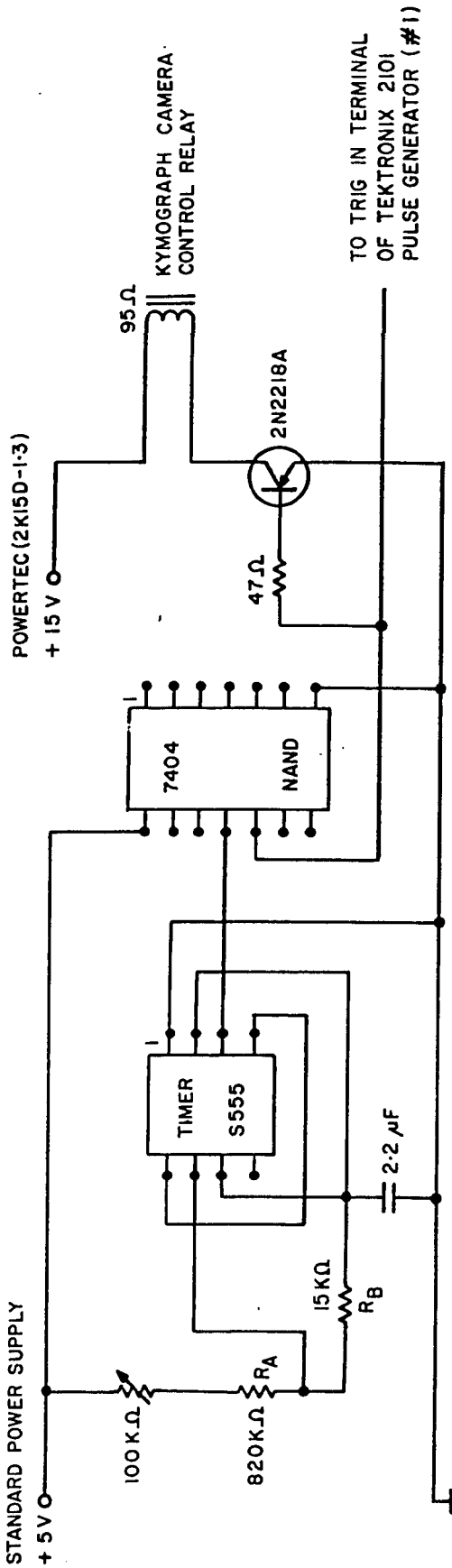

Fig. A. 4-1. Clock and Kymograph camera control

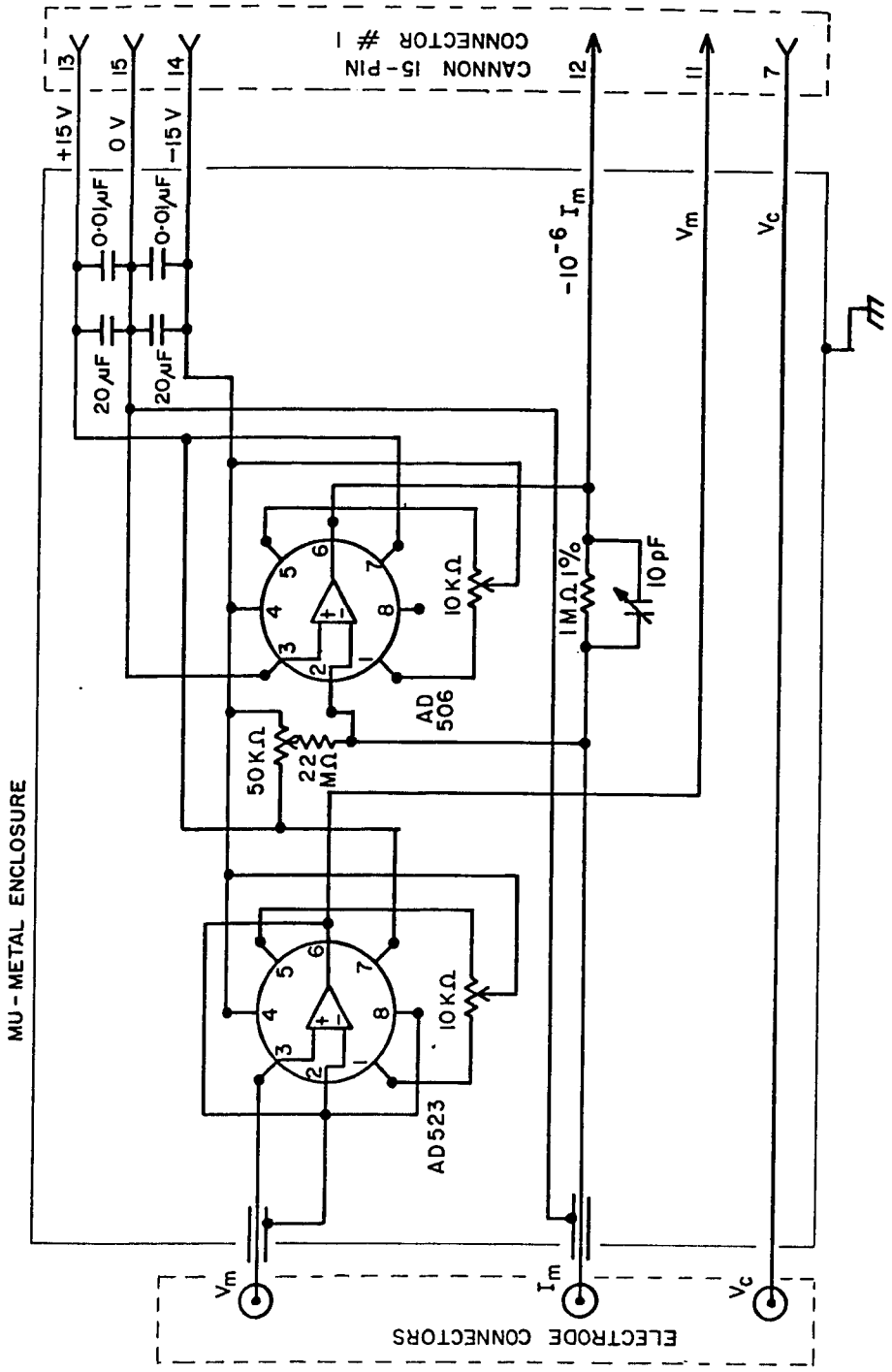

Fig. A.4-2. Voltage preamplifier and current-to-voltage converter

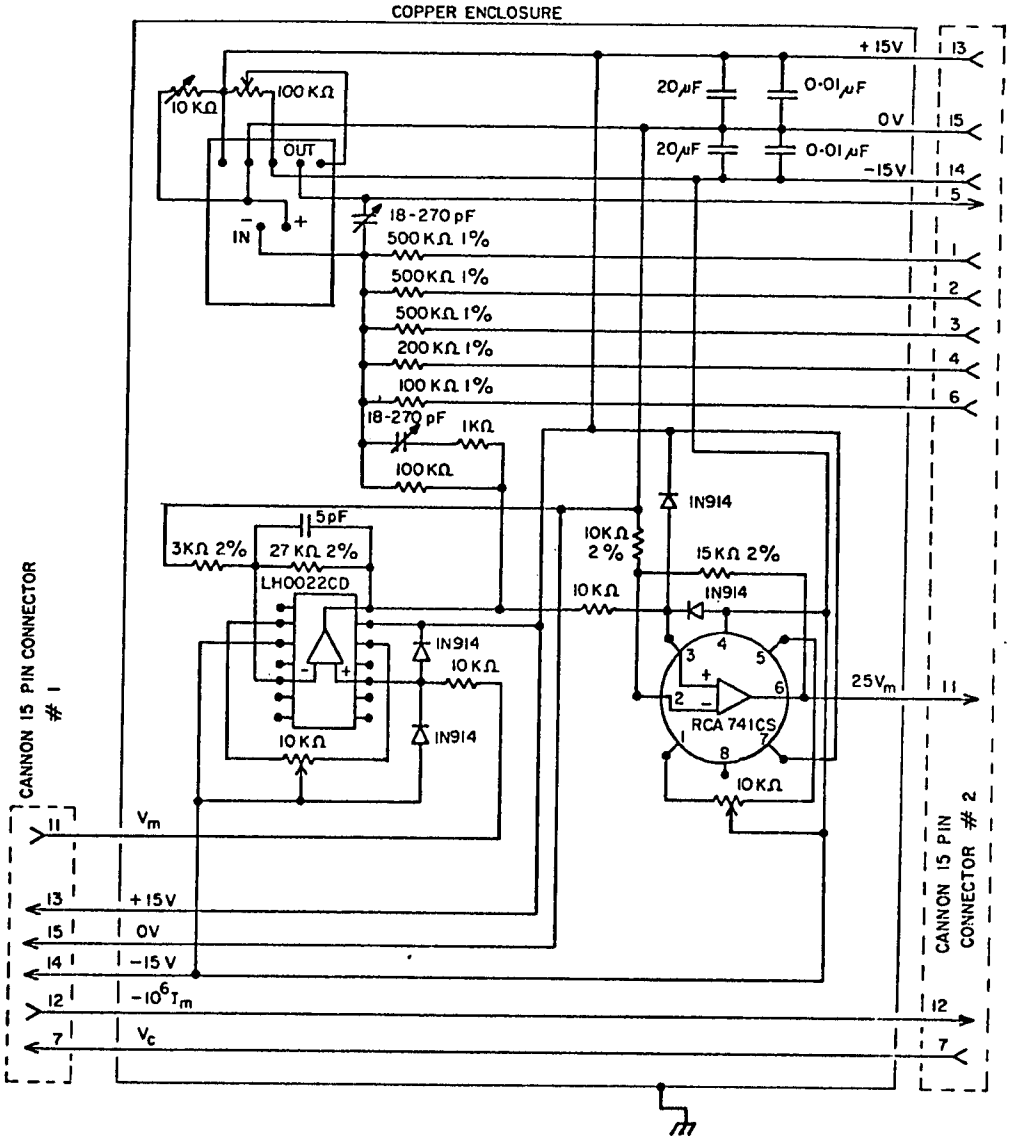

Fig. A.4-3. Buffer and control amplifiers

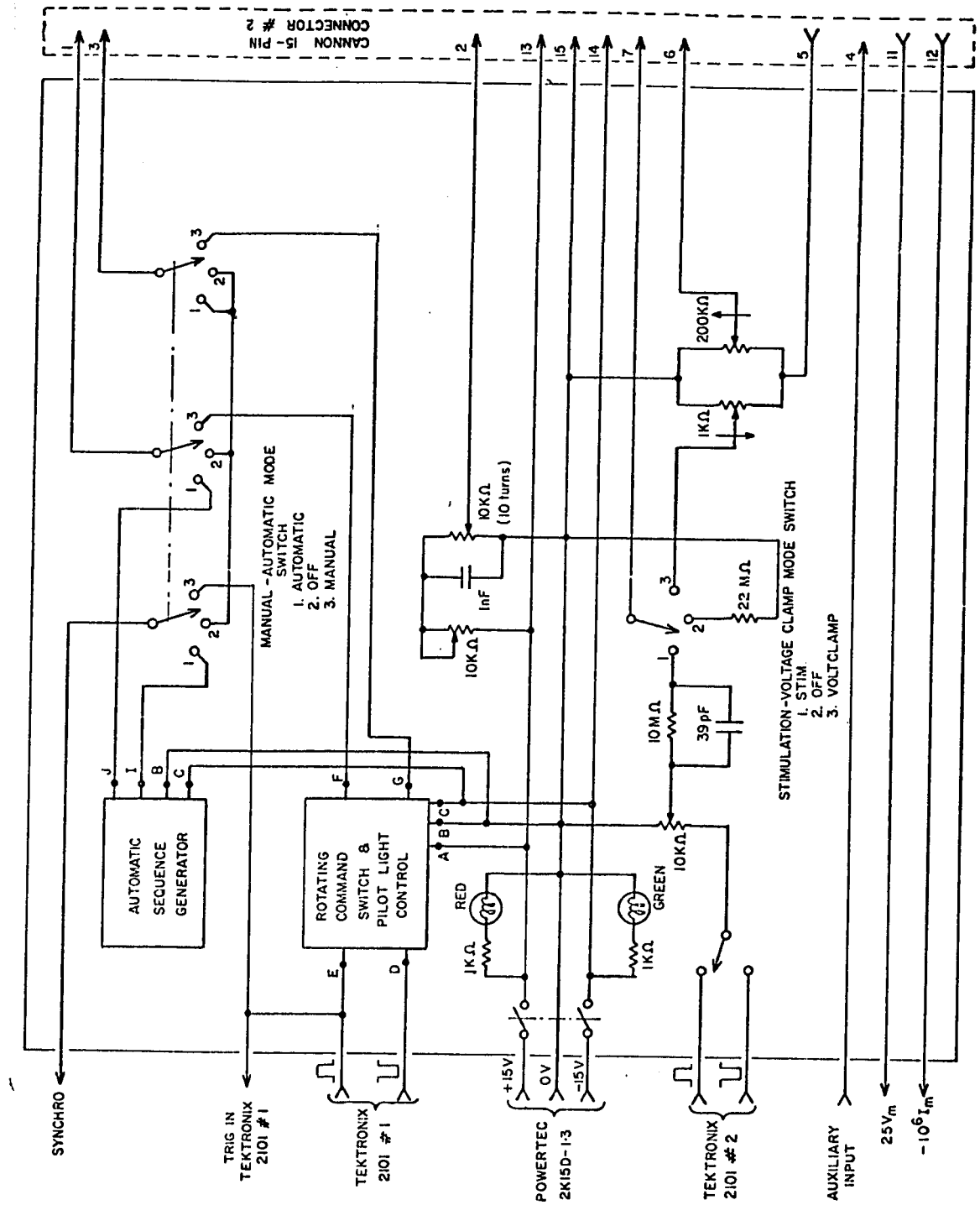

Fig. A.4-4 Control panel

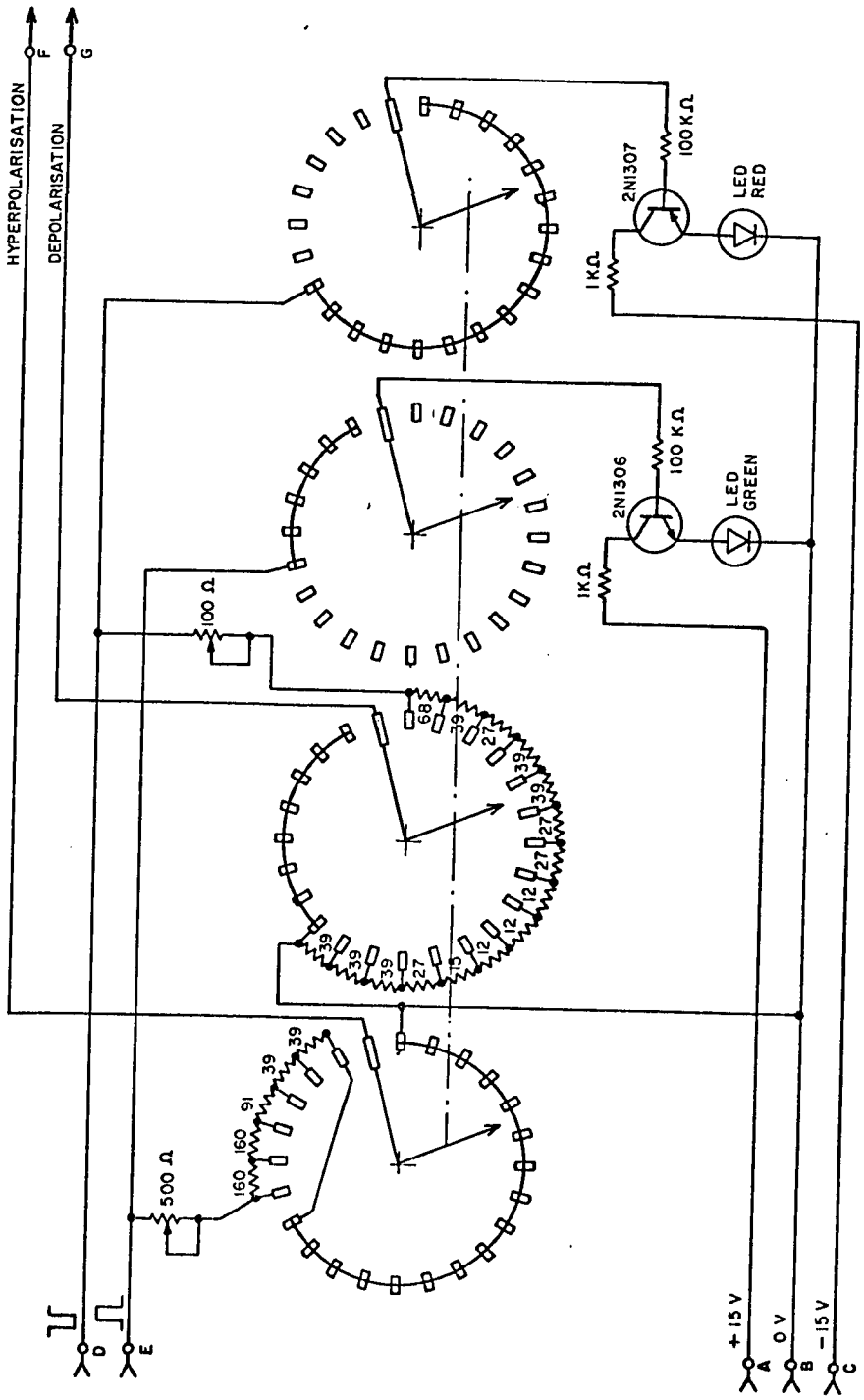

Fig. A.4-5. Rotating command switch and pilot light control

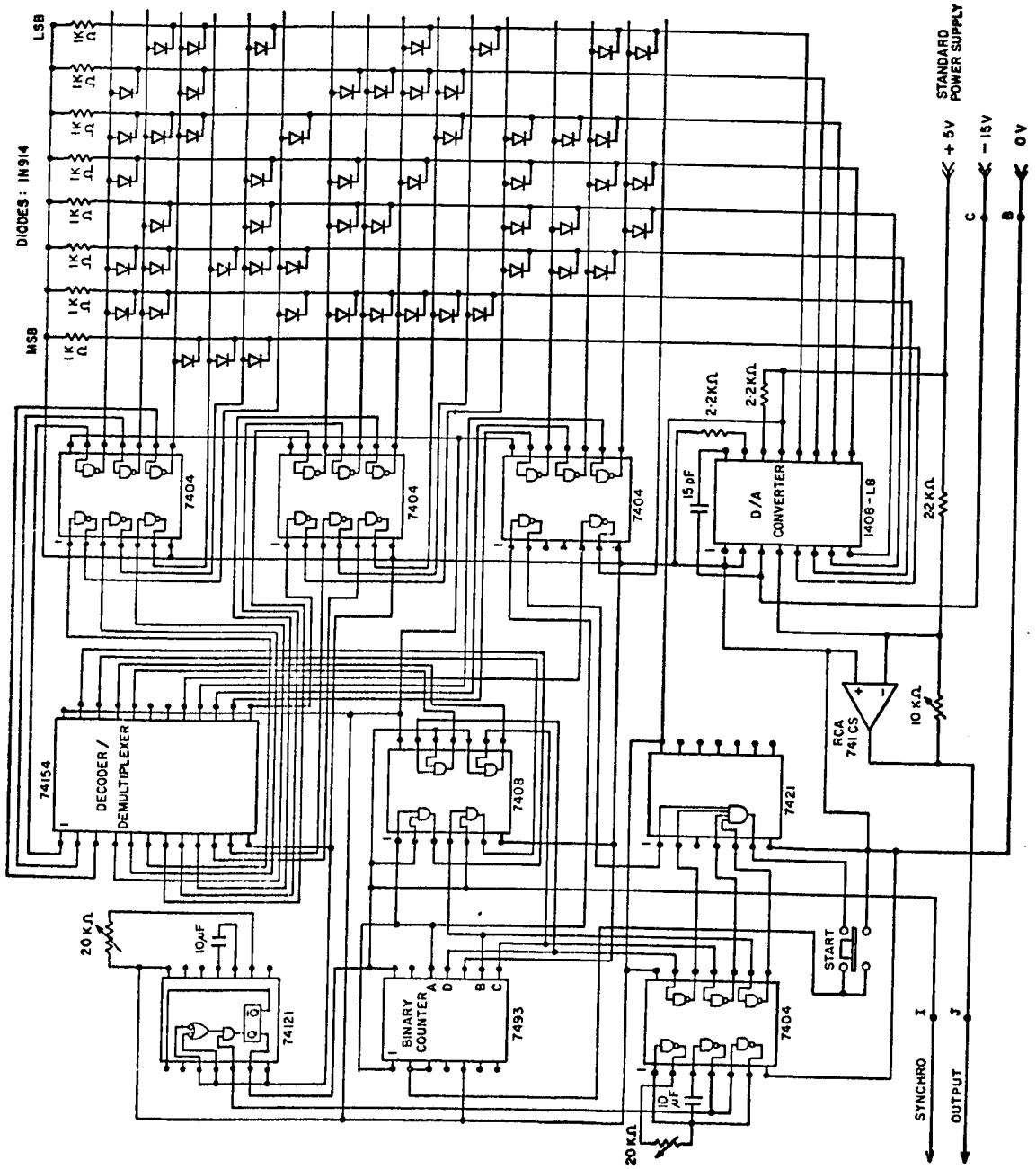

Fig. A.4-6. Automatic command signal sequence generator (circuit diagram)

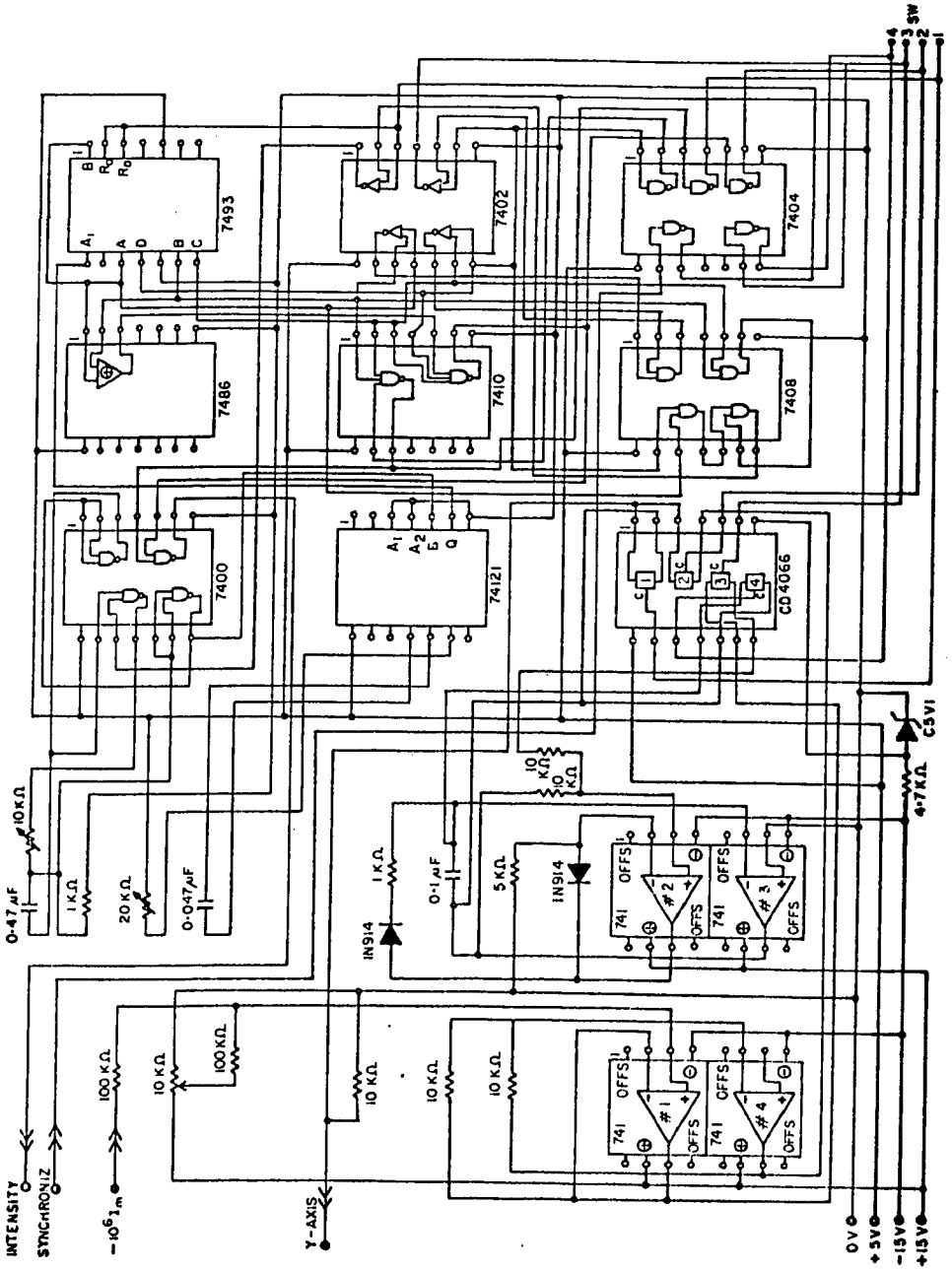

Fig. A.4-7. I vs V processor (circuit diagram)

APPENDIX A.5

AUTOMATIC COMMAND SIGNAL SEQUENCE GENERATOR

Automatic operation presents the advantages of speed (the pulse repetition rate can be increased) and versatility, and simple modifications of a programming diode matrix also provide other command sequences at will. The design uses the principle of digital-to-analog conversion. Fig. A.5-1 represents the circuit(*) that automatically generates the sequence of hyperpolarizing pulses (Schwartz, 1976).

An independent clock is used to trigger the binary counter (Signetics N7493). Counting starts when the start button is depressed and stops automatically when the sequence is over. The output of the counter is then fed to a set of 4 AND gates, together with the clock pulse, in order to always provide a 0000 signal when no pulse is present. The output of the AND gates is then connected to a 4-16 demultiplexer-decoder (Signetics N74154), which has 16 output lines connected to the 16 x 8 programming diode matrix that generates the input words of the digital-to-analog converter (Motorola 1408L-8). Its output (which is a current proportional to the weighted input word and the reference voltage) is added to the constant current that constitutes the bias of the sequence. The sum is then converted into a proportional voltage by means of the current-to-voltage converter (RCA 741 CS), the gain of which can be adjusted in order to obtain the suitable pulse levels. The output of the amplifier is then fed directly through the MODE switch to the command input of the control amplifier of the voltage-clamp electronic circuit.

(*) The detailed wiring diagram is given in Appendix A.4, Fig. A.4-6.

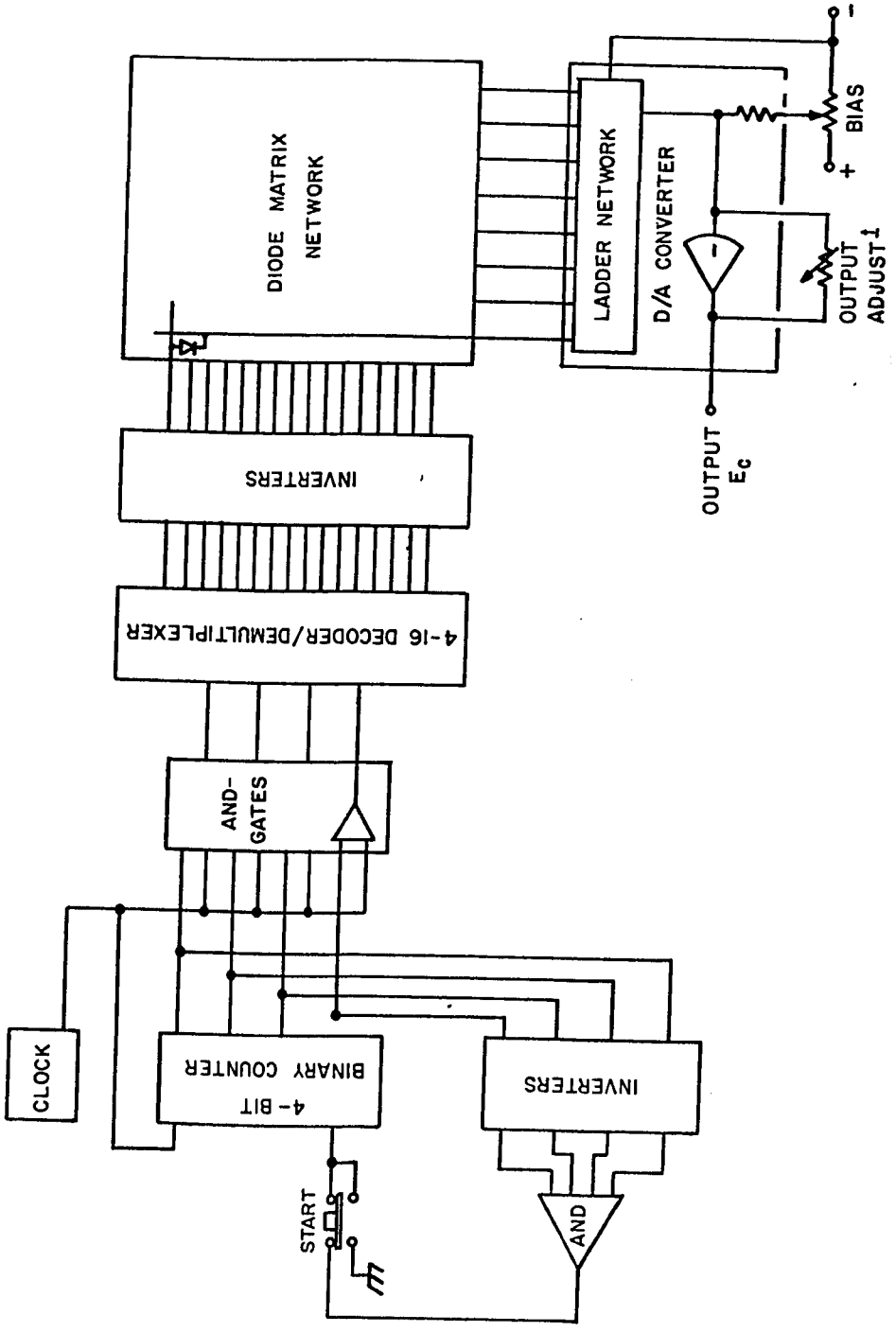

Fig. A.5-1. Automatic command signal sequence generator

APPENDIX A.6

SIGNAL PROCESSOR FOR DIRECT PLOTTING OF CURRENT vs VOLTAGE DATA OF VOLTAGE-CLAMP EXPERIMENTS

Since the introduction of voltage-clamp techniques in excitable membrane biophysics and electrophysiology, a great amount of information has been extracted from the current-voltage characteristics of the cells under study (I-V curves), both in the transient and steady-state behaviour. Unfortunately, there is no direct way to obtain these characteristics. The usual method is to plot the current versus voltage manually or by means of a processing machine, thereby eliminating the time parameter from the current and voltage responses. In order to facilitate this procedure, an electronic system(*) that permits the direct and immediate display of the current-voltage characteristics of excitable membranes under voltage-clamp has been designed (Schwartz, 1977). It detects the peak transient current and the steady-state current corresponding to each voltage-clamp step, and feeds the detected values into a storage cathode ray oscilloscope (CRO) used in the X-Y mode with intensity modulation, which serves as a convenient display device.

The system functions as follows (fig. A.6-1): when the clamping pulse is applied to the specimen, the counter is triggered by the synchronization pulse. The membrane current, after preamplification, is amplified and shifted to make it acceptable by the peak detector (the closing of switch SW3 has been delayed to avoid detecting the capacitive transient, and switch SW4 is in the HOLD mode). When the peak has been detected, switch SW1 closes and simultaneously an intensifying pulse is sent to the intensity modulation input of the oscilloscope so that a dot will appear on the CRO screen. At the end of the intensifying

---

(*) The detailed wiring diagram is given in Appendix A.4, Fig. A.4-7.

pulse, SW4 goes to RESET and SW1 opens. After a time necessary to reach the steady-state, SW2 closes and a second intensifying pulse displays the steady-state value of I_m. This in turn stops the counter and the whole circuit is reset to be ready for the next voltage-clamp pulse.

From the above description, it can be seen that this signal processing circuit is basically made out of a logic and an analog circuit. TTL logic has been used to implement the circuit that controls a quadruple bilateral electronic switch (RCA-CD 4066). The analog circuit consists in an inverting positive peak detector (Graeme et al., 1971), and two operational amplifiers (RCA 741) for biasing the input signal and recovering the steady-state output value in the correct phase.

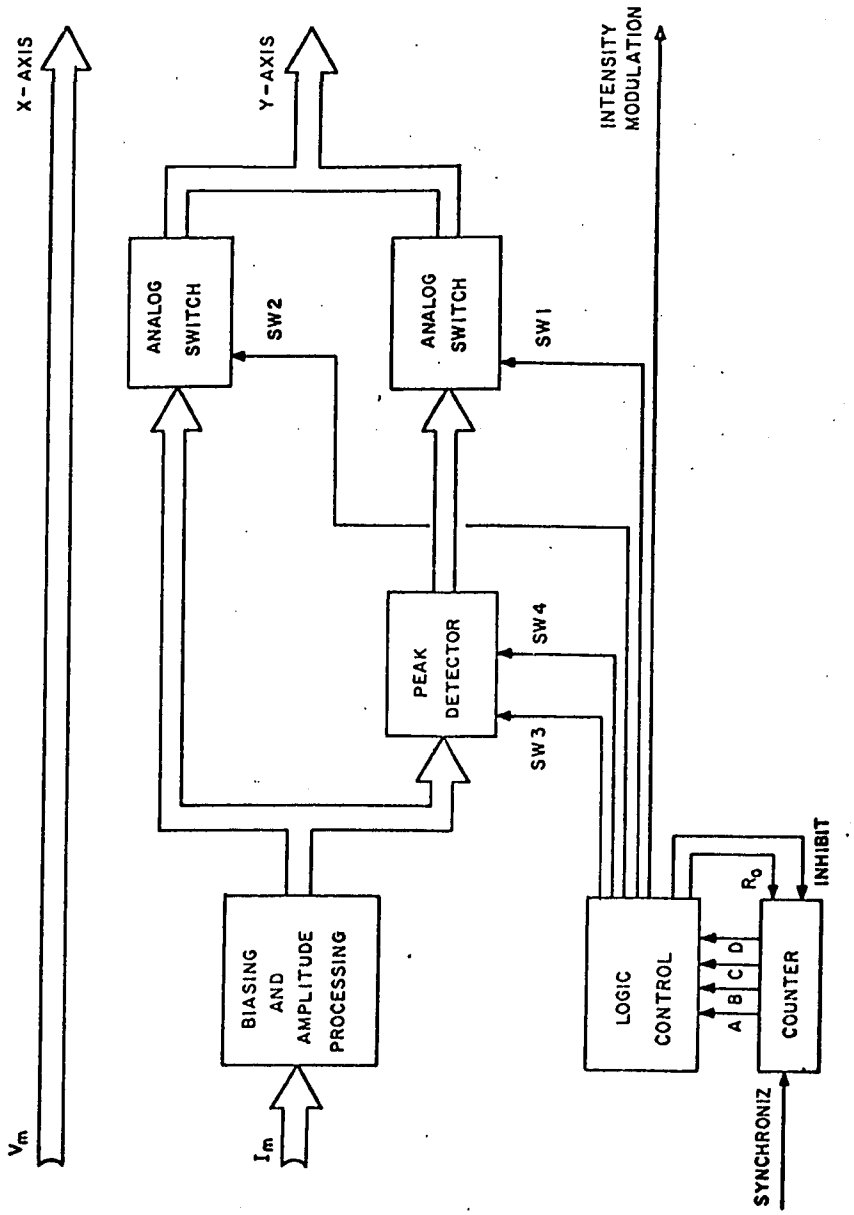

Fig. A.6-1. Block-diagram of current-voltage processor

APPENDIX A.7

VOLTAGE-CLAMP OPERATION: DETAILED CALCULATIONS

This appendix contains the complete derivation of the equations given in Chapt. III, section III.3.4, that describe the operation of the electronic measurement and control system used in this biomagnetic experiment.

The basic assumptions are identical to those made for the simplified treatment in Chapt. III. They are repeated here, as are the related figures III-9 and III-11 of Chapt. III, to make this appendix self-contained.

These assumptions are (see fig. A.7-1 and A.7-2):

(i) amplifier No 1 is an electrometer amplifier. It has therefore a very high input impedance and draws a negligible current. Its gain is set at unity.

(ii) amplifier No 2 (gain of 10) and amplifier No 3 (gain of 2.5) are operational amplifiers. Their gain is constant over the frequency range concerned.

(iii) amplifier No 5 is connected in a current-to-voltage configuration. The input terminal B is therefore at virtual ground.

(iv) the voltage drop across the series resistance R_{asw} is negligible. This assumption introduces a systematic error that can be eliminated in the actual system by substracting electronically from the measured membrane potential a voltage that is proportional to the membrane current (Poindessault et al., 1976).

In what follows, the symbols are taken from Fig. A.7-1 and Fig. A.7-2. Voltages are taken with respect to ground (virtual or

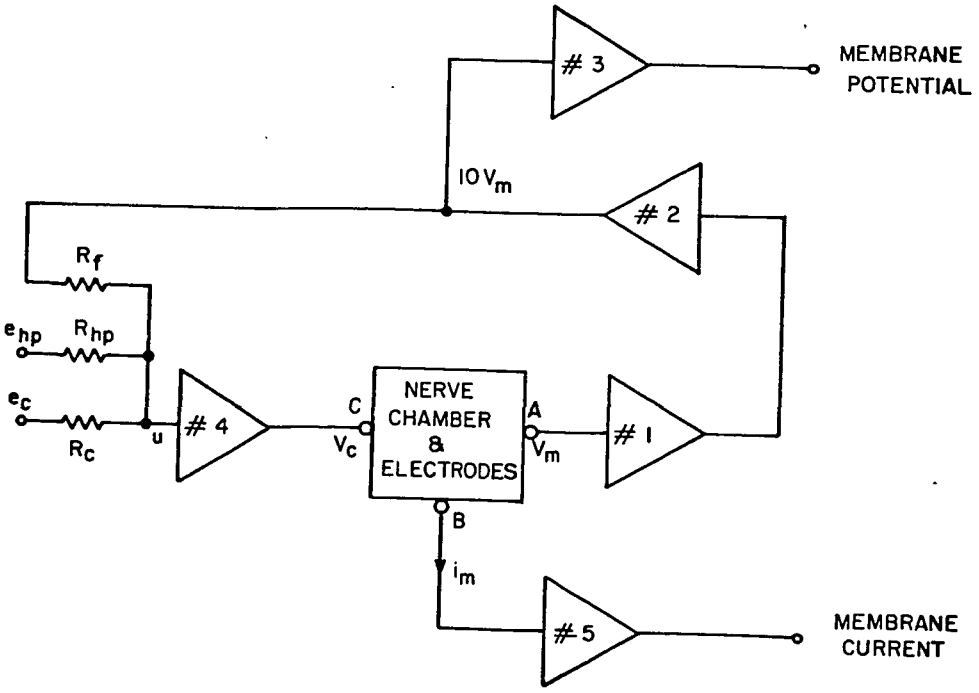

Fig. A.7-1. Simplified diagram of the measurement and control system

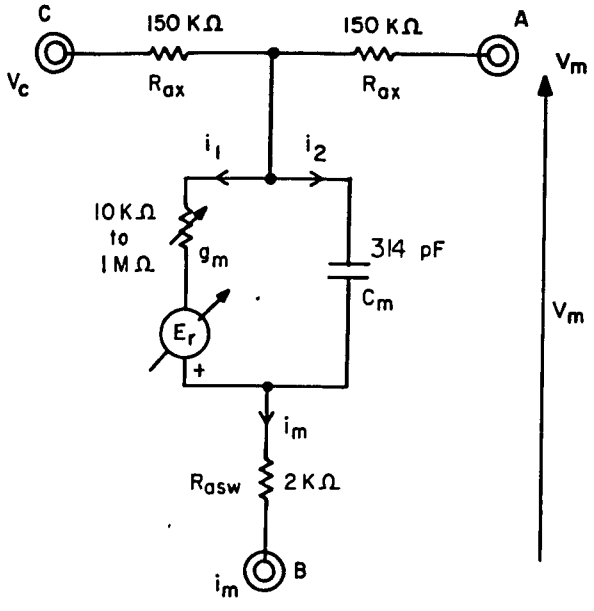

Fig. A.7-2. Equivalent T-network membrane model in double sucrose gap arrangement

signal ground).

1) Membrane transfer function

$$v_m = -E_r + r_m i_1$$

$$v_m = \frac{1}{sC_m} i_2$$

$$v_m = v_c - R_{ax} i_m$$

$$i_m = i_1 + i_2$$

thus

$$v_c = R_{ax} g_m E_r + (1 + R_{ax} g_m + sR_{ax} C_m) v_m \qquad (A.7\text{-}1)$$

2) Control amplifier equation

In addition to the command potential, there is another input connected to the summing junction of the control amplifier. This input e_{hp}, the holding potential, is used to maintain the membrane potential to a predetermined value between the command signals.

Assuming that the open-loop gain of amplifier No 4 is A_4, and that the sum of the currents entering the summing junction is equal to zero, the following equations hold for the control amplifier:

$$v_c = -A_4 u$$

$$\frac{10v_m - u}{R_f} + \frac{e_c - u}{R_c} + \frac{e_{hp} - u}{R_{hp}} = 0$$

Thus, using equation (A.7-1), the control amplifier equation(*) is obtained :

$$\left\{\frac{10}{R_f} + \frac{1}{A_4}\left(\frac{1}{R_f} + \frac{1}{R_c} + \frac{1}{R_{hp}}\right)(1 + R_{ax} g_m + sR_{ax} C_m)\right\} v_m +$$

$$\frac{1}{A_4} R_{ax} g_m \left(\frac{1}{R_f} + \frac{1}{R_c} + \frac{1}{R_{hp}}\right) E_r + \frac{e_c}{R_c} + \frac{e_{hp}}{R_{hp}} = 0 \qquad (A.7\text{-}2)$$

(*) equ. (1), chapt. III, paragraph III.3.4.2

It should be mentioned here that the gain of the operational amplifiers No 1 and No 2 has been assumed constant over the whole frequency range of the overall system operation. This is quite valid as both amplifiers are used at low gain. Of course, these amplifiers are selected in such a way that their frequency response is compatible with the constant gain requirement.

3) Resting state operation

When the membrane is at rest, it displays a resting potential that is equal to E_r^o. The command potential e_c being equal to zero, equation (A.7-2) becomes :

$$\left\{\frac{10}{R_f} + \frac{1}{A_4}\left(\frac{1}{R_f} + \frac{1}{R_c} + \frac{1}{R_{hp}}\right)\left(1 + 2R_{ax}g_m^o\right)\right\} E_r^o + \frac{e_{hp}}{R_{hp}} = 0 \qquad (A.7\text{-}3)$$

which simply reduces to the following resting state equation(*) :

$$\frac{10}{R_f} E_r^o + \frac{e_{hp}}{R_{hp}} = 0 \qquad (A.7\text{-}4)$$

if A_4 tends to infinity.

4) Active state operation

In the active state, the instantaneous membrane voltage v_m can be expressed as :

$$v_m = E_r^o + \Delta v_m \qquad (A.7\text{-}5)$$

Substituting in equat. (A.7-1) and taking into account equat. (A.7-3) we get :

$$\left\{\frac{10}{R_f} + \frac{1}{A_4}\left(\frac{1}{R_f} + \frac{1}{R_c} + \frac{1}{R_{hp}}\right)\left(1 + R_{ax}g_m\right)\right\}\Delta v_m + \frac{e_c}{R_c} + \frac{R_{ax}}{A_4}\left(\frac{1}{R_f} + \frac{1}{R_c} + \frac{1}{R_{hp}}\right)\left(2\Delta g_m E_r^o + g_m \Delta E_r\right) = 0 \qquad (A.7\text{-}6)$$

(*) equ. (2), chapt. III, paragraph III.3.4.3 :

with $g_m = g_m^o + \Delta g_m$

and $E_r = E_r^o + \Delta E_r$

It can be seen from equation (A.7-6) that in order to clamp the membrane voltage displacement Δv_m to the assigned value e_c, it is necessary to make the terms that contain A_4 as small as possible. Typical data as obtained experimentally for the excited membrane in the double sucrose gap arrangement(*) impose the choice of high values for the resistances that are connected to the summing junction of amplifier No 4, together with a high gain A_4. It can be shown that resistances of 100 kΩ minimum and a gain A_4 of 80 dB or more are suitable for the control system used here. Under these conditions, the third term of the sum in equ. (A.7-6) is negligible with respect to the two others. The control equation(**) then takes the following form :

$$\left\{\frac{10}{R_f} + \frac{1}{A_4}\left(\frac{1}{R_f} + \frac{1}{R_c} + \frac{1}{R_{hp}}\right)(1 + R_{ax}g_m)\right\}\Delta v_m + \frac{e_c}{R_c} = 0 \qquad (A.7\text{-}7)$$

5) Tight control requirements

Equ. (A.7-7) can be rewritten in the following form:

$$\Delta v_m = -\frac{R_f}{10R_c}\, e_c \times \left\{\frac{1}{1 + \frac{1}{10A_4}\left(1 + \frac{R_f}{R_c} + \frac{R_f}{R_{hp}}\right)(1 + R_{ax}g_m)}\right\}$$

or:

$$\Delta v_m \cong -\frac{R_f}{10R_c}\, e_c \left\{1 - \frac{1}{10A_4}\left(1 + \frac{R_f}{R_c} + \frac{R_f}{R_{hp}}\right)(1 + R_{ax}g_m)\right\}$$

(*) $R_{ax} = 150$ kΩ, $E_r^o = 100$ mV, $g_m^o = 1$ μS, $g_m/g_m^o \cong 100$

(**) equ. (4), chapt. III, paragraph III.3.4.4

In other words:

$$\left| \frac{|\Delta v_m| - \frac{R_f}{10R_c}|e_c|}{\frac{R_f}{10R_c}|e_c|} \right| \simeq \frac{1}{A_4}\left(1 + \frac{R_f}{R_c} + \frac{R_f}{R_{hp}}\right)(1 + R_{ax}g_m) \qquad (A.7\text{-}8)$$

By choosing $R_f = 100\ k\Omega$, $R_c = R_{hp} = 500\ k\Omega$, with a typical axoplasmic resistance $R_{ax} = 150\ k\Omega$, and assuming that we are in the worst case, i.e. that r_m takes its minimum value of about 1 kΩ, a 1% control of the membrane voltage will be realized if A_4 is greater than 2000, according to equation (A.7-8). Therefore, if the open-loop gain of amplifier No 4 is 10 000 or more, a tight control of v_m is achieved. The analysis given in the previous paragraphs is only valid for low frequency operation. Good control however will still be realized at higher frequencies if the control amplifier is chosen with a wide enough bandwidth, which is equivalent to setting a high open-loop gain for A_4.

6) Approximate equation for low frequency operation

As shown in the previous paragraphs, the choice of a high gain control amplifier together with high values for its summing junction resistors is critical for good control of the membrane potential. If these requirements are met, equation (A.7-2) reduces to the very simple equation(*) that follows:

$$\frac{10}{R_f}\Delta v_m + \frac{e_c}{R_c} \simeq 0 \qquad (A.7\text{-}9)$$

assuming that the resting potential has been exactly balanced by means of the holding potential e_{hp} as indicated by equat.(A.7-4).

(*) equ. (5), chapt. III, paragraph III.3.4.4

APPENDIX A.8

THERMOREGULATION CIRCUIT DIAGRAM

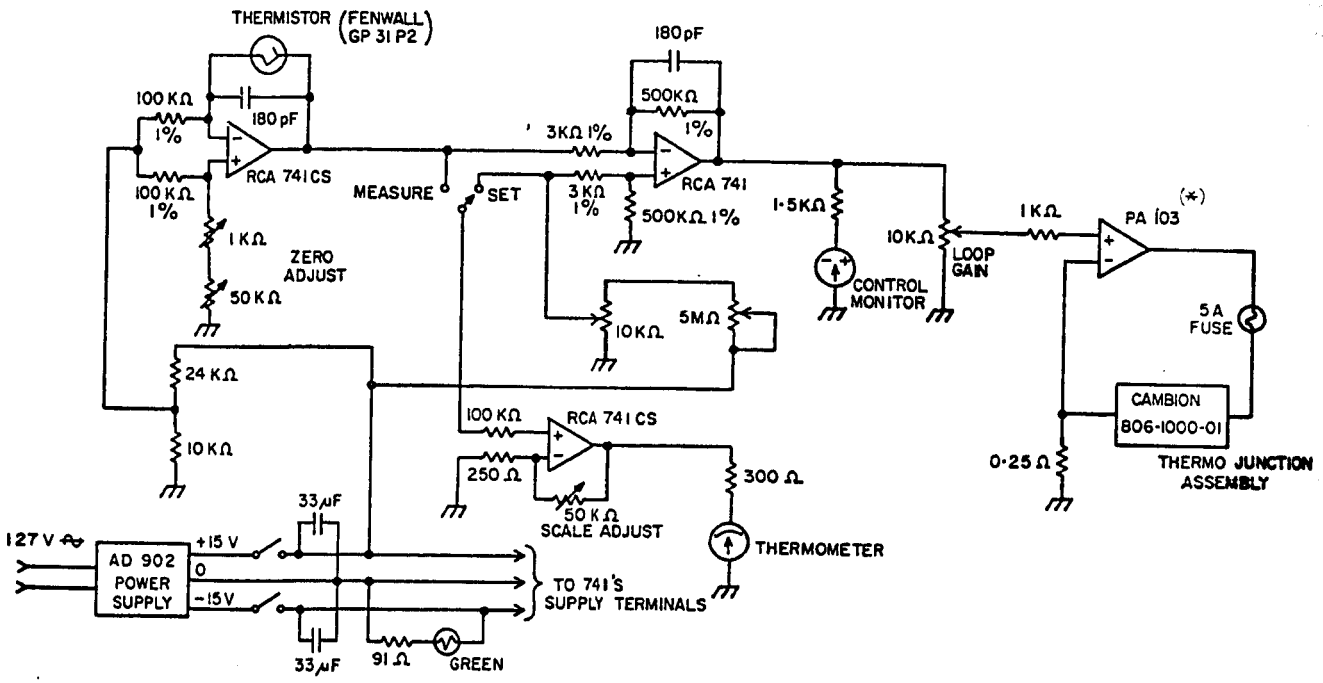

Fig. A.8-1. Thermoregulation circuit diagram

(*)

The PA 103 power amplifier (Torque Systems Inc.) is energized by two 12 V, 80 A-h automotive batteries that are also used to energize the microscope illumination system.

APPENDIX A.9

CIRCUIT DIAGRAMS OF TWO NERVE MEMBRANE MODELS

This appendix contains the following circuit diagrams:

Fig. A.9-1 T-network passive membrane model

Fig. A.9-2 Modified Neurofet(*) active membrane model

(*) Roy, 1972

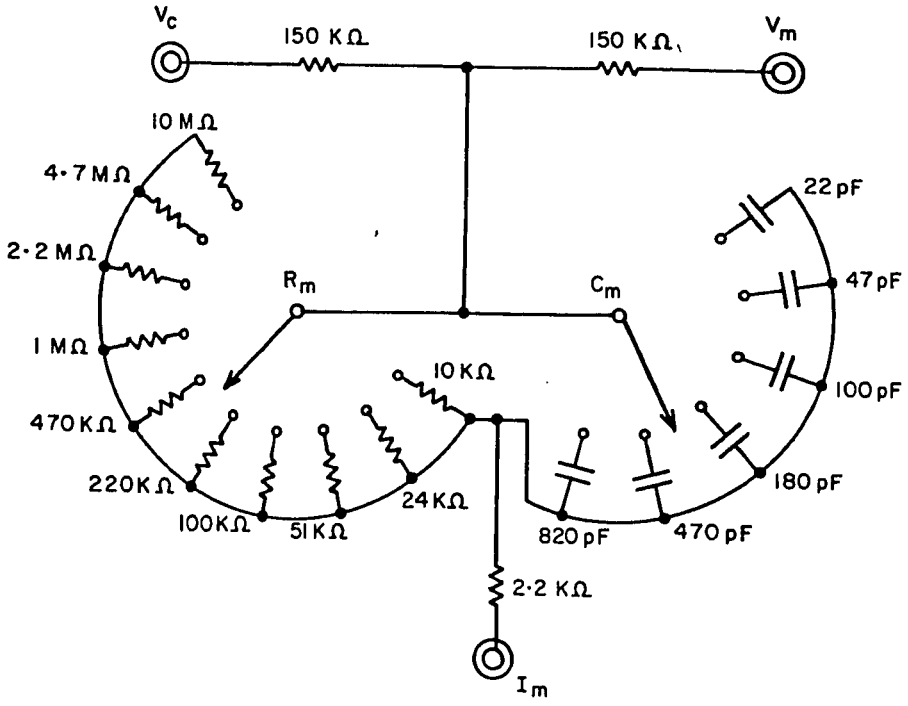

Fig. A.9-1. T-network passive membrane model

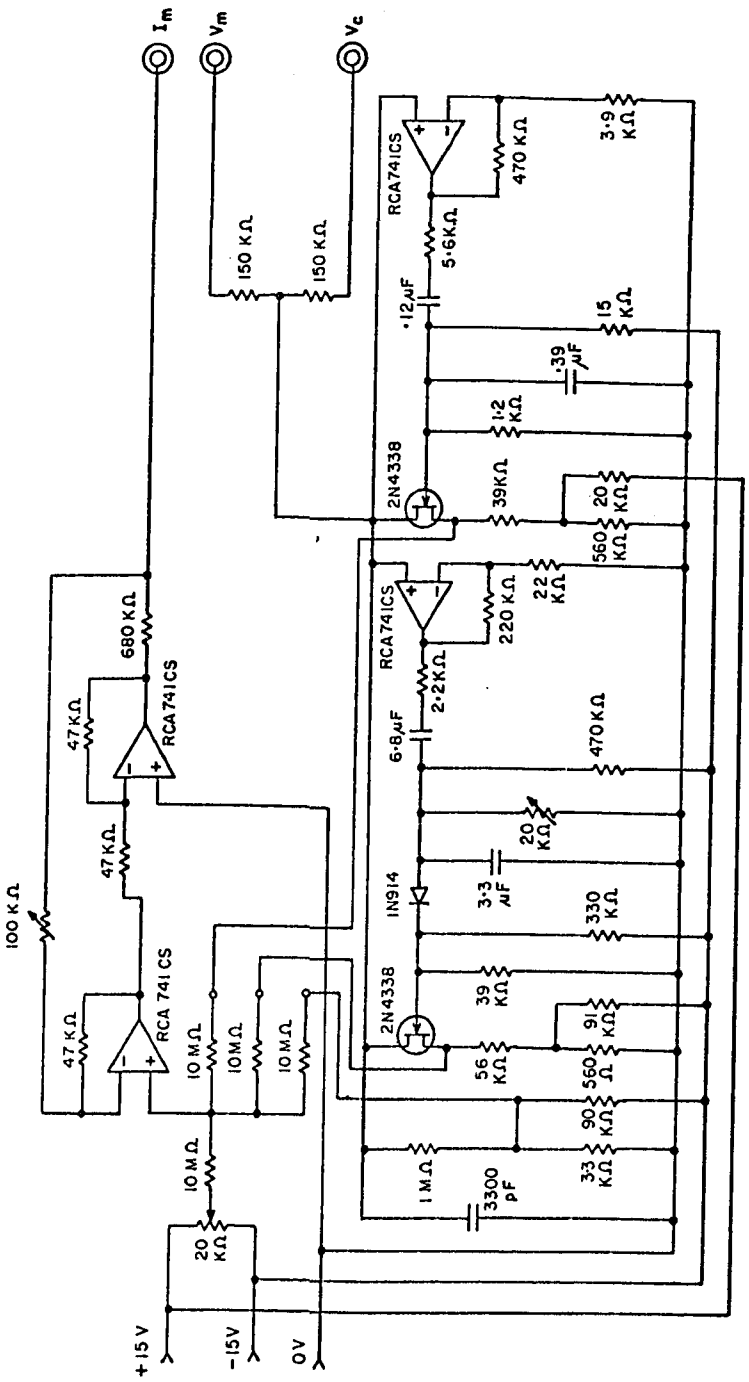

Fig. A.9-2. Modified Neurofet active membrane model

REFERENCES

ABASHIN, V.M. and EVTUSHENKO, G.I., 1975
Problems of effect of constant magnetic field on biological systems. Biofizika 20(2): 276-280.

ABASHIN, V.M. and EVTUSHENKO, G.I., 1975
Constant magnetic field and conductance of impulse along nerve. Biofizika 20(2): 281-282.

ACETO, H., TOBIAS, C.A. and SILVER, I.L., 1970
Some studies on the biological effects of magnetic fields. IEEE Trans. Magnetics 6(2) : 368-373.

ALEXANDER, H.S., 1962
Biomagnetics' - The biological effects of magnetic fields. Am. J. Med. Electr. 1 : 181-187.

AMER, N.M., 1966
Effects of homogeneous magnetic fields, ambient gas composition, and temperature on the metamorphosis of Tribolium Confusum. Ph.D. thesis, Berkeley.

ARMSTRONG, C.M., 1975
Evidence for ionic pores in excitable membranes. Biophys. J. 15 : 932-933.

AUDUS, L.J. and WHISH, J.C., 1964
Magnetotropism. In: Biological Effects of Magnetic Fields, M.F. Barnothy (ed.), Plenum Press, Vol. 1 : 170-182.

BALERNA, M., FOSSET, M., CHICHEPORTICHE, R., ROMEY, G. and LAZDUNSKI, M., 1975
Constitution and properties of axonal membranes of crustacean nerves. Biochemistry 14(25) : 5500-5511.

BARNOTHY, J.M., 1960
Biological effects of magnetic fields. In: Medical Physics, O. Glasser (ed.), The Year Book Publ., Vol. 3: 61-64.

BARNOTHY, J.M., 1964a
Development of young mice, and rejection of transplanted tumors in mice. In: Biological Effects of Magnetic Fields, M.F. Barnothy (ed.), Plenum Press, Vol. 1: 93-108.

BARNOTHY, J.M., 1964c
Introduction. In: Biological Effects of Magnetic Fields, M.F. Barnothy (ed.), Plenum Press, Vol. 1: 3-24.

BARNOTHY, M.F. 1963
Biological effects of magnetic fields on small mammals. In: Biomedical Science Instrumentation, Plenum Press, Vol. 1: 127-135.

BARNOTHY, M.F., 1964b
Reduction of irradiation mortality through pretreatment, and hematological changes in mice. In: Biological Effects of Magnetic Fields, M.F. Barnothy (ed.), Plenum Press, Vol. 1: 109-131.

BARNOTHY, M.F. and SÜMEGI, I., 1969
Effects of the magnetic field on internal organs and the endocrine system of mice. In: Biological Effects of Magnetic Fields, M.F. Barnothy (ed.), Vol. 2: 103-126.

BECKER, R.O., 1963
The biological effects of magnetic fields - A survey. Med. Electron. Biol. Eng. 1: 293-303.

BECKER, R.O., 1965
The neural semiconduction control system and its interaction with applied electrical current and magnetic fields. Proc. of the XIth International Congress of Radiology: 1753-1759.

BECKER, R.O., 1969
The effect of magnetic fields upon the central nervous system. In: Biological Effects of Magnetic Fields, M.F. Barnothy (ed.), Plenum Press, Vol. 2: 207-214.

BEISCHER, D.E., 1963
Biomagnetics. In: Lectures in Aerospace Medicine, AF-SAM-Q-16, U.S. Air Force Sch. Aerospace Med., Brooks AFB, Texas: 367-386.

BEISCHER, D.E. and KNEPTON, J.C., 1964
Influence of strong magnetic fields on the electrocardiogram of squirrel monkey (Saimiri Sciureus). Aerosp. Med. 35: 939-944.

BELLOSSI, A., BRESSON, Y. et de CERTAINES, J., 1971
Quelques effets d'un champ magnétique uniforme sur le sang. C.R. Société de Biologie (Ouest Africain) 169(6): 1503-1508.

BELLOSSI, A. et FAURAN, F., 1972
Effet d'un champ magnétique uniforme sur le sérum et le plasma. Etude spectrophotométrique.' C.R. Société de Biologie (Ouest Africain) 166(6-7): 980-983.

BELLOSSI, A., LANGUILLON, J. et DUCLOS, M., 1974
Effet d'un champ magnétique uniforme sur les leucocytes. Etude du test de migration des leucocytes chez les lépreux. Bull. Société Pathologie Exotique 67(1): 25-30.

BEZANILLA, F. and ARMSTRONG, C.M., 1975
Kinetic properties and inactivation of the gating currents of sodium channels in squid axon. Phil. Trans. R. Soc. Lond. 270: 449-458.

BIANCHI, A., CAPRARO, V. and GUALTIEROTTI, T., 1963
Decrease of the sodium transport across frog skin in a steady magnetic field.
Proc. Phys. Soc.: 61P-62P.

BINSTOCK, L., ADELMAN, W.J. Jr., SENFT, J.P. and LECAR, H., 1975
Determination of the resistance in series with the membrane of giant axons. J. Membr. Biol. 21(1-2): 25-48.

BITTMAN-COROS, L. und MACELARIU, A., 1969
Experimentelle Untersuchen und theoretische Betrachtungen über die Wirkungweise der durch den "Magnetodiaflux" Apparat erzeugten niederfrequenten Elektromagnetfelder. Archiv Physic. Therapie 2: 126-134.

BLAUSTEIN, M.P. and GOLDMAN, D.E., 1966a
Competitive action of calcium and procaine on lobster axon - A study of the mechanism of action of certain anesthetics.
J. Gen. Physiol. 49: 1043-1063.

BLAUSTEIN, M.P. and GOLDMAN, D.E., 1966b
Origin of axon membrane hyperpolarization under sucrose gap. Biophys. J. 6: 453-470.

BRESLER, S.E. and BRESLER, V.M., 1974
The liquid crystal structure of biological membranes. Dokl. Biophys. (Engl. Transl. Dokl. Akad. Nauk SSSR Ser. Biofiz.): 214-216.

BRESSON, Y. et BELLOSSI, A., 1969
Etude préliminaire des effets d'un champ magnétique uniforme sur le sang. Bull. Soc. Med. Afr. Noire lgue fr. t. XIV(3): 612-614.

BRINLEY, F.J., 1965
Sodium, potassium and chloride concentrations and fluxes in the isolated giant axon of Homarus. J. Neurophysiol. 28: 742-772.

BROWN, B.H., 1968
Theoretical and experimental waveform analysis of human compound nerve action potentials using surface electrodes. Med. and Biol. Eng. 6: 375-386.

BULLOCK, T.H. and HORRIDGE, G.A., 1965
Structure and function in the nervous systems of invertebrates. W.H. Freeman and Company.

BUSBY, D.E., 1968
Space biomagnetics. Space Life Sciences 1: 23-63.

BUTLER, B.C. and DEAN, W.W., 1964
The inhibitory effect of a magnetostatic field upon the tissue culture growth of K.B. cells. Med. Research Eng. 3: 123-125.

CHALAZONITIS, N. et ARVANITAKI, A., 1964
Effets du champ magnétique constant sur l'autoactivité des fibres myocardiques d'Helix Pomatia. C.R. Société de Biologie (Marseille) 158: 1902-1908.

CHIZHENKOVA, R.A., 1966
EEG changes in rabbit under the influence of a permanent magnetic field. Biulleten Eksperimental'nay Biologii i Meditsiny 61(6): 11-15.

COHEN, D., 1968
Magnetoencéphalography: Evidence of magnetic fields produced by α-rythm currents. Science 161: 784-786.

COHEN, L.B., 1973
Changes in neuron structure during action potential propagation and synaptic transmission. Physiol. Rev. 53: 373-418.

COHEN, L.B., HILLE, B., KEYNES, R.D., LANDOWNE, D. and ROJAS, E., 1971
Analysis of the potential-dependent changes in optical retardation in the squid giant axon. J. Physiol. (London) 218: 205-237.

COHEN, L.B., KEYNES, R.D. and HILLE, B., 1968
Light scattering and birefringence changes during nerve activity. Nature 218: 438-441.

COLE, K.S., 1949
Dynamic electrical characteristics of the squid axon membrane. Arch. Sci. Physiol. (CNRS) 3: 253-258.

COLE, K.S., 1956
Electro-ionics of nerve action. IRE Trans. PGME 6: 28-48.

COLE, K.S., 1968
Membranes, ions and impulses. University of California Press.

COLE, K.S. and MOORE, J.W., 1960
Ionic current measurements in the squid giant axon membrane. J. Gen. Physiol. 44: 123-167.

CONTI, F., DE FELICE, L.J. and WANKE, E., 1975
Potassium and sodium ion current noise in the membrane of the squid giant axon. J. Physiol. (London) 248: 45-82.

CONTI, F., TASAKI, I. and WANKE, E., 1971
Fluorescence signals in ANS-stained squid giant axons during voltage-clamp. Biophysik. 8: 58-70.

DALMAN, J.A. and GOODMAN, L.S., 1957
Variable and reversible magnetic fields obtained from a permanent magnet. Rev. Sci. Instr. 28: 961-962.

DALTON, J.C., 1958
Effects of external ions on membrane potentials of a lobster giant axon. J. Gen. Physiology 41: 529-542.

DALTON, J.C. and ADELMAN, W.J., 1960
Some relations between action potential and resting potential of the lobster giant axon. J. Gen. Physiology 43: 597-607.

DALTON, J.C. and HENDRIX, D.E., 1962
Effects of temperature on membrane potentials of lobster giant axon. Am. J. Physiol. 202: 491-494.

DAVIS, L.D., PAPPAJOHN, K. and PLAVNIEKS, I.M., 1962
Bibliography of the biological effects of magnetic fields. Fed. Proc. 21(supl. 12): 1-38.

DELCASTILLO, J., LETTVIN, J.Y., McCULLOCH, W.S. and PITTS, W., 1957
Membrane currents in clamped vertebrate nerve. Nature 180: 1290-1291.

DELEVIE, R. and ABBEY, K.M., 1976
Unified approach to ion-transport through membranes: 1. Membrane-soluble ions. J. Theor. Biol. 56: 151-173.

DODGE, F.A. and FRANKENHAEUSER, B., 1958
Membrane currents in isolated frog nerve fiber under voltage-clamp conditions. J. Physiol. (London) 143: 76-90.

DUNLOP, D.W. and SCHMIDT, B.L., 1969
Sensitivity of some plant material to magnetic fields. In: Biological Effects of Magnetic Fields, M.F. Barnothy (ed.), Plenum Press, Vol. 2: 147-170.

EASTON, D.M. and SWENBERG, C.E., 1975
Temperature and impulse velocity in giant axon of squid. Am. J. Physiol. 229(5): 1249-1253.

EHRENSTEIN, G. and LECAR, H., 1972
The mechanism of signal transmission in nerve axon. Annual Rev. Bioph. and Bioeng. 1: 347-368.

EISELEIN, J.E., BOUTELL, H.M. and BIGGS, M.W., 1961
Biological effects of magnetic fields - Negative results. Aerosp. Med. 32(5): 383-386.

ERDMAN, G.M., 1955
The problem of the effect of a constant magnetic field on nerve. Akad. Nauk SSSR Institut Biol. Fiziki Trudy (Moscow) 1: 35-39.

FERGASON, J.L., 1964
Liquid crystals. Scientific American, 211: 77-85.

FISHMAN, H.M., 1969
Direct recording of K and Na current-potential characteristics of squid axon membrane. Nature 224: 1116-1118.

FISHMAN, H.M., MOORE, L.E. and POUSSART, D.J.M., 1975
Potassium ion conduction noise in squid axon membrane. J. Membr. Biol. 24(3-4): 305-328.

FISHMAN, H.M., POUSSART, D.J.M. and MOORE, L.E., 1975
Noise measurements in squid axon membrane. J. Membr. Biol. 24(3-4): 281-304.

FRASER, A. and FREY, A.H., 1968
Electromagnetic emission at micron wavelengths from active nerves. Biophys. J. 8(6): 731-734.

FREI, E.H., 1972
Biomagnetics. IEEE Trans. Magnetics MAG-8(3): 407-413.

GAUQUELIN, M., 1966
Effets biologiques des champs magnétiques. Année Biologique, 5(11-12): 595-611.

GETZEL, W.A. and WEBSTER, J.G., 1976
Minimizing silver-silver chloride electrode impedance. IEEE Trans. Biomed. Engineering BME-23(1): 87-88.

GITLER, C., 1972
Plasticity of biological membranes. Annual Rev. Bioph. and Bioeng. 1: 51-92.

GONET, B., 1975
The effect of constant magnetic field on electrocardiogram in experimental animals. Acta Physiol. Pol. (Engl. Transl.) 26(2): 165-168.

GREAME, J.G. TOBEY, G.E. and HUELSMAN, L.P., 1971
Operational amplifiers. McGraw-Hill.

GROSS, L., 1963
A study of the biological effects of magnetic fields. Ph.D thesis, New York University.

GROSS, L., 1964
Distortion of the bond angle in a magnetic field and its possible magnetobiological implications. In: Biological Effects of Magnetic Fields, M.F. Barnothy (ed.), Plenum Press, Vol. 1: 74-79.

GROSS, L., 1964
Bibliography of the biological effects of static magnetic fields. In: Biological Effects of Magnetic Fields, M.F. Barnothy (ed.), Plenum Press, Vol. 1: 297-311.

GUALTIEROTTI, T., 1964
Decrease of the sodium pump activity in the frog skin in steady magnetic field. The Physiologist 7: 150.

HALL, E.J. and BEDFORD, J.S., 1964
Some negative results in the search of a lethal effect of magnetic fields on biological materials. Nature 203: 1086-1087.

HAMA, K., 1961
Some observations on the fine structure of the giant fibers of the crayfishes (Cambarus Virilus and Cambarus Clarkii) with special reference to submicroscopic organization of the synapses. Anat. Rec. 141: 275-293.

HEINMETS, F. and HERSCHMAN, A., 1961
Considerations of the effects produced by superimposed electric and magnetic fields in biological systems and electrolytes. Phys. Med. Biol. 5: 271-288.

HILLE, B., 1966
Common mode of action of three agents that decrease the transient change in sodium permeability of nerves. Nature 210: 1220-1222.

HILLE, B., 1968
Pharmacological modifications of the sodium channels of frog nerve. J. Gen. Physiol. 51: 199-219.

HILLE, B., 1972
Ionic permeability changes in active axon membranes. Arch. Intern. Med. 129: 293-298.

HILLE, B., 1975
Ionic selectivity, saturation and block in sodium channels - A 4-barrier model. J. Gen. Physiol. 66: 535-560.

HILLE, B., 1976
Gating in sodium channels of nerve. Annual Rev. Physiol. 38: 139-152.

HODGKIN, A.L., 1939
The relation between conduction velocity and the electrical resistance outside a nerve fibre. J. Physiol. (London) 94: 560-570.

HODGKIN, A.L. and HUXLEY, A.F., 1952b
A quantitative description of membrane current and its application to conduction and excitation in nerve. J. Physiol. (London) 117: 500-544.

HODGKIN, A.L., HUXLEY, A.F. and KATZ, B., 1952a
Measurement of current-voltage relations in the membrane of the giant axon of Loligo. J. Physiol. (London) 116: 424-448.

HOEKMAN, T.B. and DETTBARN, W.D., 1971
Electrophysiological characteristics of giant axons of the lobster Homarus Americanus and their response to cholinergic compounds. Comp. Gen. Pharmac. 2: 99-105.

HOWARTH, J.V., KEYNES, R.D. and RITCHIE, J.M., 1968
The origin of the initial heat associated with a single impulse in mammalian non-myelinated nerve fibres. J. Physiol. (London) 194: 745-793.

HUXLEY, A.F., 1959
Ion movements during nerve activity. Ann. N.Y. Acad. Sci. 81(art.2): 221-246.

IRWIN, D.D., RUSH, S., EVERING, R., LEPESCHKIN, E., MONTGOMERY, D.B. and WEGGEL, R.J., 1970
Stimulation of cardiac muscle by a time-varying magnetic field. IEEE Trans. Magnetics 6(2): 321-322.

ISRAELI, E., KARNI, Z., SCHUR, Z. and BARZILAI,D., 1971
Collagen development in tissue cultures in vitro under static magnetic field. Israel J. Med. Sci. 7(3): 465-468.

JACOB, R.H., 1973
Electronic modification of external current for an artificially segmented giant axon of the lobster. Med. Biol. Eng. 11(2): 138-145.

JIROUNEK, F. and STRAUB, R.W., 1971
The potential distribution and the short-circuiting factor in the sucrose gap. Biophys. J. 11: 1-10.

JOHNSON, G.E., 1924
Giant nerve fibers in crustaceans with special reference to Cambarus and Palaemonetes. The J. Comp. Neurol. 36(4): 323-373.

JOHNSTON, P.V. and ROOTS, B.I., 1972
Nerve membranes: A study of the biological and chemical aspect of neuron-glia relationships. Pergamon Press (Oxford).

JONNARD, R.J., 1963
Peripatetic views on some premature biomagnetic investigations. In: Biomedical Science Instrumentation, Plenum Press, Vol. 1: 95-101.

JULIAN, F.J., MOORE, J.W. and GOLDMAN, D.E., 1962a
Membrane potentials of the lobster giant axon obtained by the sucrose gap technique. J. Gen. Physiol. 45: 1195-1216.

JULIAN, F.J. MOORE, J.W. and GOLDMAN, D.E., 1962b
Current-voltage relations in the lobster giant axon membrane under voltage-clamp conditions. J. Gen. Physiol. 45: 1217-1238.

KATZ, B., 1966
Nerve, muscle and synapse. McGraw Hill.

KATZ, G.M. and SCHWARTZ, T.L., 1974
Temporal control of voltage-clamped membranes: An examination of principles. J. Membr. Biol. 17: 275-291.

KHOLODOV, Yu. A., 1964
Effects on the central nervous system. In: Biological Effects of Magnetic Fields, M.F. Barnothy (ed.), Plenum Press, Vol. 1: 196-200.

KHOLODOV, Yu. A., 1967a
The effect of electromagnetic and magnetic fields on the central nervous system. NASA TT F-465: 223-250.

KHOLODOV, Yu. A., 1967b
The effect of a constant magnetic field on the electrical activity of the rabbit brain. In: The Effects of Electromagnetic and Magnetic Fields on the Central Nervous System, NASA TT F-465: 101-116.

KHOLODOV, Yu.A., 1973
Magnetism in biology. Joint Publication Research Service FLD/GP 6S, Arlington (Va).

KHOLODOV, Yu. A., ALEXANDROVSKAYA, M.M., LUKJANOVA, S.N. and UDAROVA, N.S., 1969
Investigations of the reactions of mammalian brain to static magnetic fields. In: Biological Effects of Magnetic Fields, M.F. Barnothy (ed.), Plenum Press, Vol. 2: 215-225.

KNOLL, J., 1962
Sodium and chromate ion movement across isolated frog and fish skins with the effect of magnetic fields upon such movement. Ph.D thesis, Michigan State University.

KOLIN, A., 1968
Magnetic fields in biology. Physics Today 21: 39-50.

KOLTA, P., 1973
Strong and permanent interaction between peripheral nerve and a constant inhomogeneous magnetic field. Act. Physiol. Acad. Sci. Hung. 43(1): 89-94.

KOOTSEY, J.M., 1975
Voltage-clamp simulation. Fed. Proc. 34(5): 1343-1349.

LABES, M.M., 1966
A possible explanation for the effect of magnetic fields on biological systems. Nature 211: 968.

LENZI, M., 1966
Sulla possibilità di effetti biologici del campo magnetico a livello cellulare. Med. Aeron. e Sp. XIX: 24-44.

LEVENGOOD, W.C., 1967
Morphogenesis as influenced by locally administered magnetic fields. Biophys. J. 7: 297-307.

LIBERMAN, E.A., VAINTSVAIG, M.N. and TSOFINA, L.M.,1959
The effect of a constant magnetic field on the excitation threshold of isolated frog nerve. Biofizika 4: 505-506.

LIBOFF, R.L., 1965
A biomagnetic hypothesis. Biophys. J. 5: 845-853.

LIBOFF, R.L., 1969
Biomagnetic hypotheses. In: Biological Effects of Magnetic Fields, M.F. Barnothy (ed.), Plenum Press, Vol. 2: 171-175.

LIBERMAN, E.M., 1970
Ultraviolet radiation effects on isolated nerve fibers. Adv. Biol. Med. Phys. 13: 329-350.

MALING, J.E., WEISSBLUTH, M. and JACOBS, E.E., 1965
Enzyme substrate reactions in high magnetic fields. Biophys. J. 5: 767-776.

MARMONT, G., 1949
Studies of the axon membrane: A new method. J. Cellular Comp. Physiol. 34: 351-382.

McALEAR, J.H., MILBURN, N.S. and CHAPMAN, G.B., 1958
The fine structure of Schwann cells, nodes of Ranvier and Schmidt-Lanterman incisures in the central nervous system of the crab. Cancer Irroratus. J. Ultrastructure Res. 2: 171-176.

Mc GUIGAN, J.A.S., 1974
Some limitations of the double sucrose gap and its use in a study of the slow outward current in mammalian ventricular muscle. J. Physiol. (London) 240: 775-806.

MEGLITSCH, P.A., 1975
Zoologie des invertébrés. In: Arthropodes Mandibulates et Deutérostomiens, Doin (ed.), Vol. 3.

MEYER, S.L., 1975
Data analysis for scientists and engineers. John Wiley.

MOORE, J.W., ANDERSON, N., BLAUSTEIN, M., TAKATA, M., LETTVIN, J.Y., PICKARD, W.F., BERNSTEIN, T. and POOLER, J., 1966
Alkali cation selectivity of squid axon membrane. Ann. N.Y. Acad. Sci. 137(2): 818-829.

MOORE, J.W. and COLE, K.S., 1963
Voltage-clamp techniques. In: Physical Techniques in Biological Research, Nastuk (ed.), Academic Press, Vol. 6: 263-321.

MOORE, J.W., RAMON, F. and JOYNER, R.W., 1975
Axon voltage-clamp simulations. Double sucrose gap method. Biophys. J. 15(1): 25-35.

MULAY, I.L. and MULAY, L.N., 1964
Effect on Drosophila Melanogaster and S-37 tumor cells; postulates for magnetic fields interactions. In: Biological Effects of Magnetic Fields, M.F. Barnothy (ed.), Plenum Press, Vol. 1: 146-169.

MULLINS, L.J., 1975
Ion selectivity of carriers and channels. Biophys. J. 15: 921-931.

MURAYAMA, M., 1965
Orientation of sickled erythrocytes in a magnetic field. Nature 206: 420-422.

MUTSCHALL, Vl., 1969
Biological effects of magnetic fields. For. Sci. Bull. 5: 13-36.

NEURATH, P.W., 1964
Simple theoretical models for magnetic interaction with biological units. In: Biological Effects of Magnetic Fields, M.F. Barnothy (ed.), Plenum Press, Vol. 1: 25-32.

NOBLE, D., 1966
Applications of Hodgkin-Huxley equations to excitable tissues. Physiol. Reviews 46(1): 1-50.

OXFORD, G.S. and POOLER, J.P., 1975a
Selective modification of sodium channel gating in lobster axons by 2, 4, 6 trinitro-phenol: evidence for two inactivation mechanisms. J. Gen. Physiol. 66(6): 765-779.

OXFORD, G.S. and POOLER, J.P., 1975b
Ultraviolet photoalteration of ion channels in voltage-clamped lobster giant axon. J. Memb. Biol. 20: 13-30.

OZHIGOVA, A.P. and OZHIGOV, I. Ye., 1966
Effect of a permanent magnetic field on the movement of Paramecia. Biofizika (Biophysics) 2(6): 1026-1033.

PALMER, J.D., 1963
Organismic spatial orientation in very weak magnetic fields. Nature 198: 1061-1062.

PALTI, Y. and ADELMAN, W.J., 1969
Measurement of axonal membrane conductances and capacity by means of a varying potential control voltage-clamp. J. Membr. Biol. 1: 431-458.

PICKARD, W.F., 1966
On the propagation of the nervous impulse down medullated and unmedullated fibres. J. Theoret, Biol. 11: 30-45.

PIRUZYAN, L.A., CLEZER, V.M., DEMENT'YEV, V.A., LOMONOSOV, V.A. and CHIBRIKIN, V.M., 1970
The mechanism of the biological effect of constant magnetic fields. Izvestiya Akademii Nauk SSSR. Seriya Biologicheskaya 4: 535-539.

PLONSEY, R., 1974
The active fiber in a volume conductor. IEEE Trans. Biomed. Eng. 21: 371-381.

POINDESSAULT, J.P., DUVAL, A. and LEOTY, C., 1976
Voltage-clamp with double sucrose gap technique: External series resistance compensation. Biophys. J. 16(2 Part 1): 105-120.

POOLER, J., 1968
Light-induced changes in dye treated lobster giant axons. Biophys. J. 8: 1009-1026.

POOLER, J.P., 1972
Photodynamic alteration of sodium currents in lobster axons. J. Gen. Physiol. 60: 367-387.

POOLER, J.P. and OXFORD, G.S., 1972
Low membrane resistance in sucrose gap - A parallel leakage path. Biochim. Biophys. Acta 255: 681-684.

POUSSART, D.J.M., 1971
Membrane current noise in lobster axon under voltage-clamp. Biophys. J. 11: 211-234.

PRESMAN, A.S., 1970
Electromagnetic Fields and Life. Plenum Press.

RABINOVITCH, B., MALING, J.E. and WEISSBLUTH, M., 1967a
Enzyme substrate reactions in very high magnetic fields I. Biophys. J. 7: 187-204.

RABINOVITCH, B., MALING, J.E. and WEISSBLUTH, M., 1967b
Enzyme substrate reactions in very high magnetic fields II. Biophys. J. 7: 319-327.

RAGLE, J.L., 1964
On possible effects of magnetic fields. Aerosp. Med. 35: 469-471.

RENO, V.R., 1969
Conduction velocity in nerve exposed to a high magnetic field. NASA Report NAMI-1089, Pensacola Florida (Oct.).

RENO, V.R. and BEISCHER, D.E., 1966
Cardiac exitability in high magnetic field. Aerosp. Med. 37: 1229-1232.

RENO, V.R. and NUTINI, L.G., 1963
Effect of magnetic field on tissue respiration. Nature 198: 204-205.

ROJAS, E. and KEYNES, R.D., 1975
On the relation between displacement currents and activation of the sodium conductance in the squid giant axon. Phil. Trans. R. Soc. Lond. 270: 459-482.

ROY, G., 1972
A simple electronic analog of the squid axon membrane: the Neurofet. IEEE Trans. Biomed. Eng. BME-19: 60-63.

RUSSEL, D.R., 1969
Effect of a constant magnetic field on invertebrate neurons. In: Biological Effects of Magnetic Fields, M.F. Barnothy (ed.), Plenum Press, Vol. 2: 227-232.

SACHAVA, T.S. and SAMOKHVALOVA, L.I., 1970
Change in the membrane potential of the cells of the alga Nitella Flexilis on exposure to a permanent magnetic field. Biofizika 15(1): 89-93.

SAMUELSON, O., 1952
Ion exchangers in analytical chemistry. Almquist and Wiksells (Upsala).

SCHWARTZ, J.L., 1976
Générateur automatique de séquence de commande pour dispositif de potentiel imposé. Med. Biol. Eng. 14: 356-358.

SCHWARTZ, J.L., 1977
Signal processor for direct current-voltage plotting of voltage-clamp data. Med. Biol. Eng. (in press).

STÄMPFLI, R., 1954
A new method for measuring membrane potentials with external electrodes. Experientia X(12): 508-509.

TAKATA, M., PICKARD, W.F., LETTVIN, J.Y. and MOORE, J.W. 1966
Ionic conductance changes in lobster axon membrane when lanthanum is substituted for calcium. J. Gen. Physiol. 50: 461-471.

TASAKI, I., 1974
Energy transduction in the nerve membrane and studies of excitation processes with extrinsic fluorescence probes. Ann. N.Y. Acad. Sciences, 227: 247-267.

TASAKI, I. and BAK, A.F., 1958
Current-voltage relations of single nodes of Ranvier as examined by voltage-clamp technique. J. Neurophysiol. 21: 124-137.

TASAKI, I. and FRANK, K., 1955
Measurement of the action potential of myelinated nerve fiber. Amer. J. Physiol. 182: 572-578.

TASAKI, I., WATANABE, A., SANDLIN, R. and CARNAY, L.,1968
Changes in fluorescence, turbidity and birefringence associated with nerve excitation. Proc. Nat. Acad. Sci. USA 61: 883-888.

TAYLOR, R.E., 1963
Cable theory. In: Physical Techniques in Biological Research, Nastuk (ed.), Academic Press, Vol. 6: 219-262.

TAYLOR, R.E., MOORE, J.W. and COLE, K.S., 1960
Analysis of certain errors in squid axon voltage-clamp measurements. Biophys. J. 1: 161-202.

VAIDHYNATHAN, V.S., 1974
Current status of theory of transport of ions across membranes. Bioelectrochem. Bioenerg. 1(3-4): 378-388.

VALENTINUZZI, M., 1965
Notes on magnetic actions upon the nervous system. Bull. Math. Biophys. (Special Issue) 27: 203-214.

VALENTINUZZI, M., 1966
A survey of theoretical approaches to magnetic growth inhibition. Am. J. Med. Electr. 5: 35-39.

VOVK, M.I. and TKACH, V.K., 1971
Influence of a permanent magnetic field on the fluctuations in the threshold of stimulation of isolated skeletal muscle. Biofizika 16(5): 833-866.

VYALOV, A.M. and LISISHKILA, J.C., 1966
Characteristics of some clinical and physiological changes in workers exposed to the action of dispersed, constant magnetic fields under industrial and laboratory conditions. Gigiyena Truda i Professional'ayye Zabolevaniya 5: 39-43.

WATERMAN, T.H., 1961
The Physiology of Crustacea. Academic Press, Vol. 2.

WIERSMA, C.A.G., 1947
Giant nerve system of the crayfish. A contribution to comparative physiology of synapse. J. Neurophysiol. 10: 23-38.

WRIGHT, E.B. and REUBEN, J.P., 1958
A comparative study of some excitability properties of the giant axons of the ventral nerve cord of the lobster, including the recovery of excitability following an impulse. J. Cell. Comp. Physiol. 51: 13-28.